Stackes

MONTHLY WEATHER REVIEW

VOLUME 81 NUMBER 7

JULY 1953

CONTENTS

U. S. DEPARTMENT OF COMMERCE • WEATHER BUREAU

PUBLICATIONS OF THE U. S. WEATHER BUREAU

As the national meteorological service for the United States, the Weather Bureau issues several periodicals, serials, and miscellaneous publications on weather, climate, and meteorological science as required to carry out its public service functions. The principal periodicals and serials are described on this page and on the inside of the back cover. A more complete listing of Weather Bureau publications is available upon request to Chief, U. S. Weather Bureau, Washington 25, D. C.

Orders for publications should be addressed to the Superintendent of Documents, Government Printing Office, Washington 25, D. C.

MONTHLY WEATHER REVIEW

First published in 1872, the Monthly Weather Review serves as a medium of publication for technical contributions in the field of meteorology, principally in the branches of synoptic and applied meteorology. In addition each issue contains an article descriptive of the atmospheric circulation during the month over the Northern Hemisphere with particular reference to the effect on weather in the United States. A second article deals with some noteworthy feature of the month's weather. Illustrated. Annual subscription: Domestic, $3.50; Foreign, $4.50; 30 cents per copy. Subscription to the *Review* does not include the *Supplements* which have been issued irregularly and are for sale separately.

CLIMATOLOGICAL DATA—NATIONAL SUMMARY

This monthly publication contains climatological data such as pressure, temperature, winds, rainfall, snowfall, severe storms, floods, etc., for the United States as a whole. A short article describing the weather of the month over the United States, tables of the observational data, and a description of flood conditions are supplemented by 15 charts. An annual issue summarizes weather conditions in the United States for the year. More detailed local data are provided in the Climatological Data (by sections) for 45 sections representing each State or a group of States, and Hawaii, Alaska, and the West Indies. Subscription price for either the National Summary or for a Section: $1.50 per year (including annual issue), 15¢ per copy.

(Continued on inside back cover)

The Weather Bureau desires that the *Monthly Weather Review* serve as a medium of publication for original contributions within its field, but the publication of a contribution is not to be construed as official approval of the views expressed.

The issue for each month is published as promptly as monthly data can be assembled for preparation of the review of the weather of the month. In order to maintain the schedule with the Public Printer, no proofs will be sent to authors outside of Washington, D. C.

The printing of this publication has been approved by the Director of the Bureau of the Budget, February 11, 1952.

DEPARTMENT OF COMMERCE
SINCLAIR WEEKS, Secretary

WEATHER BUREAU
F. W. REICHELDERFER, Chief

MONTHLY WEATHER REVIEW

Editor, JAMES E. CASKEY, JR.

Volume 81
Number 7

JULY 1953

Closed September 15, 1953
Issued October 15, 1953

A STUDY OF LOW LEVEL AIR TRAJECTORIES AT OAK RIDGE, TENN.*

FRANK GIFFORD, JR.

U. S. Weather Bureau, Washington, D. C.

[Manuscript received April 10, 1953; revised August 31, 1953]

ABSTRACT

Approximately 2,000 zero-lift, double-theodolite pilot balloon observations made at Oak Ridge, Tenn., are analyzed in order to study low level air trajectories over hilly terrain. Paths of air parcels are found to fall into characteristic groups, depending on wind speed and stability conditions. Eddy patterns for these groups are determined, and these are found to resemble similar patterns determined for different types of terrain. The properties of low level air flow, particularly of vertical velocity patterns, are displayed in various ways. Slope winds due to thermal-dynamical effects appear to contribute more to these patterns than does a purely mechanical lifting effect.

INTRODUCTION

This report summarizes the main results of a study of low level air trajectories observed at Oak Ridge, Tenn. A Weather Bureau meteorological group assigned there at the request of the Atomic Energy Commission to study the micrometeorology of the area, made almost a thousand neutral, or zero-lift, pilot balloon observations between January 1949 and February 1950, as part of an intensive program of observations. This unique body of data will be analyzed for what light it can throw on local air flow patterns over the hilly terrain at Oak Ridge, as well as on the character of low level turbulence in general.

The use of neutral pilot balloons for such a purpose is not new. Lange's studies, in connection with the Rhön-Rossitten glider society, [3, 4, 5], are probably the best known example. Other interesting studies have been made, particularly by Höhndorf and Müller [2], and by Nitze [9]. The principal object of Lange's work was the determination of vertical velocities associated with lee eddies which he observed to form to the leeward of dunes, hills, or coastal cliffs, then to detach themselves and travel downwind. These studies are characterized by meticulous attention to observational techniques and sources of error and a thorough analysis of results, using the detailed case-study approach. Certain properties of low level air trajectories (such as vertical velocity patterns) were recorded for the first time, and then were observed to be reproduced, qualitatively, under similar meteorological conditions. Forty ground and 41 air releases are reported in Lange's work, all daytime and made mostly during the midafternoon. The present study deals with a far larger body of data. This permits several new types of analysis and yields correspondingly more complete information, while substantially verifying the earlier results, where these apply.

LOCALE AND TECHNIQUE OF THE OBSERVATIONS

The town of Oak Ridge is located in eastern Tennessee in the broad northeast-southwest valley lying between the Cumberland Mountains and the Great Smokies. The Smokies rise to over 5,000 feet about 40 miles east-southeast of Oak Ridge, and the Cumberland Plateau reaches a general elevation of 2,000 feet some 20 miles to the west-northwest. In between, and running parallel to the main valley, are a number of smaller ridges and valleys of which Blackoak Ridge, from which the town gets its name, is one. The valley floors near Oak Ridge are at nearly 800 feet above sea level, and the ridges rise from 300 to 500 feet above that. Drainage in the valleys is to the southwest into the Clinch River. The land consists of wooded ridges and mainly cleared valleys. Figure 1 is a topo-

*This report was prepared under a research contract between the U. S. Atomic Energy Commission and the U. S. Weather Bureau.

FIGURE 1.—Topographical map of the Oak Ridge area. Numbered dots indicate locations of stations continuously recording wind, temperature, humidity, and rainfall.

graphical map showing the area for several miles around the balloon release point, which was a platform 30 feet high near the middle of Bethel Valley, approximately 8 miles south-southwest of the town of Oak Ridge.

The technique of neutral pibals is quite simple [10]. An ordinary balloon, in this case a 10-gram ceiling ballon, is inflated until its free-lift is just zero. It is released and then followed with two theodolites. In the present experiment a baseline of about 800 feet, running across the valley, was used, and readings were made at intervals of 30 seconds. The diameter of the balloons averaged about 10 inches. Neutral runs were made successively during two 45-minute periods each day starting at 1100 and 2300 LST, weather and personnel permitting. A balloon was released, followed until it was lost, and then a new release was made. In this way, groups of from 1 or 2 to as many as 6 runs were obtained. Azimuth and elevation angles were recorded on punched cards, and the balloon's distance and height, direction and magnitude of the velocity vector, vertical velocity component, and horizontal distance components were calculated by punched-card machine. With a 30-second reading interval, about 25,000 observations were obtained during the course of the experiment. For a particular run only those observations involving horizontal distances from the release point of less than 10,000 feet are considered in this study. This reduced the total number of individual observations to about 18,000. The length of the baseline was such that the calculations for greater distances were not sufficiently reliable.

There are certain limitations and sources of error peculiar to neutral pilot balloon observations. The slight pressure excess causes diffusion through the balloon's wall; radiational heating or cooling of the balloon occurs; if the vertical temperature gradient is not adiabatic, buoyancy forces arise. All these affect the free lift. Such sources of error were studied theoretically in detail by Lange [3], who concluded that the possible free lift which might occur is not excessively large, and that the balloons remain reasonably balanced. A second kind of error arises in a continued experiment such as the present one because of the difficulty of weighing off the balloons in an exactly balanced condition in all kinds of weather. To the extent that this sort of error is random, it will tend to be minimized when large numbers of observations are considered.

SUPPLEMENTARY METEOROLOGICAL INFORMATION

In addition to the usual meteorological information, a wide variety of supplementary material was available at Oak Ridge for comparison with the neutral data. A network of stations continuously recording wind, temperature, humidity, and rainfall was in operation. These stations were located at the numbered dots on figure 1, and they give a detailed meteorological coverage of the area. Winds and temperature measurements at several heights up to 210 feet were available at the neutral release point. Detailed single theodolite pilot balloon runs were made just before and just after each neutral period. For the portion of the neutral experiment from June 1949 on, frequent temperature soundings by captive blimp were available [7]. A summarization of the essential features of much of these data, including wind speed, shear, and stability measures, was available for each hour in the form of a 10-digit classification code, and this information was punched into the neutral card deck.

THE NEUTRAL TYPES

As a starting point in the analysis, a number of neutral trajectories, position plots in x-y and x-z coordinates, were drawn. One hundred observing periods, or about 250 individual runs were examined. It soon became clear that these could be grouped qualitatively into four classes according to the appearance of the x-z trajectory, the plot of distance against height of a group of runs. The general appearance of each of these is shown, schematically, in figure 2. Type A, a daytime, light wind type associated with unstable lapse rates in the lowest few hundred feet, appears to be the result of convective heating. Balloons are carried upward rapidly and do not travel much horizontally before being carried back down to near the ground. Some balloons have been observed to go up into cumulus clouds during this type of run. Type B also occurs during the daytime, but is associated with stronger winds and often with more cloudiness and less instability than is Type A. Type C occurs at night, with moderate to strong winds. The balloons go out in steady paths, two or more often being virtually superimposed. The fourth type, D, is associated with stable conditions and light surface winds at night. The balloons slowly rise, then drift slowly back down, often without moving very far out.

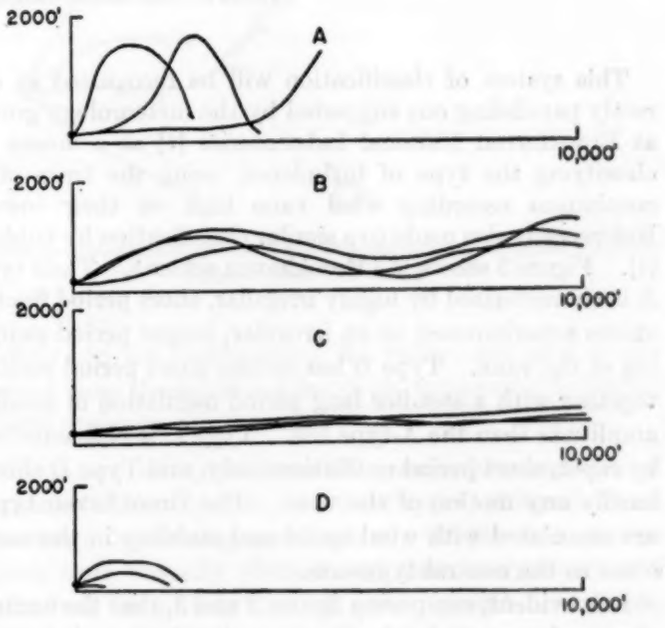

FIGURE 2.—Schematic distance—height trajectories illustrating the four basic neutral balloon run types.

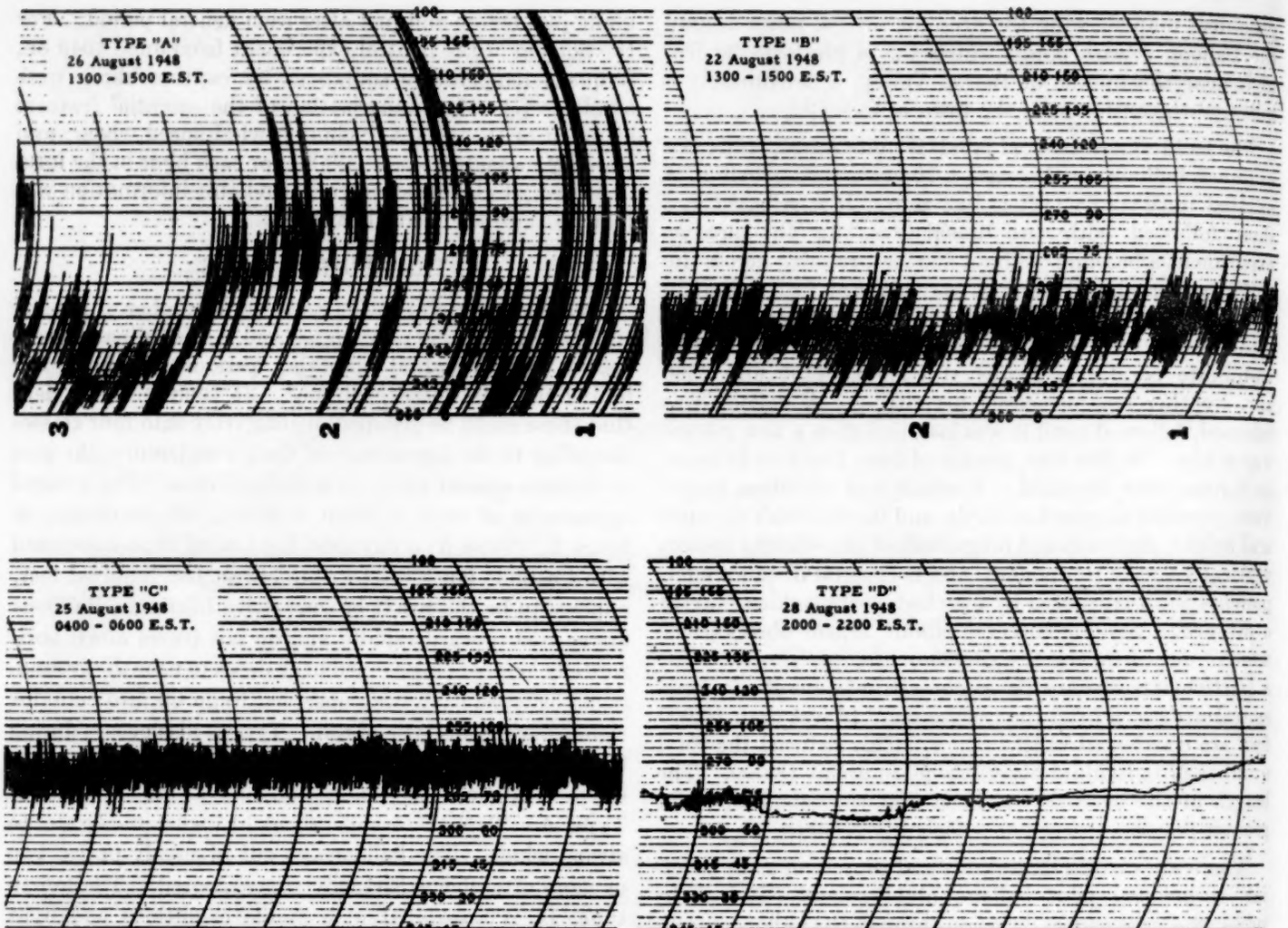

FIGURE 3.—Wind direction traces illustrating the Brookhaven turbulence types [6].

This system of classification will be recognized as directly paralleling one suggested by the meteorology group at Brookhaven National Laboratories [6] as a means of classifying the type of turbulence, using the trace of a continuous recording wind vane high on their tower. Reference is also made to a similar classification by Giblett [1]. Figure 3 shows the Brookhaven scheme. Their type A is characterized by highly irregular, short period fluctuations superimposed on an irregular, longer period swinging of the vane. Type B has similar short period motion together with a steadier long period oscillation of smaller amplitude than the A-type has. Type C is characterized by rapid, short period oscillations only, and Type D shows hardly any motion of the vane. The Brookhaven types are associated with wind speed and stability in the same sense as the neutral types are.

It is evident, comparing figures 2 and 3, that the neutral observations completely filter out the short period oscillations of types B and C. Continuous wind direction traces at a height of 210 feet were available for 30 of the neutral periods comprising 54 individual runs. These were classified according to the Brookhaven typing system and the result compared with the corresponding neutral types. Over 90 percent agreement was found. This result fits the neutral observations into the general picture of low level turbulent flow as it is already understood. Furthermore, it is possible in the light of these observations, to infer from a wind-direction trace what sort of paths the air parcels are following.

Because it separates what appear to be essentially different patterns of flow, or turbulence regimes, this classification scheme has been used as a basis for the remainder of the analysis.

SOME TYPICAL NEUTRAL RUNS

From the many plotted runs, two sets representative of each turbulence type are presented in this section.

Figure 4 shows typical A-groups. Panel (a) contains

distance vs. height and distance vs. azimuth plots of a group of three consecutive runs made on a clear August day. There was a flat High centered just east of the Oak Ridge area, near Bristol, Tenn., giving light easterly winds aloft. The micronet stations (fig. 1) in valley locations (001, 003, 004) followed the general circulation with light, northeasterly winds, whereas the slope stations (005, 010, 012) showed evidence of upslope winds. The lapse rate was strongly superadiabatic below 200 feet but more stable above. Dots and crosses give the balloon's position at the end of each 30-second interval, so that the distance between them is proportional to wind speed. All these balloons show a good deal of vertical motion, the maximum vertical velocities being about ±4 mph. Panel (b) shows a second A-group. The principal features of the first group are repeated.

Two typical B-groups are shown in figure 5. The first group of runs, panel (a) was made on a clear December day. A ridge of high pressure extended north-south over the eastern part of the country, causing a somewhat stronger easterly flow than in the first A-case. Valley and ridge micronet stations showed northeasterly winds, with slight upslope components at the slope stations. The balloons followed a wavelike path in the vertical with peaks about every 2,000 feet at first. The maximum height the balloons reached is only about 1,000 feet. The second B-group, panel (b) of figure 5, was made on a clear November day with moderate westerly flow over the area. The undulation here has a length of around 4,000 feet.

Figure 6 shows two C groups. In the first, panel (a), the balloons are responding to a strong southwesterly gradient associated with a trough through the central United States. The sky was overcast, base 2,000 feet, and there was intermittent rain in the area, preceding a polar outbreak in January. Micronet winds were mainly southerly, following the general circulation. The balloons follow nearly identical paths, displaced from one another slightly more horizontally than vertically. They cross Chestnut Ridge at about 5,000 and Pine Ridge at about 10,000 feet out, but any topographic effect is evidently slight. The second C-group (panel (b)), made on a partly cloudy November night when the area was being affected by a moderate northwesterly flow due to a High over the Plains States, duplicates the appearance of the first, except that there is even more disparity between horizontal and vertical dispersion of the balloons.

Figure 7 shows two D-groups. The first, panel (a), was made on a partly cloudy February night with a High centered near Oak Ridge. Valley micronet winds were calm, and ridgetop winds light, westerly. Two of the balloons rose slowly, traveled out a short distance, and sank. The third became imbedded in the stronger flow aloft, above the ground inversion, and was carried away more rapidly, much as a C-type. The second D-group was made on a June night with an indefinite trough giving a weak, southerly flow over the area. The balloons rose slightly, drifted slowly across the valley, and sank to the ground near the southeastern slope, apparently following a local drainage circulation.

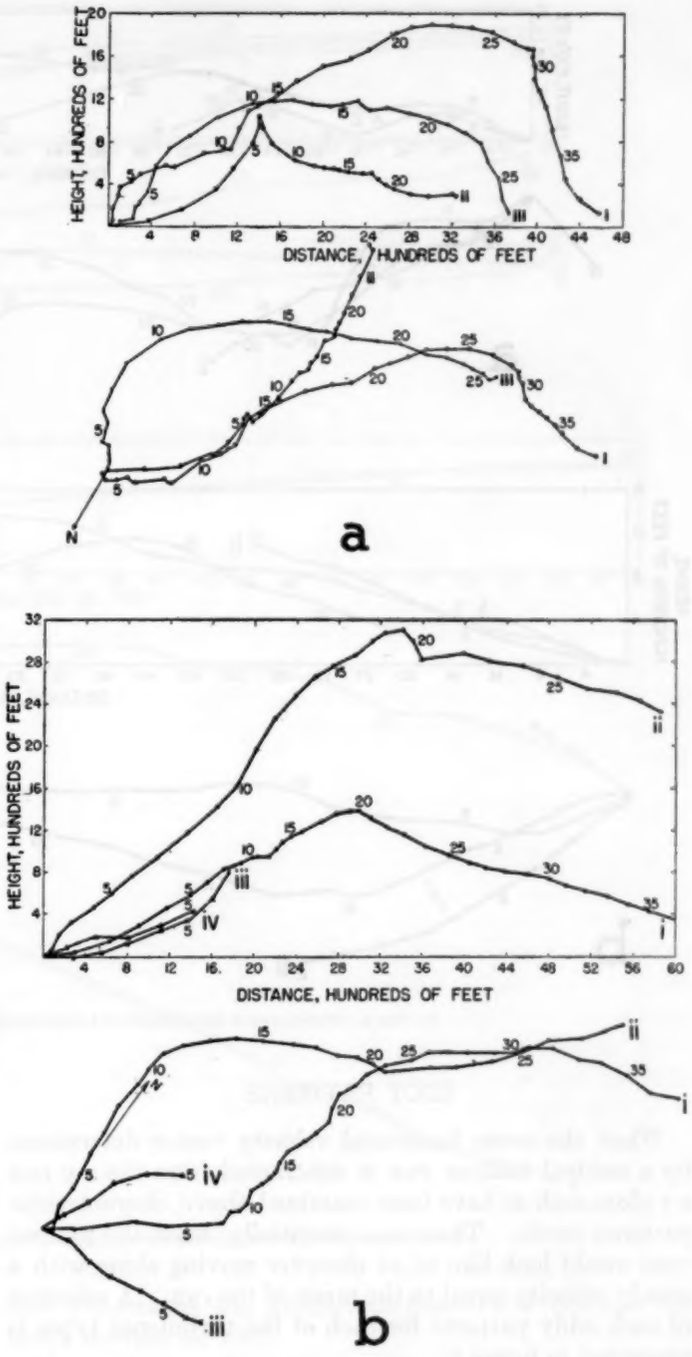

FIGURE 4.—Trajectories in the vertical and horizontal planes of two typical A-groups of neutral balloon observations.

These are all typical neutral runs. Most groups of neutrals fall readily into 1 of the 4 types, although there are many interesting peculiarities. Of the 100 groups which were actually plotted and examined, about 250 individual runs, only 1 or 2 were out-and-out misfits, defying classification.

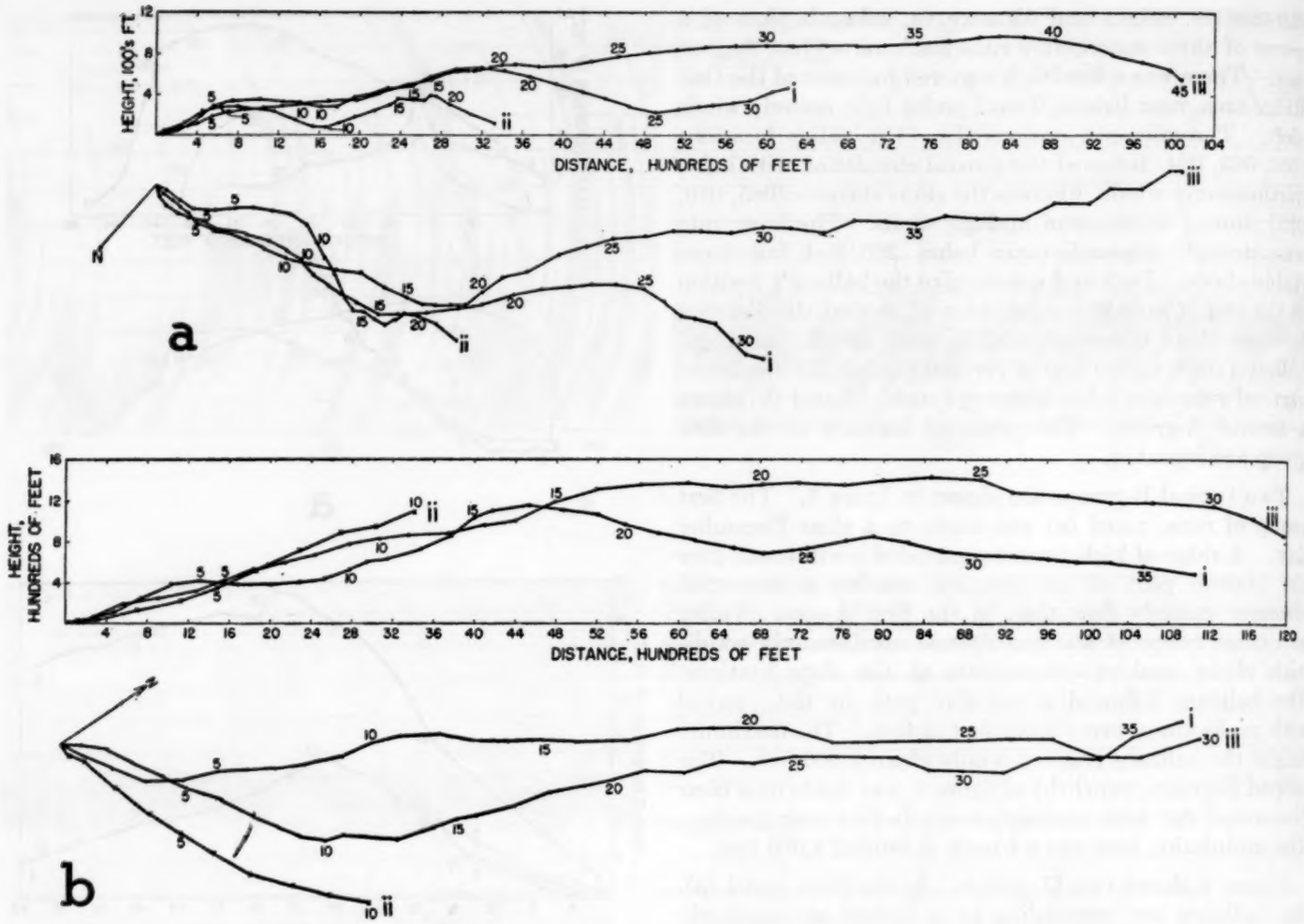

FIGURE 5.—Trajectories in the vertical and horizontal planes of two typical B-groups of neutral balloon observations.

EDDY PATTERNS

When the mean horizontal velocity vector determined by a neutral balloon run is subtracted from the x-y and x-z plots such as have been examined above, characteristic patterns result. These are, essentially, what the neutral runs would look like to an observer moving along with a steady velocity equal to the mean of the run. A selection of such eddy patterns for each of the turbulence types is presented in figure 8.

The A types correspond to the trajectories of figure 4. The eddies are elongated in the vertical and transverse directions, and have dimensions of around 1,000 to 2,000 feet. It is a very interesting feature of this particular group that the sense of rotation of the center run, in both the horizontal and vertical patterns, is opposite to that of the two others. The end balloons, runs i and iii, rose with a velocity deficit and went to the left of the main stream, then picked up speed and returned to the right while lowering. Run ii, in contrast, rose with an excess velocity, actually faster than the mean for the run, and went to the right, ultimately slowing down and lowering. These patterns indicate air motion in the form of counter-rotating horizontal helical vortices, a form suggested by Woodcock and Wyman [11] to explain their observations of a banded appearance of the sea surface under similar weather conditions, but which they were unable, at that time, to observe directly.

The panel of figure 8 labeled Type B shows eddy patterns due to the B-types. The B eddies are smaller than the A's, just as were the waves in the trajectory plot. Once again, the sense of rotation of the second eddy is reversed. Some small loops, about 100 to 200 feet in diameter, are evident.

These patterns, both A- and B-types, are comparable in dimension, appearance, and sense of the rotation with similar ones found by Lange. Except that no lee eddies, such as Lange occasionally observed ([3], p. 22, fig. 21, turbulence element #52) were found, the resemblance between the Oak Ridge patterns and those Lange found over much different terrain types is very striking. Lange's observations were usually made either over rather flat terrain or in the area of some such bluff obstacle as a dune

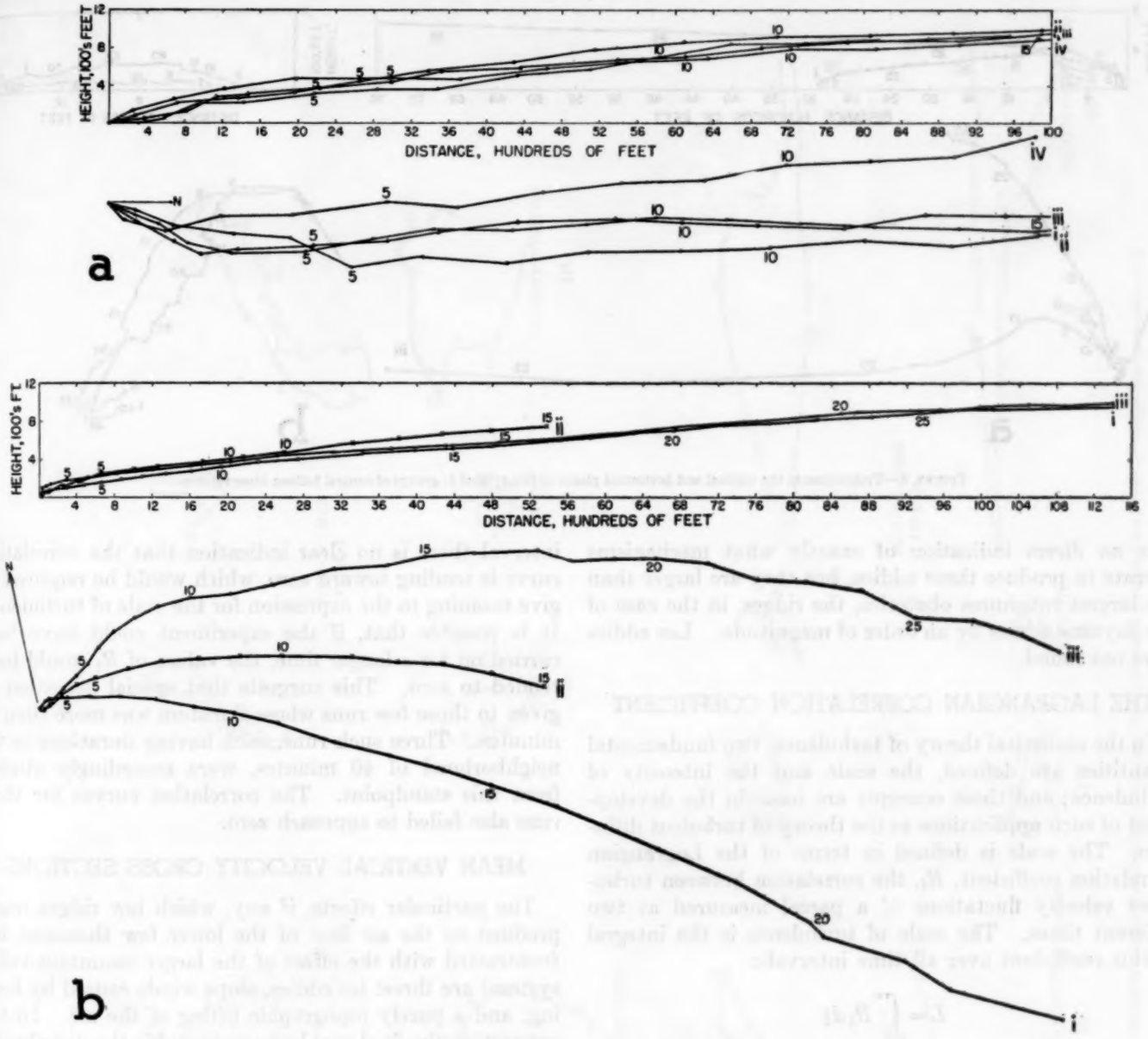

FIGURE 6.—Trajectories in the vertical and horizontal planes of two typical C-groups of neutral balloon observations.

or a cliff. The Oak Ridge observations, being made over low, comparatively gently sloping ridges, lie on a scale of terrain ruggedness somewhere in between. The similarity of eddy patterns of the A- and B-types to Lange's indicate that these particular eddies are characteristic properties of low level air flow and that their properties do not depend on the presence of large ground obstacles.

There is no true eddy pattern for type C, (fig. 8), either in the horizontal or in the vertical. The apparent half-rotation in the vertical plane is simply a depiction of the vertical velocity gradient. Of the D-type eddy patterns (fig. 8), the first two have a slow clockwise rotation, the pattern being this time elongated horizontally. The third run of this group looks like a C-type; the balloon in this case penetrated the ground inversion and reached the faster moving air aloft.

It seems clear from these patterns, that the neutrals respond primarily to large eddies, probably thermal in origin, when these are present but show little indication of the small-scale mechanical turbulence which we know, from fixed wind measuring instruments, to exist. The size of these larger eddies is of the order of thousands of feet in the case of daytime thermals, and of hundreds for the sluggish, nighttime eddies. During the day, with light winds and instability, the eddies are elongated vertically, during the night horizontally. The nighttime eddies are of the proper size and character to be explained by slope and valley drainage circulations. The neutrals

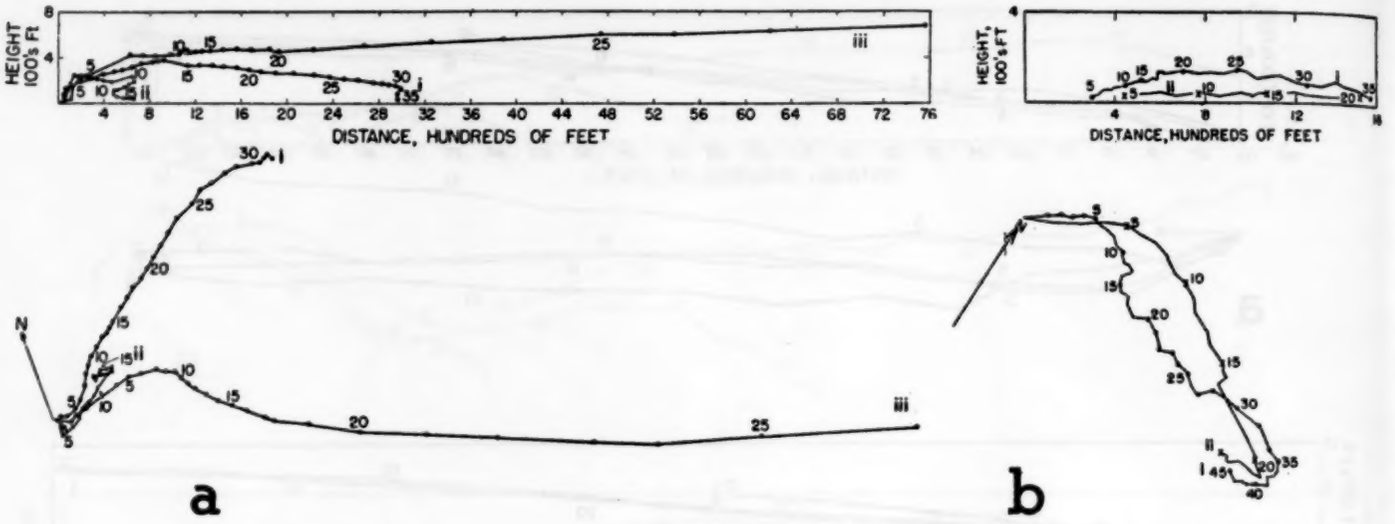

FIGURE 7.—Trajectories in the vertical and horizontal planes of two typical D-groups of neutral balloon observations.

give no direct indication of exactly what mechanisms operate to produce these eddies, but they are larger than the largest roughness obstacles, the ridges, in the case of the daytime eddies by an order of magnitude. Lee eddies were not found.

THE LAGRANGIAN CORRELATION COEFFICIENT

In the statistical theory of turbulence, two fundamental quantities are defined, the scale and the intensity of turbulence; and these concepts are basic in the development of such applications as the theory of turbulent diffusion. The scale is defined in terms of the Lagrangian correlation coefficient, R_ξ, the correlation between turbulence velocity fluctations of a parcel measured at two different times. The scale of turbulence is the integral of this coefficient over all time intervals:

$$L=\int_0^\infty R_\xi \, d\xi$$

The intensity of turbulence is defined as the square root of the ratio of the turbulent energy to the mean energy:

$$I=\frac{\sqrt{\overline{v'^2}}}{\bar{u}}$$

But the mean velocity, $\bar{u}$, must be taken over a time interval long enough for R_ξ to attain zero in such a way that the integral has some value. Otherwise the intensity is not defined.

Data with which to determine R_ξ in the atmosphere are not common by any means because of the difficulty of making observations on a parcel of air. Neutral pilot balloons are among the few possible methods. For this reason, the curves exhibited in figure 9 should be of interest. These are R_ξ vs. ξ curves for a selection of neutral runs representing each type. The time interval involved is, in each case, less than ten minutes ($\xi<20$). At this interval there is no clear indication that the correlation curve is tending toward zero, which would be required to give meaning to the expression for the scale of turbulence. It is possible that, if the experiment could have been carried on for a longer time, the values of R_ξ would have tended to zero. This suggests that special attention be given to those few runs whose duration was more than 30 minutes. Three such runs, each having durations in the neighborhood of 40 minutes, were accordingly studied from this standpoint. The correlation curves for these runs also failed to approach zero.

MEAN VERTICAL VELOCITY CROSS SECTIONS

The particular effects, if any, which low ridges might produce on the air flow of the lower few thousand feet (contrasted with the effect of the larger mountain-valley system) are three: lee eddies, slope winds caused by heating, and a purely topographic lifting of the air. In this connection the final problem considered is the distribution of vertical velocities over various parts of the neutral study.

Figure 10 shows the joint relation, for the 100 plotted neutral runs, between turbulence type, and measures of low level stability and 5,000-foot wind speed, these particular quantities being among those punched into each neutral IBM card. It is seen that light winds and instability correspond to the A-type, and so on. With considerable justification, a sort can be made on the stability and wind speed values indicated by the dashed lines in the figure, and the entire body of observations separated in this way by type. Notice that the A's and B's are well separated from the C's and D's by the isothermal, but that the separation between A's and B's and between C's and D's is considerably poorer.

Figure 11, showing isopleths of vertical velocity, was obtained by sorting first on turbulence type and then selecting all observations with azimuths in a 10° arc up

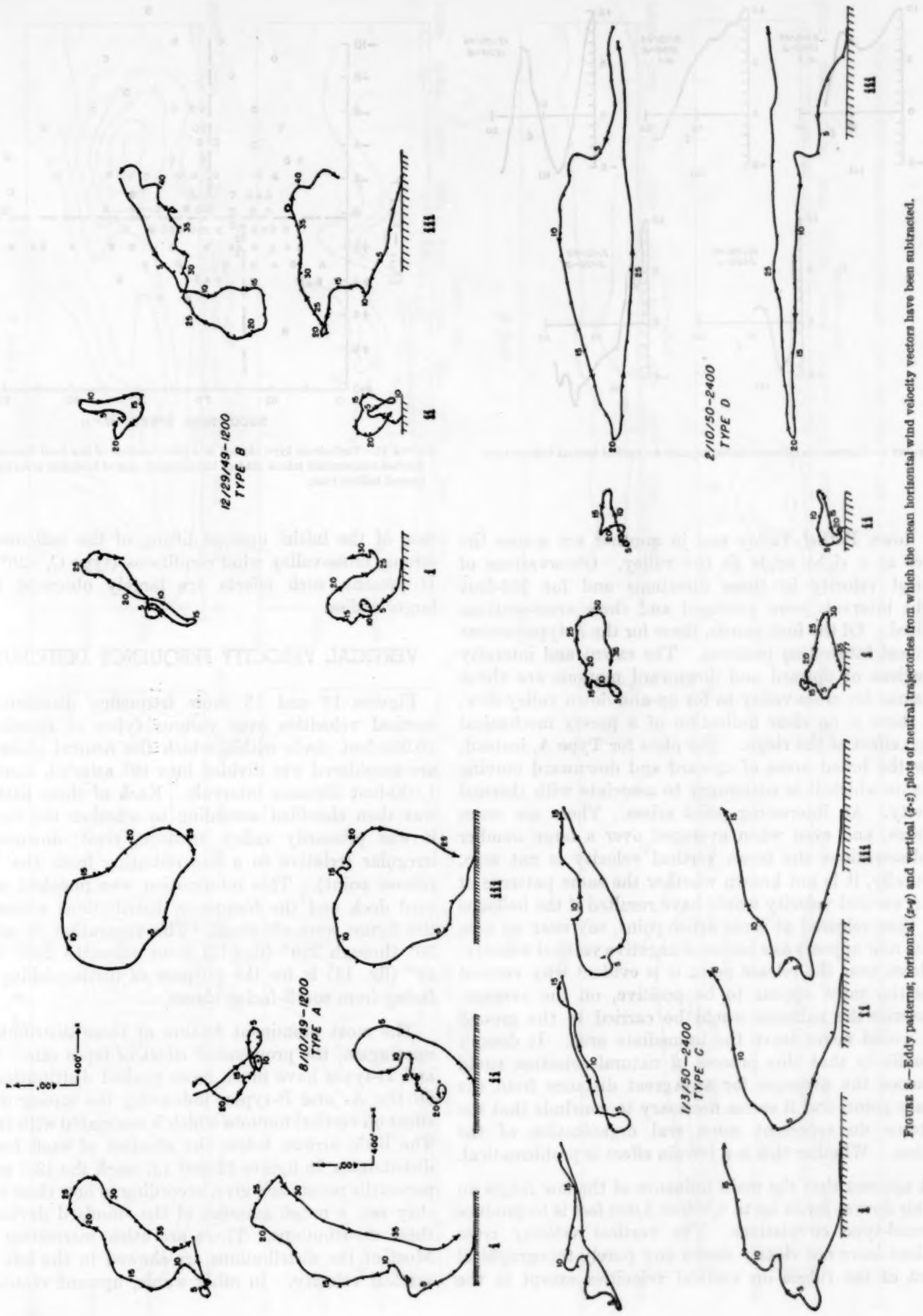

FIGURE 8.—Eddy patterns; horizontal (x-y) and vertical (x-z) plots of neutral trajectories from which the mean horizontal wind velocity vectors have been subtracted.

266962—53——2

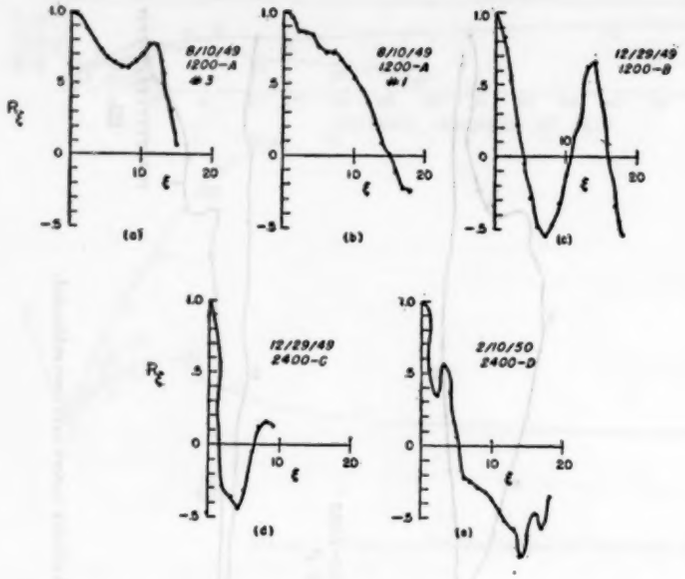

FIGURE 9.—Lagrangian autocorrelation function for typical neutral balloon runs.

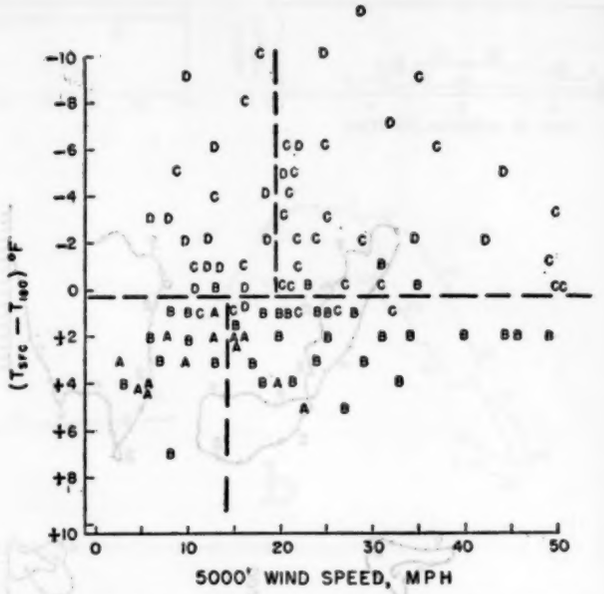

FIGURE 10.—Turbulence type plotted as a joint function of low level thermal stability (surface temperature minus 180-foot temperature) and of 5,000-foot wind speed for 100 neutral balloon runs.

and down Bethel Valley and in another arc across the ridges at a right angle to the valley. Observations of vertical velocity in these directions and for 500-foot height intervals were averaged and these cross-sections resulted. Of the four panels, those for the A-type present the most interesting patterns. The extent and intensity of regions of upward and downward motions are about the same for cross-valley as for up-and-down valley flow, and there is no clear indication of a purely mechanical lifting effect of the ridge. The plots for Type A, instead, show the broad areas of upward and downward moving currents which it is customary to associate with thermal activity. An interesting point arises. These are mean pictures, and even when averaged over a large number of observations the mean vertical velocity is not zero. Naturally, it is not known whether the same patterns of mean vertical velocity would have resulted if the balloons had been released at some other point, say near an area which now appears as a center of negative vertical velocity. At least near the release point it is evident why vertical velocities must appear to be positive, on the average. Otherwise the balloons would be carried to the ground and would never leave the immediate area. It doesn't seem likely that this process of natural selection could influence the averages for any great distance from the release point, and it seems necessary to conclude that the patterns do represent some real organization of the motion. Whether this is a terrain effect is problematical.

It appears that the main influence of the low ridges on the air flow at levels up to 2,000 or 3,000 feet is to produce thermal-type circulations. The vertical velocity cross sections have not clearly shown any purely topographical effect of the ridges on vertical velocities except in the case of the initial upslope lifting of the balloons under strong, cross-valley wind conditions (type C, 320°–329°). If present, such effects are largely obscured by the larger eddies.

VERTICAL VELOCITY FREQUENCY DISTRIBUTION

Figures 12 and 13 show frequency distributions of vertical velocities over various types of terrain. The 10,000-foot circle within which the neutral observations are considered was divided into 10° azimuth sectors and 1,000-foot distance intervals. Each of these little areas was then classified according to whether the terrain in it was primarily valley, upslope, crest, downslope, or irregular (relative to a line radiating from the balloon release point). This information was punched into the card deck and the frequency distributions appearing in the figure were obtained. The separation of azimuths 50° through 229° (fig. 12) from azimuths 230° through 49° (fig. 13) is for the purpose of distinguishing north-facing from south-facing slopes.

The most prominent feature of these distributions is, once again, the pronounced effect of lapse rate. The C- and D-types have much more peaked distributions than do the A- and B-types, indicating the strong damping effect on vertical motions which is associated with stability. The little arrows below the abscissa of each frequency distribution, in figures 12 and 13, mark the 12.5 and 50th percentile points and give, according to how close together they are, a rough measure of the standard deviations of these distributions. There are other interesting points. Most of the distributions are skewed to the left of zero vertical velocity. In other words, upward velocities are

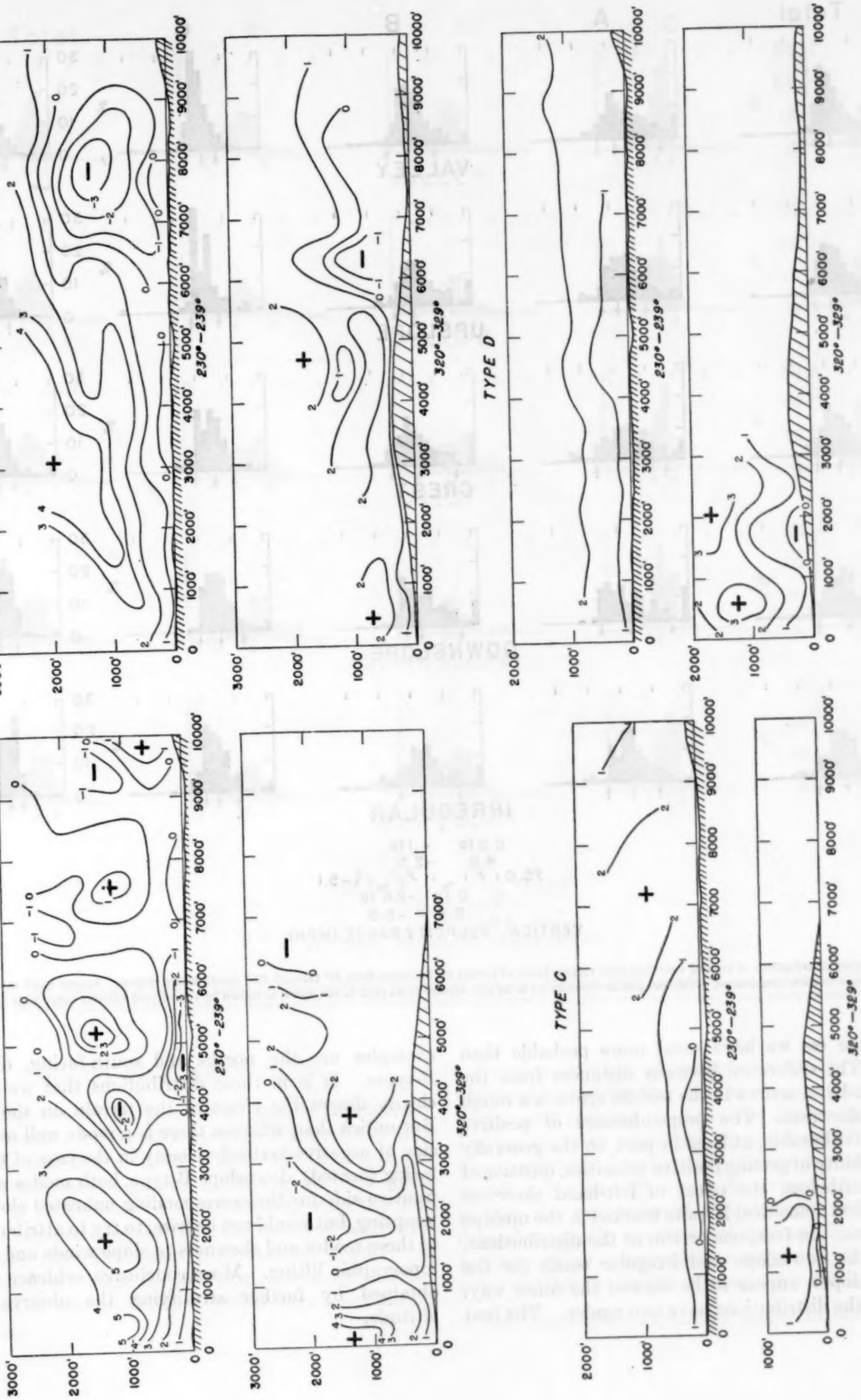

FIGURE 11.—Vertical cross-sections showing the average distribution of observed vertical velocities (m. p. h.) in 10° arcs down-valley (230° to 239°) and cross-valley (320° to 329°) from the neutral balloon release point (of fig. 1).

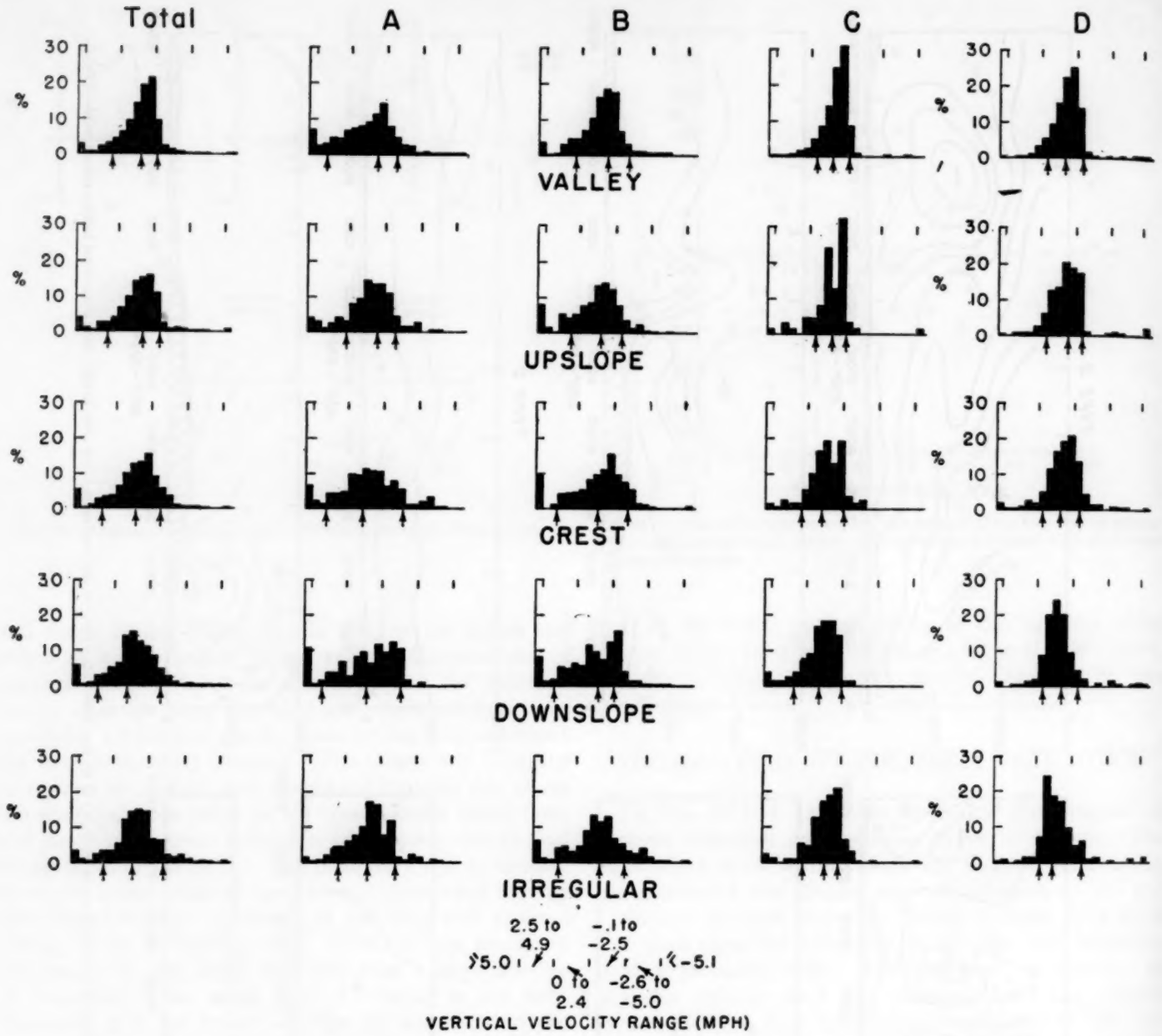

FIGURE 12.—Frequency distributions of vertical velocities over various types of terrain for azimuths from 50° through 229° (south-facing slopes). Arrows mark the ±12.5 and the 50th percentile points in each distribution. *Note that positive velocities are to the left, negative to the right in this figure,* as shown by the vertical velocity range scale at the bottom.

on the average (as we have seen) more probable than downward. The difference between distances from the right- and left-hand arrows to the middle arrow is a rough measure of skewness. The preponderance of positive velocities is attributable, at least in part, to the generally greater probability of getting positive velocities, mentioned earlier. Nevertheless, the effect of left-hand skewness (positive vertical velocities) is quite marked in the upslope and crest types. In fact, one or two of the distributions, particularly the downslope and irregular totals for the south-facing slopes, appear to be skewed the other way. Also, some of the distributions have two modes. The best examples are the north- and south-facing, downslope, B-types. It is in these distributions that we can most clearly detect the effect of the terrain on the air flow. But notice that, whereas there is a mode well over on the side of negative vertical velocity in the case of the south-facing (heated), downslope B-type, both modes are on the positive side for the corresponding unheated slope. It is tempting, but would not be wise, to try to attribute certain of these modes and skewness to slope winds and others to topographic lifting. More conclusive evidence might be obtained by further stratifying the observations by altitude.

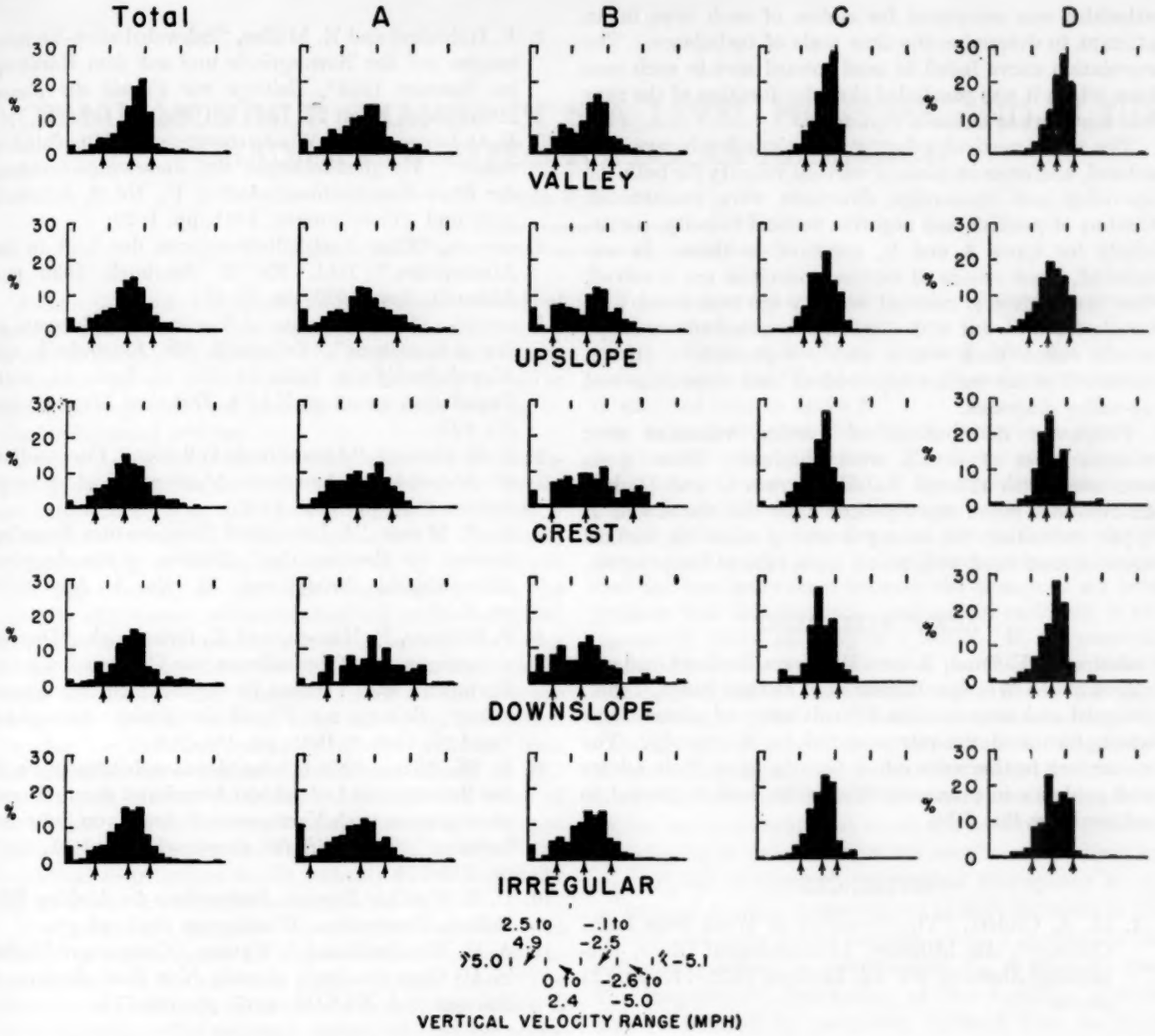

FIGURE 13.—Frequency distribution of vertical velocities over various types of terrain for azimuths from 230° through 49° (north-facing slopes). Arrows mark the ±12.5 and the 50th percentile points in each distribution. *Note that positive velocities are to the left, negative to the right in this figure,* as shown by the vertical velocity range scale at the bottom.

SUMMARY AND CONCLUSIONS

In this experiment, the paths of air parcels (represented by small, floating balloons) were observed over the hilly terrain near Oak Ridge, Tenn. These were found to fall into four characteristic groups, depending on wind speed and stability conditions. A direct analogy with the four turbulence regimes deduced from the traces of horizontal wind vanes (the Brookhaven turbulence types) was demonstrated, although the balloons necessarily can not be observed in enough detail to reveal very short period fluctuations.

From a number of trajectories, eddy patterns were obtained by subtracting out the mean horizontal velocity vector and plotting the result in x-z or x-y coordinates. During unstable conditions (types A and B), these patterns resembled ones found by Lange over much different terrain. No lee eddies were discovered. The conclusion is that the properties of the observed motions do not depend primarily on the large ground obstacles (ridges), but are, rather, characteristic properties of low level air flow; whether thermal or dynamical is not known.

The Lagrangian correlation coefficient between vertical

velocities was computed for eddies of each type in an attempt to determine the time scale of turbulence. The correlation curve failed to tend toward zero in each case from which it was concluded that the duration of the runs was too short to define a time scale.

The mean vertical velocity at various levels was considered, and cross sections of vertical velocity for both the up-valley and cross-ridge directions were constructed. Centers of positive and negative vertical velocity, particularly for types A and B, appeared in these. It was inferred, since means of vertical velocities are involved, that the centers of vertical velocity are associated with terrain features, but with thermal-dynamical effects (slope winds) rather than with a purely topographical lifting, inasmuch as the centers appeared on both cross-ridge and up-valley diagrams.

Frequency distributions of vertical velocities over various types of terrain were obtained. Those types associated with thermal stability (types C and D) had distributions much more peaked than did the A and B types, indicating the strong damping effect on vertical motions associated with stable lapse rate of temperature.

ACKNOWLEDGMENT

Joshua Z. Holland, Robert F. Myers, Barlow Goad and others of the Weather Bureau staff at Oak Ridge, Tenn., designed and executed the difficult series of observations which furnished the raw material for this study. The writer has furthermore relied heavily upon their advice and guidance in preparing this report, and is pleased to acknowledge this debt.

REFERENCES

1. M. A. Giblett, "The Structure of Wind Over Level Country", Air Ministry, Meteorological Office, *Geophysical Memoirs No. 54*, London 1932, 119 pp., 21 plates.
2. F. Höhndorf and E. Müller, "Schwebeballon-Vermessungen auf der Hornisgrinde und auf dem Hornberg im Sommer 1933", *Beiträge zur Physik der Freien Atmosphäre*, Band 22, Heft 3, 1935, pp. 132–148.
3. K. O. Lange, "Über Windströmungen an Hügelhindernissen", *Veröffentlichungen des Forschungs-Institutes der Rhön-Rossiten-Gesellschaft e. V.*, Nr. 4, Jahrbuch 1929 und Abhandlungen, 1931, pp. 1–29.
4. ———, "Über Vertikalbewegungen der Luft in der Atmosphäre," Ibid, Nr. 5, Jahrbuch 1930 und Abhandlungen, 1932, pp. 25–43.
5. ———, "Measurements of Vertical Air Currents in the Atmosphere", *Zeitschrift für Flugtechnik und Motorluftschiffahrt*, Band 22, Nr. 17, Sept. 14, 1931. Translation issued as NACA *Technical Memorandum No. 648*.
6. E. W. Hewson, "Atmospheric Pollution", *Compendium of Meteorology*, American Meteorological Society, Boston 1951, pp. 1139–1157.
7. R. F. Myers, "A Low-Level Temperature Sounding System for Routine Use", *Bulletin of the American Meteorological Society*, vol. 33, No. 1, Jan. 1952, pp. 7–12.
8. P. Mildner, F. Hänsch, and K. Griessbach, "Doppelvisierungen von Pilotballonen zur Untersuchung von Turbulenz und Vertikal-Bewegungen in der Atmosphäre", *Beiträge zur Physik der Freien Atmosphäre*, Band 17, Heft 3, 1931, pp. 181–219.
9. F. W. Nitze, "Nächtliche Austauschströmungen in der Bodennahen Luftschicht hergeleitet durch Stereophotogrammetrich Vermessene Bahnen von Schwebeballonen", *Zeitschrift für Geophysik*, Band 11, 1935, pp. 247–271.
10. U. S. Weather Bureau, *Instructions for Making Pilot Balloon Observations*, Washington 1942, 68 pp.
11. A. H. Woodcock and J. Wyman, "Convective Motion in Air Over the Sea", *Annals, New York Academy of Sciences*, vol. XLVIII, 1947, pp. 749–776.

NORMAL MONTHLY CHANGE IN SEA LEVEL PRESSURE AND IN THE GRADIENT OF EFFECTIVE SOLAR RADIATION

MILES F. HARRIS

U. S. Weather Bureau, Washington, D. C.

[Manuscript received July 17, 1953; revised manuscript received August 27, 1953]

A basic problem of meteorology is to relate the fields of pressure and motion in the atmosphere to the distribution of the incoming solar energy. The purpose of this note is to present the sea level pressure and the solar radiation data in a way that may possibly have some bearing on this fundamental problem.

Table 1 shows the normal monthly change in the northward gradient of effective solar radiation over the northern hemisphere. The data were obtained from Table V of Simpson's study on "The Distribution of Terrestrial Radiation" [1], in which are tabulated by 10° latitude zones the intensity of the effective radiation, i. e., the intensity of the solar radiation absorbed by the earth and its atmosphere. Simpson's data were based on the mean of the relationships between cloud amount and albedo found by Aldrich and Ångström, and on the average cloudiness for each latitude zone according to Brooks. To allow for the large reflection of solar radiation from the extensive snow surfaces, a constant albedo of 0.65 was adopted for the polar cap. Although the value of the albedo used in Simpson's computations is now open to question [2], the general features of the seasonal and latitudinal distributions would probably not be materially altered by the use of a different value.

The northward gradient of effective radiation was defined as the intensity at a lower latitude zone minus the intensity at the adjoining higher latitude zone. The gradients are therefore in terms of a length unit which is 10° of latitude. The monthly changes in gradient represent the gradient at a given month minus the gradient at the preceding month. The data are presented in figure 1 as an isopleth analysis.

Table 2 shows the normal monthly change in mean sea level pressure at each latitude over the Northern Hemisphere. These values were obtained from the 40-year series of Historical Weather Maps [3], and are represented in analyzed form in figure 2.

It is apparent that the isopleth patterns in figures 1 and 2 show some similarity. The linear correlation between the patterns is 0.43. If the pressure change pattern is lagged one-half month the correlation is increased to 0.55; if the lag is extended a full month, the correlation drops to a value of 0.38. It should perhaps be emphasized that the best correlation between the change in sea level pressure and the change in gradient of radiation is not necessarily found at a lag of 2 weeks. If, for example, normal data were available for a period shorter than 1 month, the highest correlation might be found at a different lag; but it is not possible to determine the most suitable lag by the use of interpolated values. In general, however, it appears that at latitudes where the gradient of effective solar radiation is increased there is a tendency for the air to accumulate; where the northward gradient of radiation is decreased (or the southward gradient increased), air is removed. A marked discrepancy in the patterns of the two figures occurs at high latitudes in the late fall and early winter months, where a decrease in the radiation gradient is accompanied by a pressure rise. The longitudinal distribution of the monthly changes may be inferred by comparing figure 2 with the more detailed data in Brier's study of changes in the Northern Hemisphere sea level circulation [4].

The representation of the solar radiation and pressure

TABLE 1.—*Normal monthly change in northward gradient of effective solar radiation, cal. cm.$^{-2}$ min.$^{-1}$ (10° lat.)$^{-1}$*

North latitude	December to January	January to February	February to March	March to April	April to May	May to June	June to July	July to August	August to September	September to October	October to November	November to December
Degrees												
80	0.000	+0.011	+0.016	−0.020	−0.013	−0.001	+0.001	+0.010	+0.024	−0.014	−0.014	0.000
70	+.007	+.029	+.042	+.008	−.011	−.005	−.003	−.004	−.009	−.020	−.023	−.019
60	+.008	+.011	−.005	−.011	−.023	+.005	+.003	+.020	+.018	−.009	−.010	−.007
50	+.001	+.001	−.008	−.009	+.007	−.018	+.017	+.029	+.006	−.005	−.012	−.009
40	−.003	+.001	−.008	−.009	−.018	+.013	+.003	+.001	+.014	+.009	+.003	−.006
30	−.001	−.008	−.009	−.016	−.021	−.033	−.008	+.016	+.032	+.028	+.015	+.005
20	+.009	−.010	−.019	−.025	−.037	−.021	−.013	+.014	+.024	+.049	+.019	+.010
10	−.008	−.011	−.021	−.035	+.005	+.009	+.022	+.019	+.010	−.009	+.010	+.009
0	−.010	−.013	−.019	−.005	−.003	−.002	+.010	−.005	+.011	+.021	+.016	−.001

TABLE 2.—*Normal monthly change in sea level pressure, mb*

North latitude	December to January	January to February	February to March	March to April	April to May	May to June	June to July	July to August	August to September	September to October	October to November	November to December
Degrees												
90	−2.0	+2.0	+3.0	+1.0	−1.0	−4.0	−1.0	+1.0	−1.0	0.0	+2.0	0.0
80	−0.7	+1.2	+3.0	+0.1	−0.4	−2.4	−1.2	−0.3	−0.9	0.0	+2.0	+0.9
70	+0.2	+1.3	+1.2	−0.2	−0.3	−2.8	−1.4	−0.4	+0.8	−1.4	+1.4	+0.8
65	+0.7	+1.0	+0.4	−0.6	0.0	−2.5	−1.5	+0.4	+0.6	−0.3	+1.1	+0.7
60	+1.2	+0.7	−0.1	−0.8	−0.2	−1.9	−1.2	+0.4	+1.2	−0.3	+0.6	+0.4
55	+1.6	0.0	−0.4	−0.9	−0.7	−1.3	−0.5	+0.7	+0.9	−0.3	+0.3	−0.2
50	+1.5	−0.5	−0.6	−1.0	−1.1	−1.1	+0.1	+0.9	+2.0	+0.3	+0.1	−0.6
45	+1.1	−1.2	−0.6	−1.1	−1.1	−1.0	+0.5	+0.9	+1.9	+1.0	+0.3	−0.7
40	+0.5	−1.5	−0.6	−1.0	−1.2	−1.3	+0.8	+0.4	+1.8	+1.6	+0.8	−0.3
35	+0.4	−1.5	−0.8	−1.1	−1.3	−1.5	+1.5	+0.1	+1.6	+2.0	+1.6	0.0
30	+0.3	−1.3	−0.9	−1.4	−1.5	−1.5	0.0	−0.2	+1.4	+2.2	+2.7	+0.8
25	+0.4	−0.7	−1.2	−1.4	−1.6	−1.5	−0.4	−0.3	+1.2	+2.2	+2.1	+1.2
20	+1.0	−0.5	−1.2	−1.2	−1.3	−1.0	−0.6	−0.4	+1.8	+0.8	+1.7	+0.9
10	+0.6	−0.2	−0.5	−0.5	−0.3	−0.2	0.0	−0.7	+0.2	+0.2	−0.3	+0.6

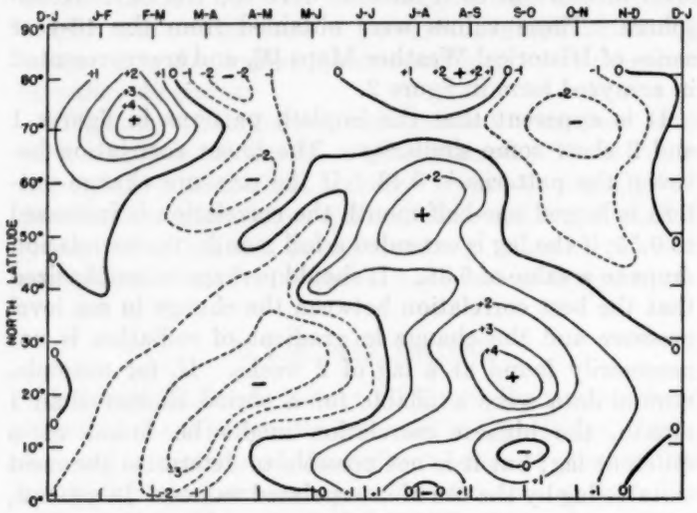

FIGURE 1.—Normal monthly change in northward gradient of effective solar radiation, 10^{-3} cal. cm.$^{-2}$ min.$^{-1}$ (10° lat.)$^{-1}$

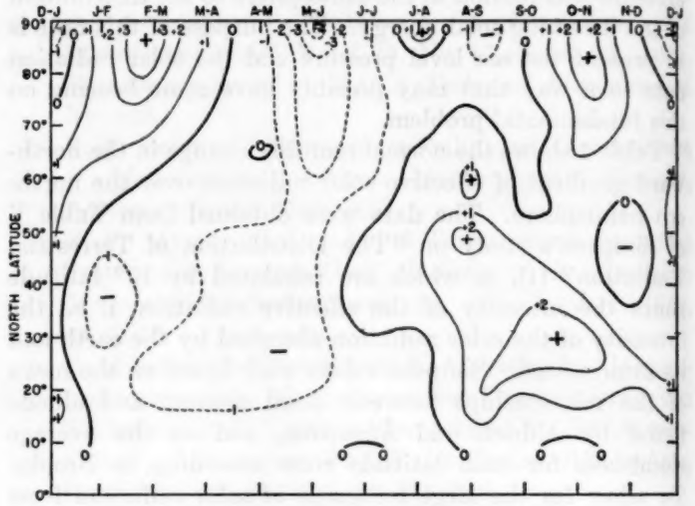

FIGURE 2.—Normal monthly change in sea level pressure, mb.

data in the form shown in figures 1 and 2, which appears to be novel, poses an interesting question, and it is for this reason the data are published.

REFERENCES

1. G. C. Simpson "The Distribution of Terrestrial Radiation," *Memoirs of the Royal Meteorological Society*, vol. III, No. 23, 1928, pp. 53–78.
2. S. Fritz, "Solar Radiant Energy and Its Modification by the Earth and Its Atmosphere", *Compendium of Meteorology*, American Meteorological Society, Boston, 1951, pp. 13–33.
3. U. S. Weather Bureau, *Historical Weather Maps, Northern Hemisphere, Sea Level*, 1899–1939, Washington, D. C.
4. G. W. Brier, "Changes in the Northern Hemisphere Sea Level Circulation in the 40-Year Period 1899–1939", *Transactions, American Geophysical Union*, vol. 29, No. 6, Dec. 1948, pp. 789–795.

THE UNPARALLELED THRALL, TEXAS RAINSTORM

GEORGE A. LOTT
Hydrologic Services Division, U. S. Weather Bureau, Washington, D. C.
[Manuscript received June 4, 1953]

INTRODUCTION

The largest observed rainstorm in the United States in terms of the depth-duration-area relation (see fig. 1) occurred at the fringe of the Edwards Plateau area of Texas on September 9–10, 1921. The purpose of this paper is to review this great storm as a matter of general interest and to present all the available data for use by those concerned with quantitative rainfall problems. This paper on the Thrall storm is one of a group on intense rainstorms which are important in American hydrologic work. The factors that produce heavy rainfall are probably more in evidence here in the great storms than in lesser more common ones.

Large flood-producing storms are more frequent over the Edwards Plateau and its escarpment than over any other area in the United States east of the 105th meridian [1]. The floods created by the torrential rains of the 1921 storm took 215 lives and caused $19,000,000 worth of property damage. Homes and crops were destroyed; bridges and railroad tracks were washed out; power and communication lines were crippled [2]. This was not only the largest storm of the Edwards Plateau group but also produced the highest official point-rainfall total recorded in the United States, 19.65 inches in 12 hours. An unofficial point-rainfall total, a record 32 inches in 12 hours, fell about 2 miles north of Thrall, Tex. This intense concentration of rain in both time and place caused unprecedented rises in the level of many streams. On the San Gabriel River the first rise, at midnight of the 9th, came as a 4-foot wall of water. Thereafter, the river

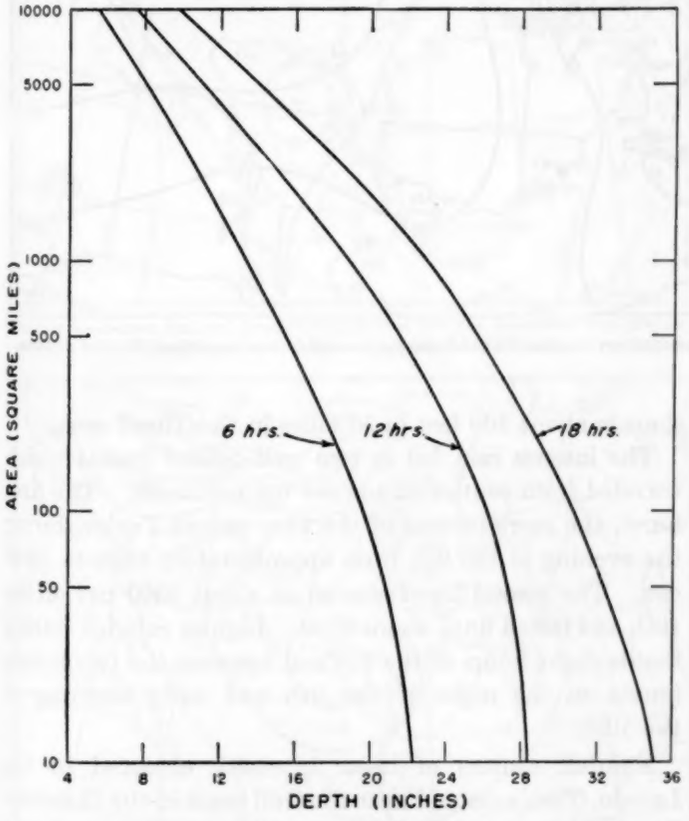

FIGURE 1.—Depth-duration-area curves for the Thrall, Tex., rainstorm during the period noon Sept. 8 to 1 p. m. Sept. 10 (local time), 1921.

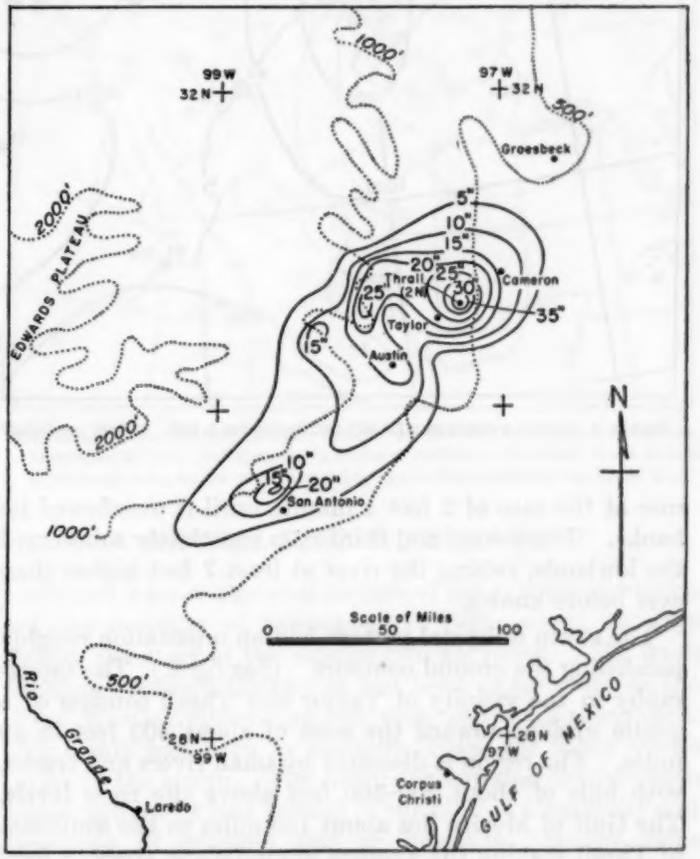

FIGURE 2.—Generalized isohyetal pattern (solid lines, in inches) for the Thrall, Tex., rainstorm, covering the period noon Sept. 8 to noon Sept. 10 (local time), 1921, superimposed on the ground contours (dotted lines, in feet). The intense rain fell in two bursts which traveled from the southwest to the northeast.

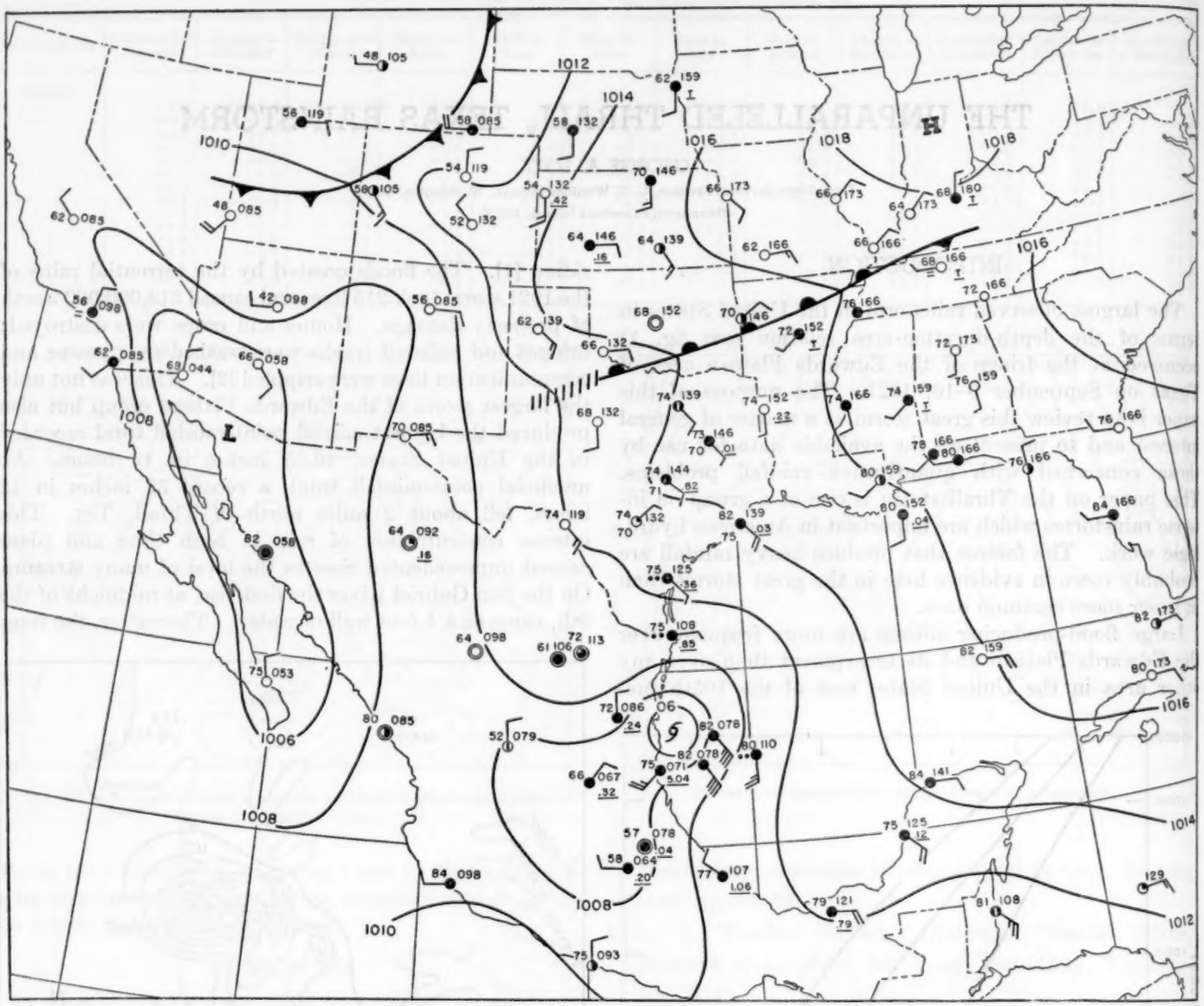

FIGURE 3.—Surface weather map for 0630 CST, September 7, 1921. 12-hour precipitation amounts are shown at United States stations and 24-hour amounts at Mexican stations.

rose at the rate of 2 feet a minute until it overflowed its banks. The second and third rises completely submerged the lowlands, raising the river at least 7 feet higher than ever before known.

The storm isohyetal pattern had an orientation roughly paralleling the ground contours. (See fig. 2.) The topography in the vicinity of Taylor and Thrall consists of a gentle upslope toward the west of about 500 feet in 50 miles. The region is dissected by small rivers and creeks, with hills of about 200–300 feet above the river levels. The Gulf of Mexico lies about 150 miles to the southeast of Thrall making the average ground-slope about 3 feet/mile from Thrall to the Gulf. In a southeast-northwest line (the approximate direction of gradient inflow wind at the time of beginning of heavy rain) the average land slope is about 300 feet in 50 miles in the Thrall area.

The intense rain fell in two well-defined bursts which traveled from southwest toward the northeast. The first burst, the more intense of the two, passed Taylor during the evening of the 9th from approximately 1900 to 2300 CST. The second burst started at about 0300 CST of the 10th and lasted until about 0700. Lighter rain fell during the daylight hours of the 9th and between the two heavy bursts on the night of the 9th and early morning of the 10th.

Rainfall centers of lesser intensity occurred in the Laredo, Tex., area and near the Gulf coast in the Houston-Beaumont region, but this study will concern itself almost exclusively with the Thrall center.

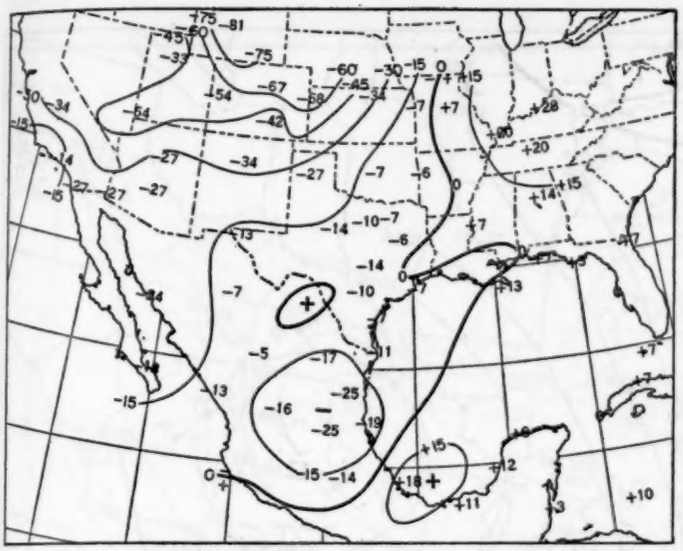

FIGURE 4.—24-hour sea level pressure change from 0700 CST, September 6 to 0700 CST, September 7, 1921. Isallobars are in tenths of millibars.

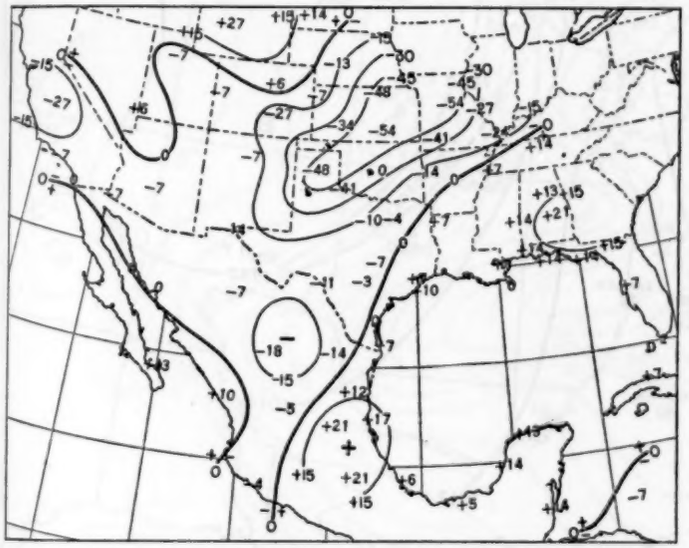

FIGURE 5.—24-hour sea level pressure change from 0700 CST, September 7 to 0700 CST, September 8, 1921. Isallobars are in tenths of millibars.

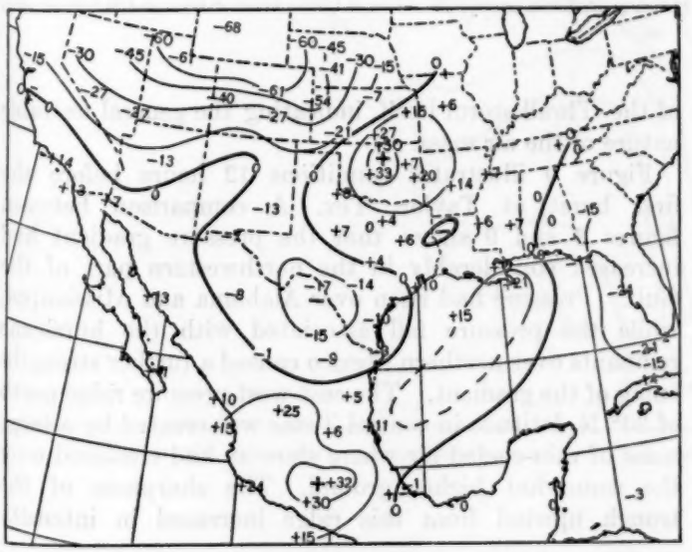

FIGURE 6.—24-hour sea level pressure change from 0700 CST, September 8 to 0700 CST, September 9, 1921. Isallobars are in tenths of millibars.

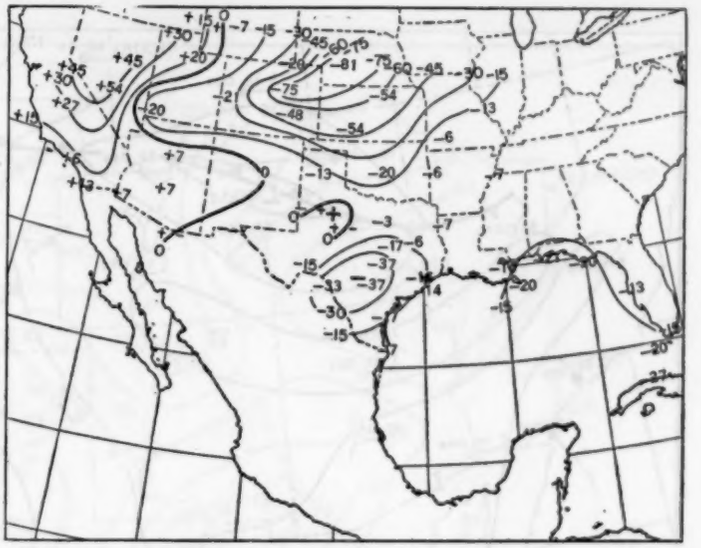

FIGURE 7.—24-hour sea level pressure change from 1900 CST, September 8 to 1900 CST, September 9, 1921. Isallobars are in tenths of millibars.

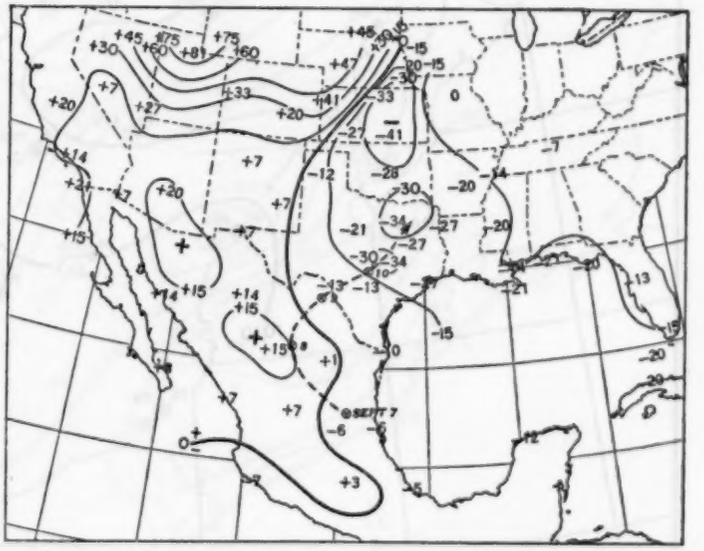

FIGURE 8.—24-hour sea level pressure change from 0700 CST, September 9 to 0700 CST, September 10, 1921. Isallobars are in tenths of millibars. The track of the 24-hour katallobaric center for the period covered by figures 4–8 is shown by the dashed arrow.

GENERAL SYNOPTIC SITUATION

Figure 3 gives a general picture of the synoptic situation on the morning of September 7, 1921, about 2½ days before the start of the intense rain at Thrall. The weak front in southern Oklahoma had been as far south as the Fort Worth-Abilene line but then retreated northward. No fronts had been in southern Texas for many weeks prior to the storm. The hurricane entering the Mexican coast in figure 3 had formed in the Gulf of Campeche and was not of unusual size or intensity. Heavy rains accompanied the storm near Tampico, however, and in the coastal range nearby. Although all traces of a surface circulation disappeared when the storm reached the Mexican Plateau, pressure falls could be followed through this region and on into southern and central Texas. Figures 4–8 are 24-hour pressure change charts covering

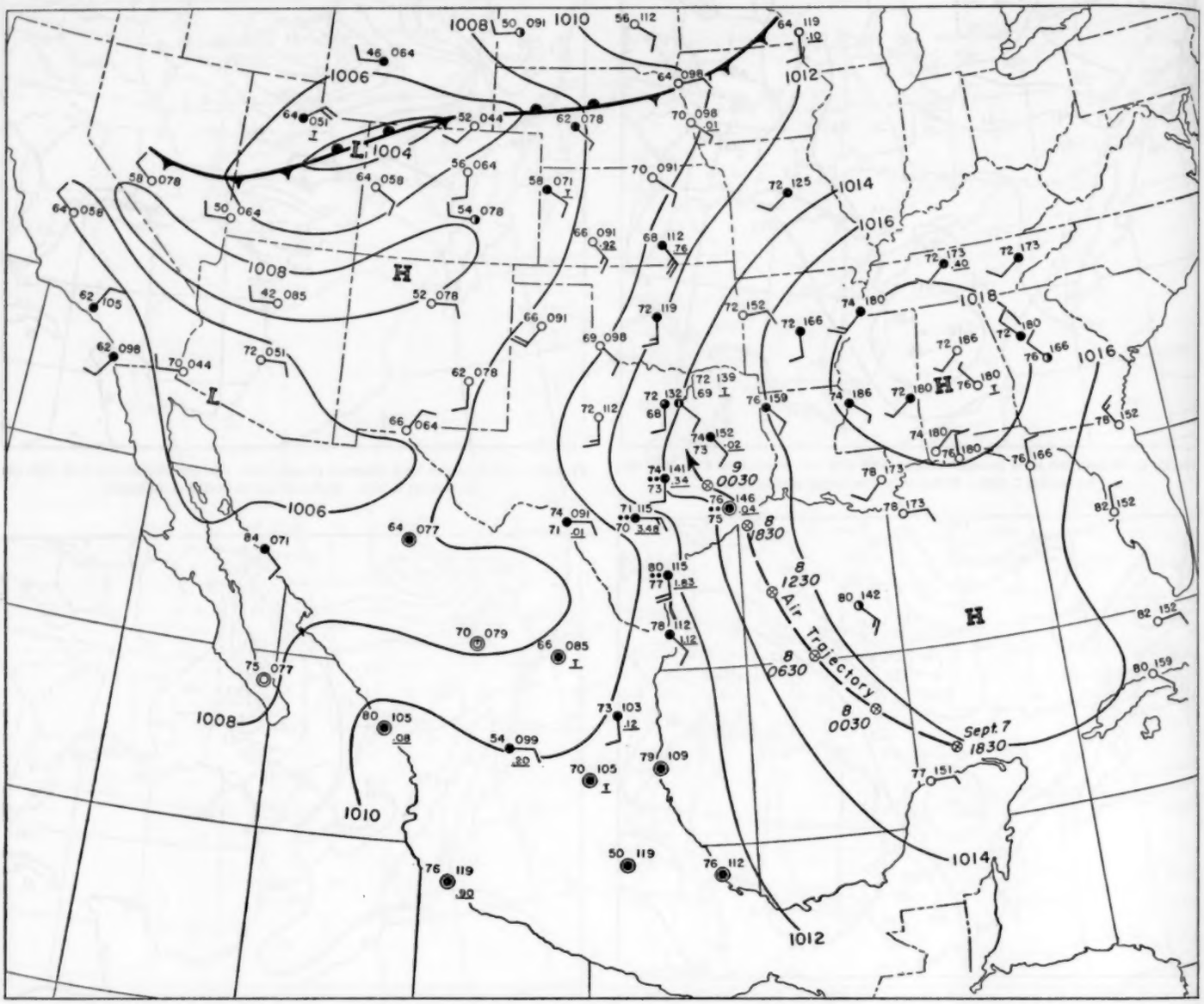

FIGURE 9.—Surface weather map for 0630 CST, September 9, 1921. The air trajectory from 1830 CST, September 7 to 0630 CST, September 9, shown by the dashed arrow, indicates the tropical maritime source of the air in the ridge in the Taylor-Groesbeck area of Texas. 12-hour precipitation amounts are shown at United States stations, and 24-hour amounts at Mexican stations.

the period September 6–10, with the path of the katallobaric center plotted on figure 8. It can be seen on this figure (in the United States where the station density is greater) that the center was double. The cause of the double nature of the center has not been ascertained, but its effect on the rainfall distribution with time was very marked. The two bursts of the Thrall storm occurred with the passage of these two fall centers.

Rain showers progressed northward over eastern Texas on the morning of September 7 reaching the San Antonio-Taylor-Groesbeck area early on the afternoon of the 7th. Scattered showers and thunderstorms were observed throughout the moist southerly current over southern and central Texas from this time until the climactic bursts of the Thrall storm itself, indicating the general unstable nature of the air mass.

Figure 9 illustrates conditions 12 hours before the first burst at Taylor, Tex. A comparison between figures 3 and 9 shows that the pressure gradient had increased considerably in the northwestern part of the Gulf. Pressure had risen over Alabama and Mississippi, while the pressure fall associated with the hurricane remnants over northern Mexico caused a further strengthening of the gradient. The east-west pressure ridge north of 30° N. latitude in central Texas was created by a large mass of rain-cooled air where showers had clustered over the somewhat higher ground. The sharpness of the trough upwind from this ridge increased in intensity

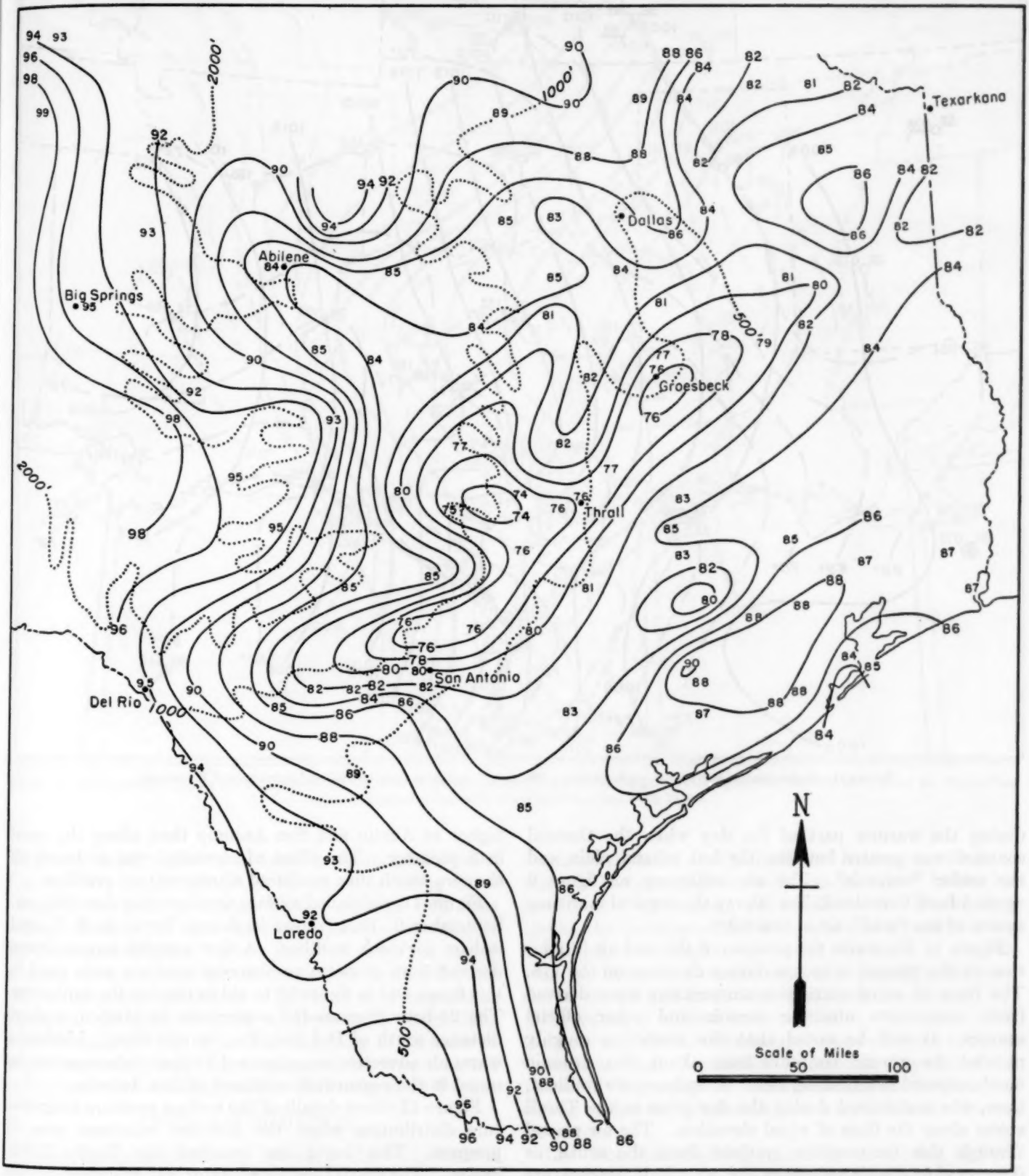

FIGURE 10.—Maximum temperature isotherms (solid lines, ° F.) for September 9, 1921, in relation to the ground contours (dotted lines, feet).

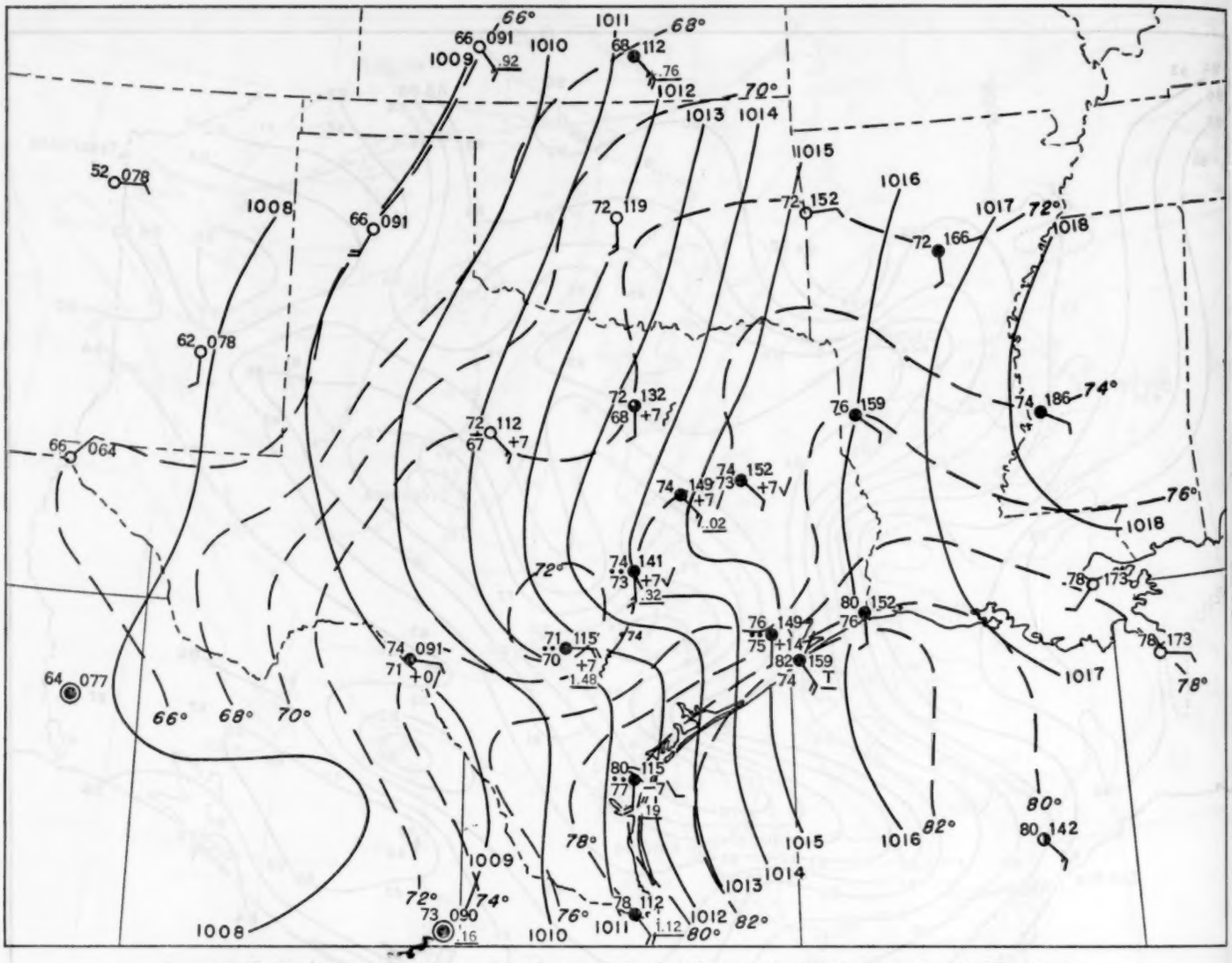

FIGURE 11.—Surface weather map for 0630 CST, September 9, 1921, showing isobars at 1-mb. intervals and isotherms at 2° F. intervals.

during the warmer part of the day when the thermal contrast was greater between the hot coastal plain and the cooler "uplands". The air trajectory on figure 9 upwind from Groesbeck, Tex. shows the tropical maritime source of the "cool" air in this ridge.

Figure 10 illustrates the position of the cool air in relation to the ground contours during daytime on the 9th. The lines of equal maximum temperature were derived from cooperative observer records and other official sources. It will be noted that the isotherms roughly parallel the ground contours from about San Antonio northeastward to Palestine, Tex. A temperature gradient, then, was maintained during the day prior to the Thrall storm along the lines of equal elevation. The air passed through this temperature gradient from the south, as illustrated in the air trajectory (fig. 9). This temperature gradient was only indirectly due to the effect of elevation, since maximum temperatures average several degrees higher at Austin and San Antonio than along the coast in September. The effect of elevation was to touch off showers which then produced a temperature gradient.

Figure 11, a detailed surface weather map for 0630 CST, September 9, 1921, shows isotherms for each 2° F. and isobars for each millibar. A few current temperatures derived from cooperative observer readings were used in this figure and in figure 12 to aid in placing the isotherms. The 24-hour pressure-fall center was in Mexico, a short distance south of Del Rio, Tex. at this time. Moderate warm air advection accompanied by heavy showers can be noted in the region just southeast of San Antonio.

Figure 12 shows details of the surface pressure-temperature distribution when the heaviest rainburst was in progress. This burst had reached the Taylor-Thrall region. The small Low near Taylor was the result of the pressure fall that originated from the Tampico hurricane. This Low was traveling northeastward and resulted in

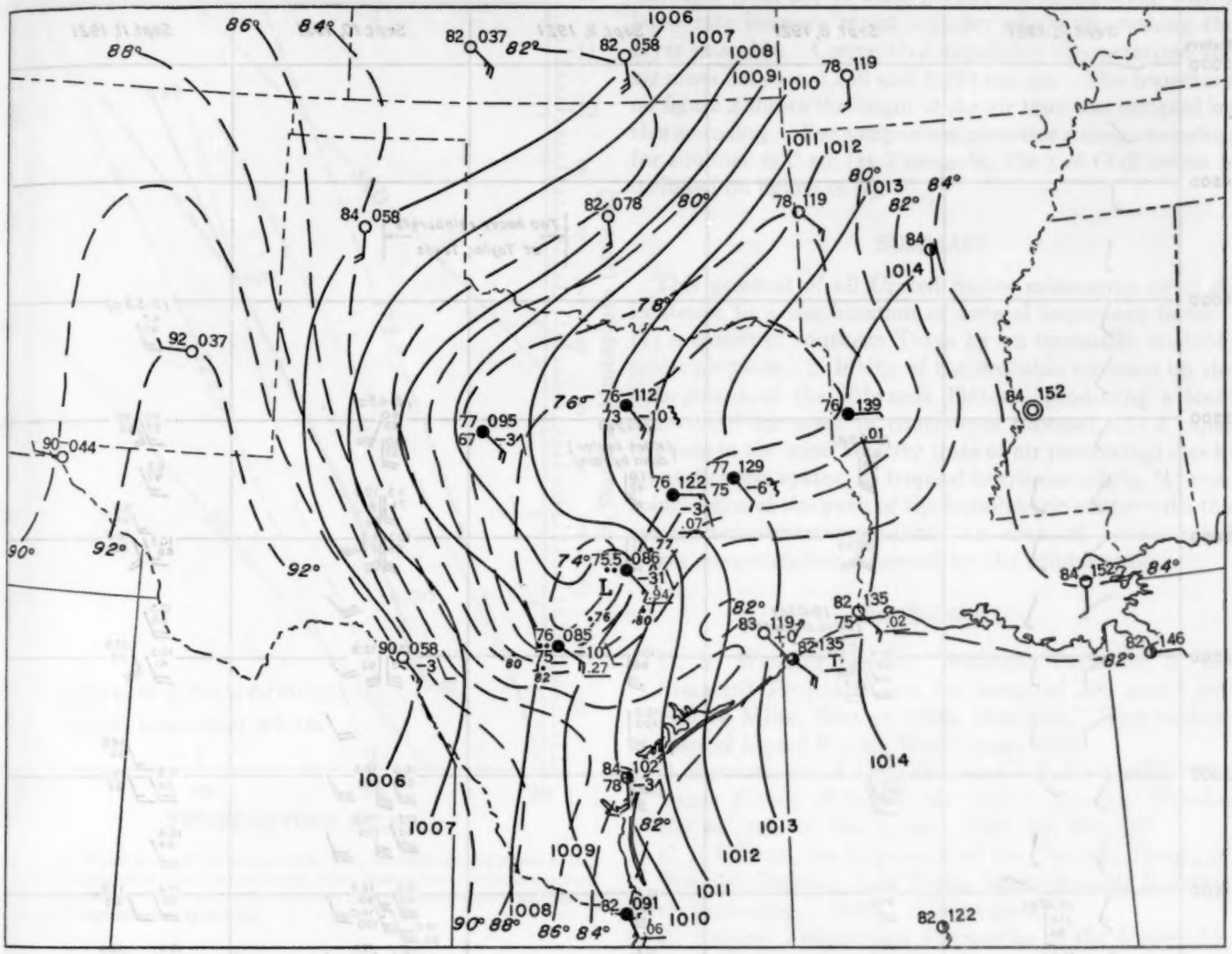

FIGURE 12.—Surface weather map for 1830 CST, September 9, 1921, showing the pressure-temperature distribution at the time the heaviest rainburst had reached the Taylor-Thrall area. The area of strong warm air advection is centered near Taylor.

temporary wind shifts to a westerly component at Del Rio, San Antonio, and Taylor. The area of strong warm air advection centered near Taylor on this map was closely associated in time and place with the beginning of the monumental burst. (For a development of the theory of warm advection as a cause of vertical motion see Gilman [3].) Heavy rain continued to fall for 3 or 4 hours after the warm advection started to decrease in magnitude. A much smaller drop in pressure resulting in an increase in gradient winds from the south-southeast was observed to accompany the second burst at about 4 a. m. at Taylor.

UPPER AIR SITUATION

Upper air data were very sparse in the early 1920's. The kite sounding and winds aloft station at Groesbeck, Tex., 75 miles northeast of the rainfall center, was the only one in operation during the storm period within many hundreds of miles of Thrall, Tex. During the 24 hours prior to the storm, Groesbeck was immersed in the low level "cool" air (see fig. 11) similar to the Taylor area. Unlike the storm area, however, the cool air surrounding Groesbeck was swept away during the night of the 9th-10th, probably as a consequence of a generally less steep rise in the ground level downwind from Groesbeck.

Figure 13 is a time cross-section of the upper wind, temperature, and relative humidity observations taken at Groesbeck from September 7 through September 11. Times of beginning of ascent, maximum height, and ending of descent (if observations were taken on descent) are given.

The Groesbeck morning soundings on the 8th and 9th were characterized by coldness, considering the time of year. The observed temperatures at the 3-km. level on both days are exceeded on 85 to 90 percent of the days in September

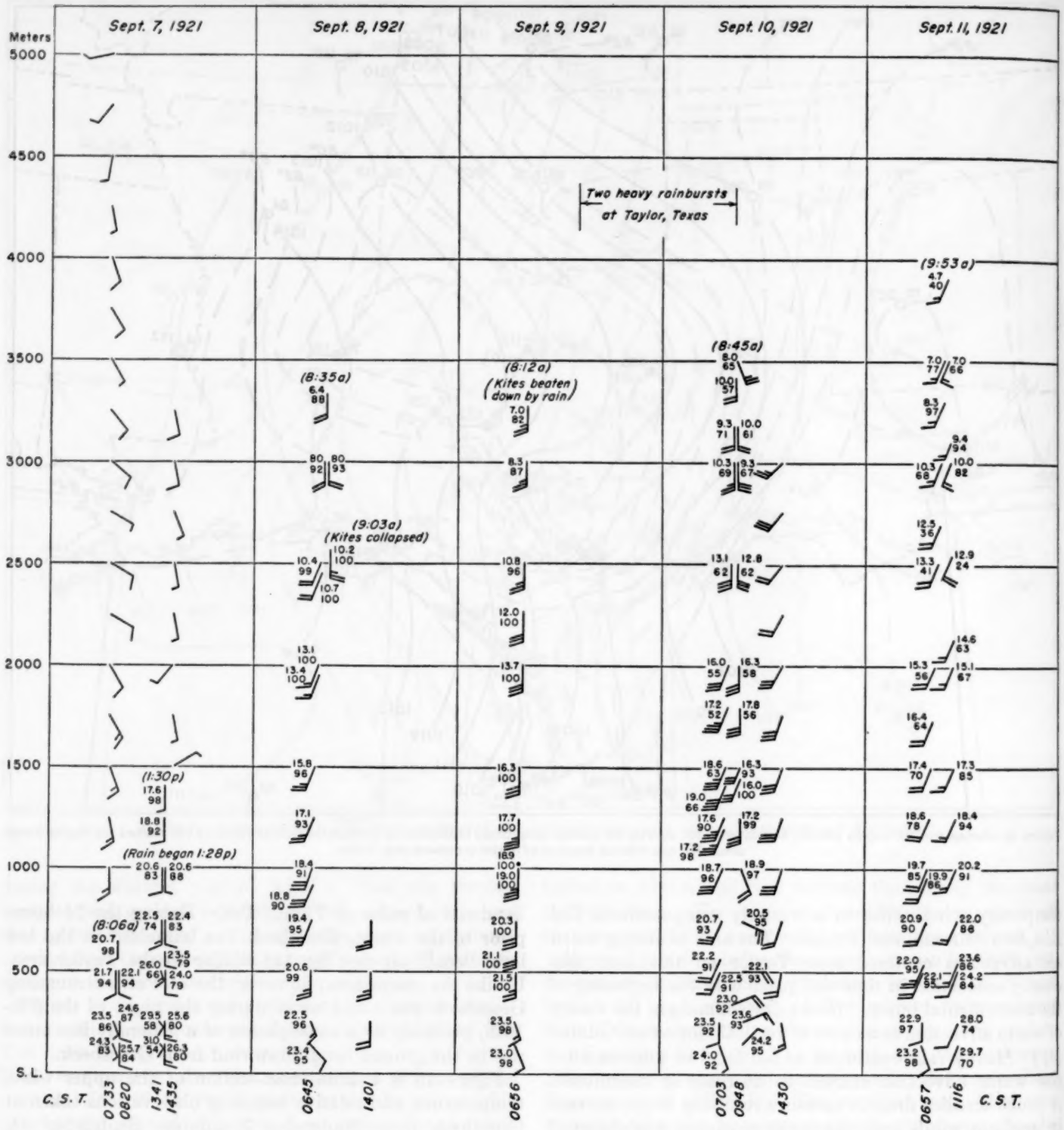

FIGURE 13.—Time cross-section of the upper wind, temperature, and relative humidity observations at Groesbeck, Tex., September 7–11, 1921. A full wind barb indicates a value of 10 m. p. h.

[4]. The moisture content in the layer between the surface and 3 km. was high on the 9th (1.65 in. of precipitable water) but it was by no means a record. The mean September precipitable water in the Groesbeck, Tex., area is about 1.05 in. and the maximum of record about 1.99 in.

[5]. Below the 1.25-km. level little change in the air mass properties is evident in the 48-hour period starting at 0700 CST on September 8. Above this level, however, the sounding on the morning of the 10th shows warming and drying accompanied by a wind shift from southerly to

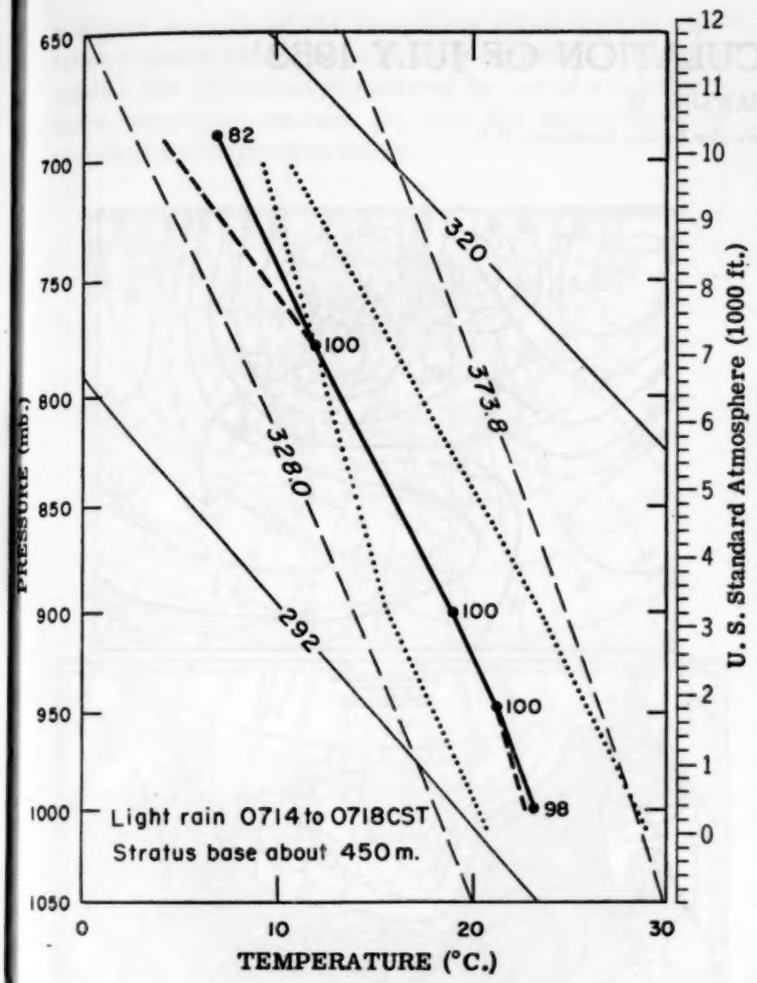

FIGURE 14.—Upper air sounding at Groesbeck, Tex., 0656–0812 CST, September 9, 1921, showing temperature (solid line) and dew point (dashed line). Numbers indicate relative humidity. The dotted temperature and humidity curves show a mean sounding for summer mT air of Gulf origin.

south-southwesterly. The bringing in aloft of drier air from the Mexican highlands was responsible for the abrupt cessation of rainfall over central Texas on the 10th.

An interesting feature of the wind record is the maximum at the 3,000–4,000-foot level as shown in the 24 hours from the morning of the 9th to the morning of the 10th. (The heavy rain occurred at Taylor and Thrall between these observation times.) A wind maximum at this level has been found in many of the greatest rainstorms of record [6].

The Groesbeck sounding for the morning of the 9th appears in figure 14. The air was completely saturated in the layer from 500 to 2,250 meters above sea level, with a lapse rate between moist and dry adiabatic, making the layer unstable. Convective instability characterized the air mass between 2,250 and 3,250 meters. The trajectory on figure 2 shows the origin of the air that was sampled by this sounding. For comparison purposes a mean sounding for summer mT air (at Pensacola, Fla.) of Gulf origin is included on figure 14 [7].

SUMMARY

This greatest of all United States rainstorms owed its existence to a combination of several important factors: (1) invasion of southern Texas by an unusually unstable moist air mass, (2) lifting of the unstable air mass up the escarpment of the Edwards Plateau, producing a local rain-cooled air mass (a continuous process), (3) a rapid increase in the wind velocity (rate of air processing) due to a katallobaric system of tropical hurricane origin, (4) near coincidence of the path of the katallobaric center with the strong temperature gradient, an area of concentrated warm advection being formed by the combination.

REFERENCES

1. U. S. Weather Bureau, "Seasonal Variation of the Standard Project Storm for Areas of 200 and 1,000 Square Miles, East of 105th Meridian," *Hydrometeorological Report* No. 29, Washington, 1953.
2. B. Bunnemeyer, J. H. Jarboe, and J. P. McAuliffe, "The Texas Floods of September 1921," *Monthly Weather Review*, vol. 49, No. 9, Sept. 1921, pp. 491–497.
3. C. S. Gilman, An Expansion of the Thermal Theory of Pressure Changes, ScD Thesis, Massachusetts Institute of Technology, 1949. (Unpublished.)
4. B. Ratner, *Temperature Frequencies in the Upper Air*, U. S. Weather Bureau, Washington, 1946.
5. A. L. Shands, "Mean Precipitable Water in the United States," Weather Bureau *Technical Paper* No. 10, Washington, April 1949.
6. G. A. Lott, "An Extraordinary Rainfall Centered at Hallett, Okla.," *Monthly Weather Review*, vol. 81, No. 1, Jan. 1953, pp. 1–10.
7. H. C. Willett, "Characteristic Properties of North American Air Masses," Contribution pp. 73–108 to *An Introduction to the Study of Air Mass and Isentropic Analysis*, by Jerome Namias, American Meteorological Society, Milton, Mass., Oct. 1940.

THE WEATHER AND CIRCULATION OF JULY 1953[1]

HARRY F. HAWKINS, JR.

Extended Forecast Section, U. S. Weather Bureau, Washington, D. C.

DISAPPEARING DROUGHT

Last month was the second successive June with record breaking drought and heat [1]. Consequently, attention during July was focused upon the critical drought area. On July 6, the *Weekly Weather and Crop Bulletin* stated: "The drought is most severe in Arkansas, Oklahoma, and the extreme western and extreme southern portions of Texas where the total rainfall for the last 7 weeks was mostly less than 10 percent of normal." It was also extremely dry in Arizona and southern Utah where the usual summer "Arizona Rains" [2] had yet to make their appearance.

FIRST DECADE OF JULY

Although early July saw the intensification of heat and drought over the Southwest, by the end of the first decade some relief occurred. Figure 1 shows the 700-mb. contours together with the temperature and precipitation anomalies for the first 10 days of July. The mean heights (fig. 1-A) are similar to those for the month of June in the location of troughs off either coast of the United States and the high over the Lower Mississippi Valley. However, the weakening and filling of the west coast trough led to a less well-defined ridge system over the central United States. As a result, cold air began to penetrate this area via the Northern Plains, as might be expected from the strength of the western Canadian ridge.

Figure 1-B shows that for July 1–10 the mean temperatures averaged below normal as far south as central Kansas where June temperatures had averaged as much as 8° F. above normal. As the weakened upper level High began to split, this cooling proceeded southward reaching southern Louisiana by the end of the decade. Nevertheless, over much of the drought area temperatures averaged well above normal for this period.

Precipitation (fig. 1-C) shows the results of the weakening of anticyclonic circulation aloft and the renewal of frontal activity. In areas of convergence associated with the movement of fronts and cyclones sensible relief was effected mainly by shower activity. However, no measurable rain was recorded in extreme southern and extreme western Texas, eastern New Mexico, and southern Colorado, while precipitation was well below normal in the Lower Mississippi Valley. Summer showers in the Far Southwest started to become effective as the drought regime weakened. Ely, Nev., and Salt Lake City, Utah, reported over 200 percent and 175 percent, respectively, of the normal 10-day precipitation amounts. Figure 1-C

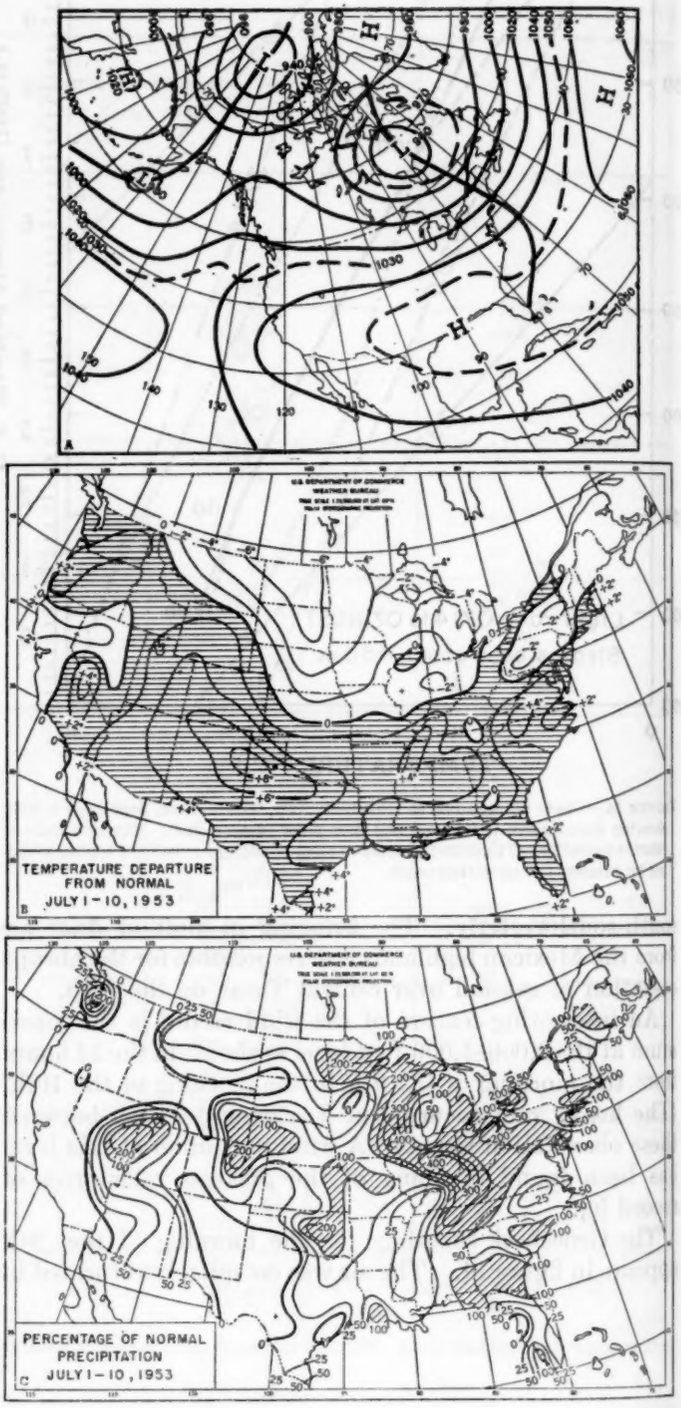

FIGURE 1.—Means for July 1–10, 1953. A. 700-mb. heights in tens of feet. Blocking in Bering Sea and cyclogenesis in the Gulf of Alaska led to filling of west coast trough and weakening of United States drought-producing ridge. B. Mean temperature departures from normal. Cooling has already invaded the Central Plains as United States ridge weakened. Drought area remained hot. C. Precipitation departure from normal showing the first significant precipitation of the mid-Plains and the initiation of the summer "Arizona Rains." Hatched area indicates areas with precipitation greater than 100 percent of normal.

[1] See Charts I–XV following page 216 for analyzed climatological data for the month.

is a good example of the complexity of summer precipitation patterns which reflect the showery nature of summer rainfall, the difficulties engendered by use of a relatively coarse rain gage network [3], and the employment of cumulative precipitation totals.

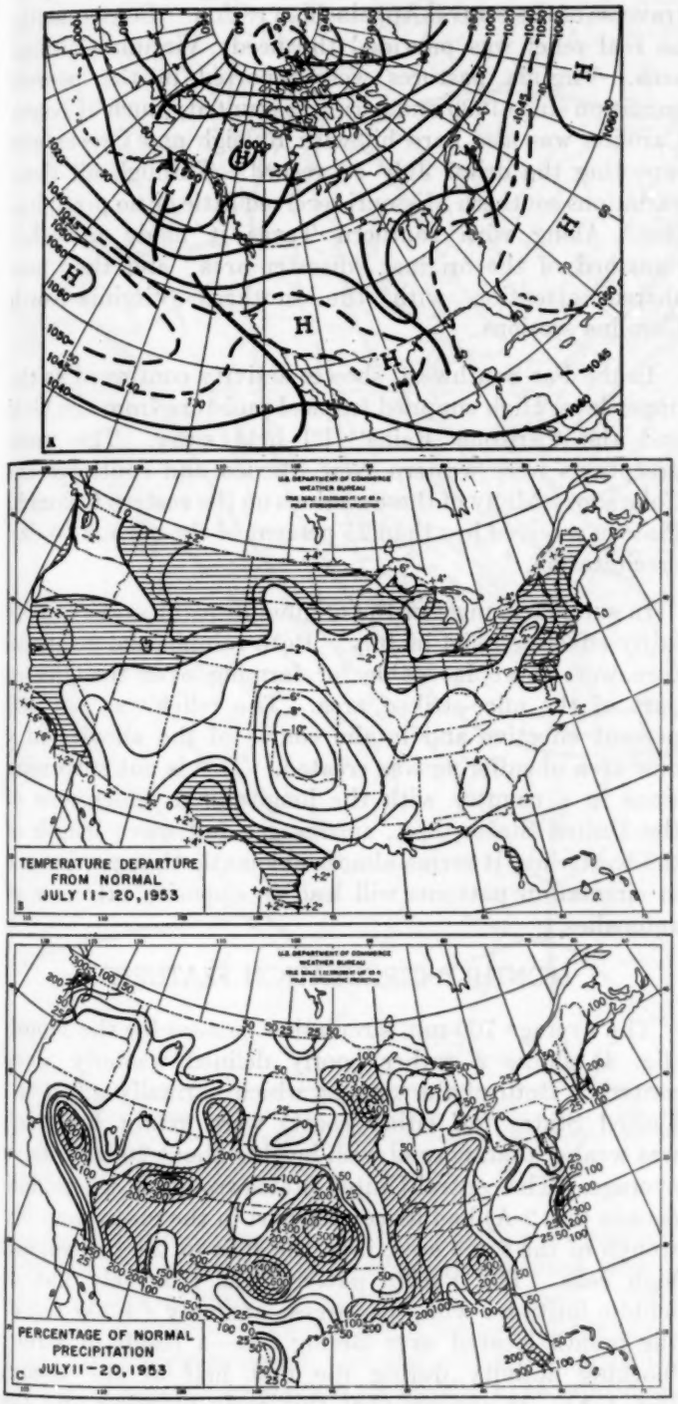

FIGURE 2.—Means for July 11–20, 1953. A. 700-mb. heights in tens of feet. Contours show trough development over central United States as west coast trough disappears. Note change in phase of westerly wave pattern from June [1] or figure 1-A and figure 3-A. B. Mean temperature departures from normal. Cool air dominates the Central Plains (in local reversal of June's heat) where cyclonic circulation aloft and persistent cloudiness prevail. C. Precipitation departure from normal. Continued drought relief over much of the Central and Lower Plains. Western showers continue. Virginia and North Carolina become increasingly dry under mean ridge.

SECOND DECADE

It was during the second decade of July that the most effectual relief arrived for the main drought areas. Figure 2-A shows the reversal of the 700-mb. circulation pattern when compared to June [1] or July 1–10 (fig. 1-A). The troughs off either coast weakened still further while the ridge formerly over the Lower Mississippi Valley was replaced by a marked trough over the Central Plains. This reversal in circulation was accompanied by pronounced cooling and fairly copious rainfall over large portions of the South Central Plains.

As shown in figure 2-B, Oklahoma, averaging 8° to 10° F. below normal, was the center of the cool anomaly. Below normal temperatures extended over the Central and most of the Southern Plains in a striking contrast to the heat of June and early July.

Precipitation was not everywhere abundant, but figure 2-C shows significant relief over most of the drought area. These rains, the result of frontal and air mass shower activity, were accompanied by considerable cloudiness which was an important factor in the below normal temperatures noted in figure 2-B. Continuation of shower activity over Arizona and adjacent regions restored most ranges to something approaching normal conditions. In spite of this, the persistent vagaries of summer showers left significant areas of the Panhandle, southern Texas, and southern Missouri-northern Arkansas critically dry.

Less fortuitous was the location of the mean ridge over the central Appalachians (fig. 2-A). This feature precluded sizable precipitation amounts over central areas of southern Virginia and North Carolina. Precipitation totals in these regions were from 0 to 10 percent of the normal amounts. Four-week precipitation totals (preceding July 20) were only 20 to 50 percent of normal. Rainfall deficiency plus normal July heat were establishing a new drought area. In fact, practically all miscellaneous crops in the Atlantic Coastal region from South Carolina to New York were reported suffering from lack of rain.

THIRD DECADE

As shown in figure 3-A, during the third decade there was a definite tendency for return of the circulation to a pattern like that of June and earlier July. The High once more became established over the southern Mississippi Valley after the mid-United States trough had worked its way eastward to the Atlantic Coast. The lower extremity of this trough trailed back toward the Delta region while the northeastern Gulf of Mexico was the scene of several (westerly moving) easterly waves.

In figure 3, sections B and C show the effects of this transition upon the anomalies of temperature and precipitation. Warming was slow over the South Central and Southeastern States with the 10-day averages near, to below, normal. The anticyclonic circulation of continental air resulted in above normal temperatures from the Central Plains eastward to Virginia and North

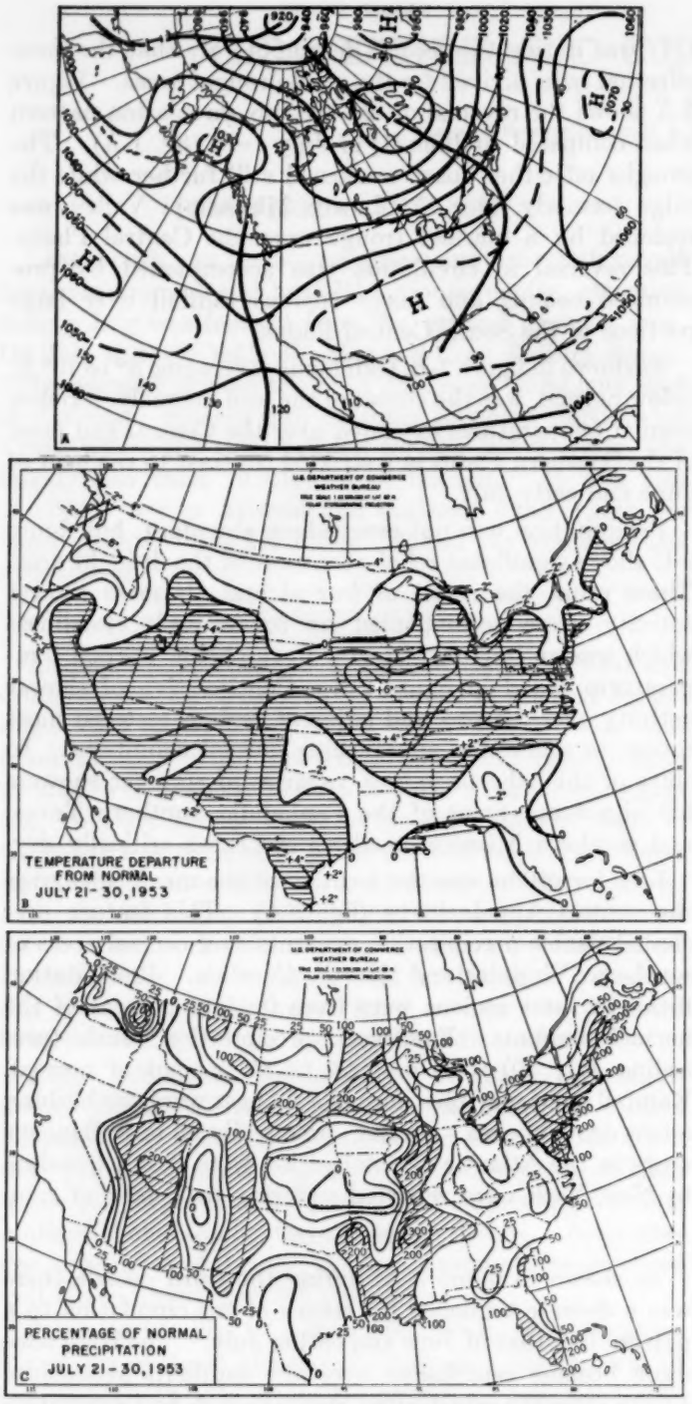

FIGURE 3.—Means for July 21–30, 1953. A. 700-mb. heights in tens of feet. Return to previous 700-mb. circulation pattern as central United States trough (fig. 2-A) moved east. B. Mean temperature departures from normal. Slow warming in southern Plains, continued heat in the mid-Appalachians. C. Precipitation departure from normal. Decreasing precipitation in southern Plains as pattern reverted toward that of June. Rains from Mississippi River to Appalachians occurred early in period as trough moved eastward. Continued rains over western ranges.

Carolina. During all three of these periods southern Texas averaged above normal and the monthly positive departure there (see Chart I) was the largest in the entire United States.

Ten-day precipitation anomalies (fig. 3-C) also reflect this transition in circulation pattern. The Central Plains received less than 25 percent of normal rainfall. Precipitation between the Mississippi Valley and the Appalachians was almost entirely an early period occurrence, most of the rain falling as the mid-United States trough (fig. 2-A) migrated eastward. Unfortunately, the trough accelerated as its downstream profile flattened during its traverse of the central Appalachian region. Consequently no real relief was provided the needy Virginia-Carolina area. Virginia pastures were reported in the poorest condition since 1930 and corn was stunted; much of North Carolina was also hard hit with Raleigh and Greensboro reporting the driest July on record. Through all these variations southern Missouri received little or no precipitation. Along with southern Texas it made up what remained of the original "disaster area" and they now shared attention with the southern Virginia-North Carolina sections.

In the Far Southwest, shower activity continued as the upper level High supplied tropical moisture from the Gulf and the "Arizona Rains" [2] held sway. The main exceptions were western New Mexico and southwestern Colorado. Many of these sections on the eastern Colorado Plateau received less than 25 percent of the normal 10-day precipitation.

In summary, most of the original drought area received fairly effective relief in July. Both rainfall and temperature were more favorable for farming over the greater part of the once-striken area. The relief was not 100 percent effective and in the course of the alleviation a new area of suffering was created. This is not surprising since in a country with the longitudinal dimensions of the United States, i. e., spanning a full wave length of the westerlies, it seems almost axiomatic that persistence in circulation patterns will lead to opposite extremes of anomalies.

MONTHLY CIRCULATION FEATURES

The average 700-mb. circulation pattern for the month (fig. 4) shows a rather poorly defined westerly wave pattern. Both of the troughs which normally affect the United States (off either coast) were extant but each was weaker than normal with heights about 70 feet above average. The central United States trough of the middle decade (fig. 2-A) had its counterpart in the mean monthly trough of the same area, i. e., the split in the subtropical high cells. The Pacific pattern was relatively flat at middle latitudes with the largest anomaly (+300 ft.) of the month located over Bering Sea—a result of strong blocking activity during the first half of the month (fig. 1-A). It appears that this early blocking and the typical cyclonic intensification to its southeast can be readily associated with the filling of the west coast trough and may, therefore, be a teleconnection in the breaking of the United States drought.

An integral part of this pattern was an unusually strong polar vortex. This center of action was a per-

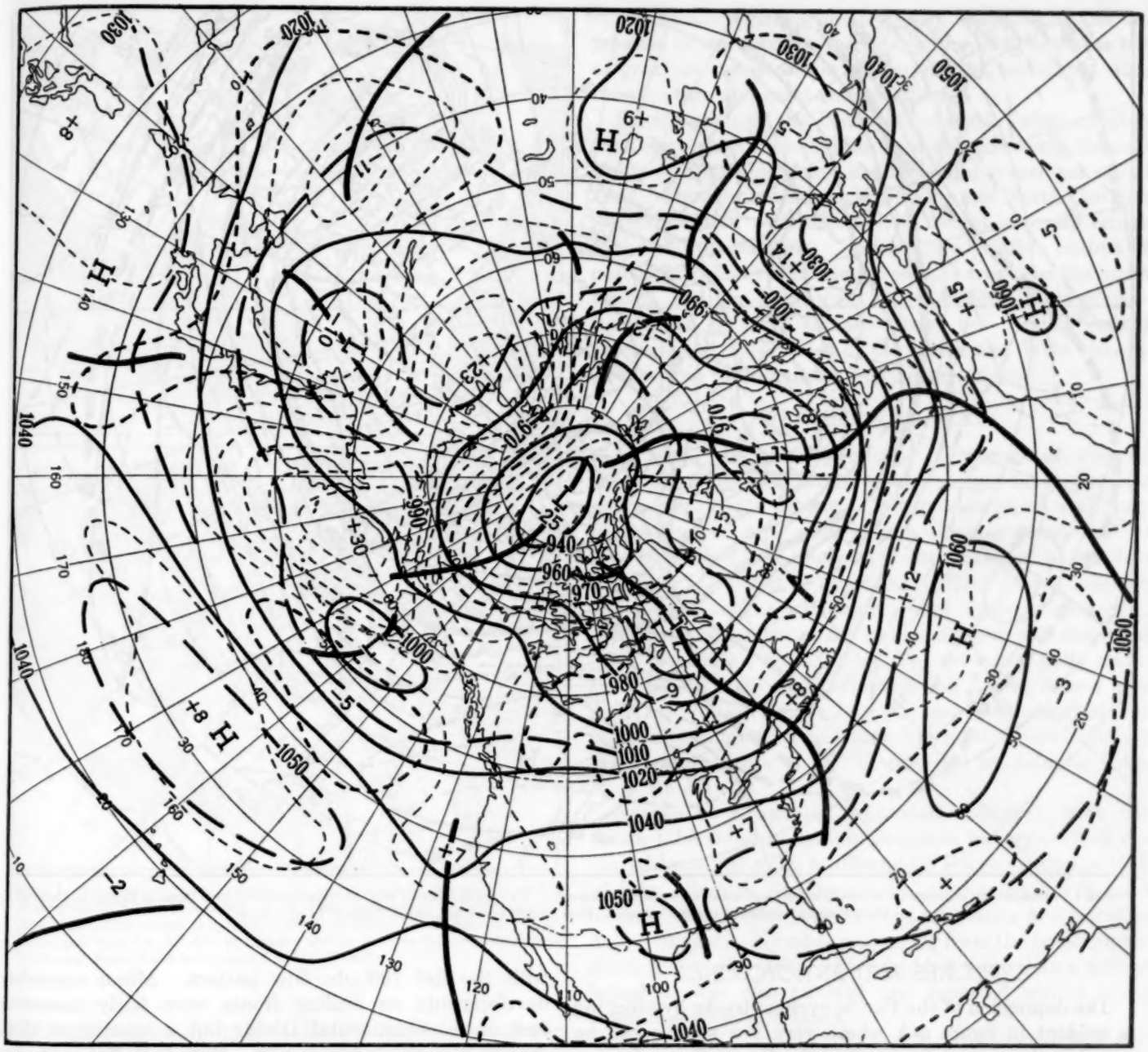

FIGURE 4.—Mean 700-mb. height contours and departures from normal (both in tens of feet) for June 30-July 29, 1953. Weakening and splitting of subtropical anticyclone over south-central United States (see June 1953 [1]) and poorly defined coastal troughs were indicative of transitions. Well developed Arctic vortex (−250 ft.) and Bering Sea blocking (+300 ft.) were major abnormalities in otherwise flat pattern.

sistent abnormal feature of the month's circulation. The 250-foot departure from normal associated with it was the largest negative anomaly on the map. These high latitude vortices are important features of the circulation since their extension into and connections with the mid-latitude westerly wave train usually have immediate effect upon the train itself.

Very similar features can be noted at the 200-mb. level (fig. 5). Most of the 700-mb. characteristics were readily identifiable at this (40,000-foot) level. The striking exceptions were the disappearance (or tremendous displacements) of the subtropical oceanic anticyclones at higher levels. Geostrophic wind speeds (isotachs dashed in fig. 5) at 200 mb. showed a well marked, almost zonal, wind speed maximum which was located between 40° and 45° N. over most of the Pacific and between 45° and 50° N. elsewhere. The United States and Atlantic sectors of the maximum were in good agreement with the "normal" location of the jet stream [4]. However, the Pacific maximum appeared to be slightly farther north than "normal" with two centers of maximum velocity separated by the longitudes most affected by blocking. To the north, an Arctic maximum was clearly discernible between 70° and 75° N.

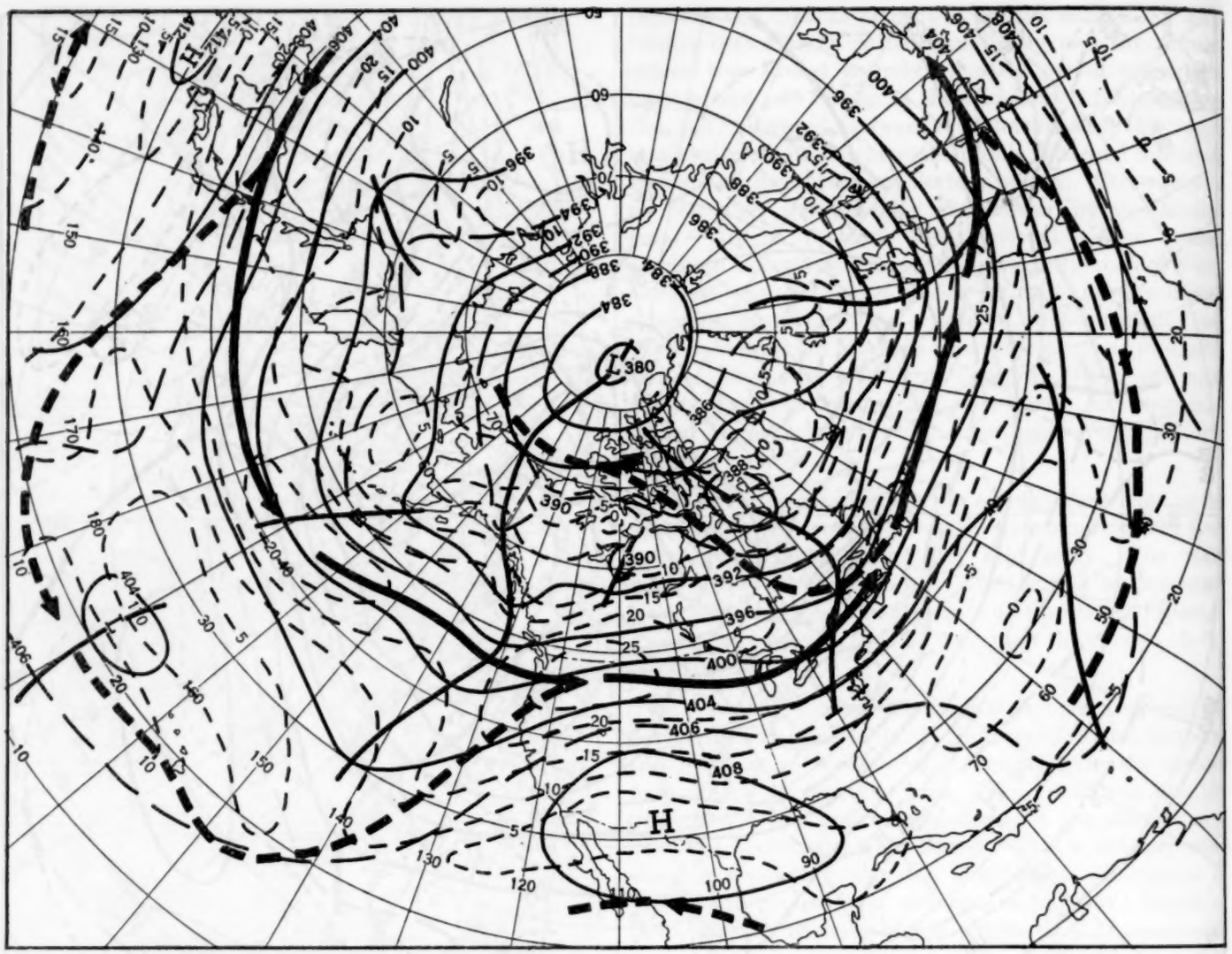

FIGURE 5.—Mean 200-mb. contours (in hundreds of feet) and isotachs (in meters per second). Well-developed west wind maximum extended from Japan to Europe at about 45° N. Arctic maximum indicated in polar latitudes. Note troughs above mid-oceanic Highs in Tropics (fig. 4).

CYCLONES AND ANTICYCLONES

The depression of the Pacific cyclone tracks by blocking is evident in figure 6-A where very few storms can be noted in their usual rendezvous, the Bering Sea. During much of July, the Gulf of Alaska and adjacent regions served this purpose while blocking Highs dominated the Bering Sea. Further evidence of this displacement can be found in the monthly mean sea level map and its departure from normal, Chart XI. Pressures averaged 4 mb. below normal just south of the Gulf of Alaska, and 7 mb. above normal in the western Bering Sea. Arctic cyclones associated with the polar vortex are also indicated both on the track map and the sea level departure from normal which averaged 11 mb. below normal at the Pole (not shown).

The major North American storm track lay about 10° north of the west wind maximum (fig. 5). Most of the trajectories were of a zonal west-to-east nature in accord with the flat 700-mb. flow pattern. Minor secondary developments on trailing fronts were fairly numerous east of the Continental Divide but a number of them dissipated more or less *in situ*. With fast, flat westerlies on across the Atlantic (fig. 4) many of the perturbations of eastern Canada travelled rapidly across the Atlantic in the well-marked channel north of the maximum westerly winds.

Anticyclonic intrusions into the United States were quite frequent for July. These Highs showed a marked preference for invasion of the United States through the Northern Plains usually turning southeastward through the Eastern Lakes. When the polar vortex was strong, surges of mP air entered western Canada and drifted southeastward as indicated in figure 6–B. Following the peaks of Arctic activity, anticyclones of Arctic origin passed eastward or southeastward along one of the branchings indicated in the far north. Only occasionally did the

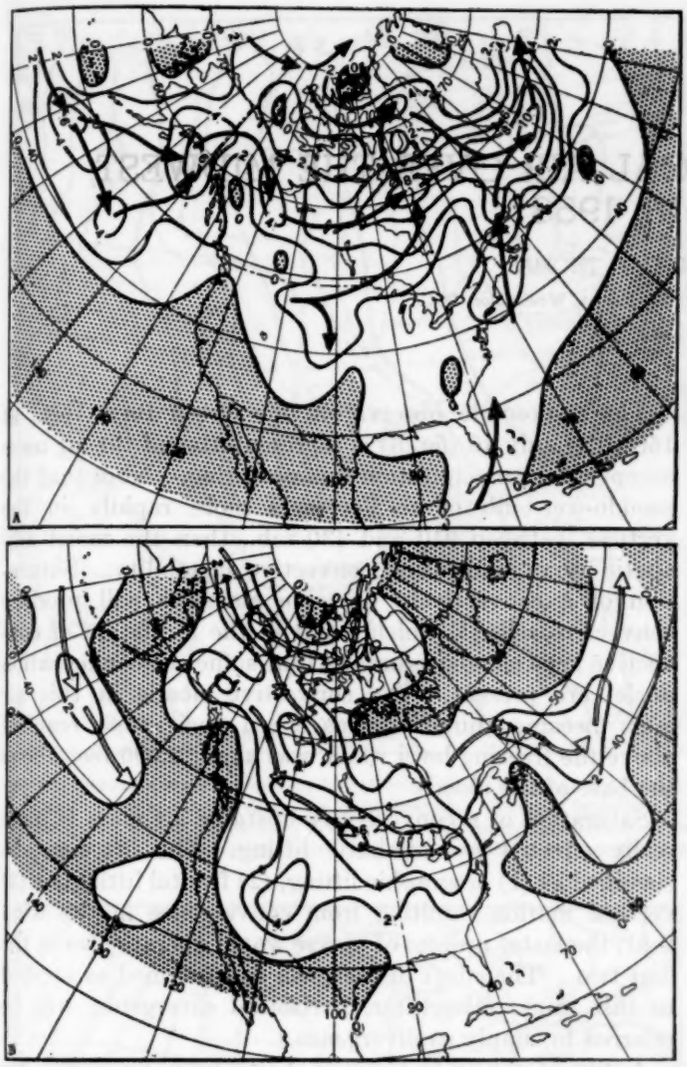

FIGURE 6.—Frequency of cyclonic passages (A) and anticyclonic passages (B) (within 5° squares at 45° N.) during July 1953. A. Depressed cyclone track in Pacific indicative of blocking. Zonal motion of cyclonic centers over eastern North America and Atlantic agree with flat, fast flow of figures 4 and 5. B. Note frequent intrusions of Pacific and Arctic Highs into United States and Canada.

Highs arriving in the eastern United States pass off the coast as closed centers. The others either stalled under the mean ridge over the Appalachians or deteriorated into weak eastward moving pressure surges.

TEMPERATURE AND PRECIPITATION

Charts I, II, and III present the mean monthly temperature and precipitation data. Below normal temperatures throughout most of the Plains and precipitation mainly between 50 and 100 percent of normal sum up the story of drought relief. Southern Texas remained hot and dry under the small upper-level Texas anticyclone shown in figure 4. Temperatures in the West under the 700-mb. ridge were appreciably above normal despite normal to greater-than-normal shower activity over much of the area. This apparently came about when the depression of the maxima due to daytime cloudiness was not as great as the elevation of the minima associated with the moisture and nighttime cloudiness.

Precipitation in the Upper Mississippi Valley resulted from convective showers plus those induced along the cold fronts of impinging cold air masses and occasional squall lines. Drought conditions in Virginia and North Carolina were associated with the positive height anomaly center over the Appalachians. Positive precipitation centers of note occurred in the northeast coastal area near the mean trough, the Far Northwest where trailing fronts of perturbations entering Canada from the Pacific caused showers, and those areas of the South and West already discussed in the detailed 10-day descriptions.

WEATHER VAGARIES

As usual the more whimsical digressions of weather made news this month too. These ranged far in distance and were varied in subject. Items: Snow plows were busy in the Italian Alps after a rare summer snowstorm of 2 to 3 inches (A. P., July 11); dust rising to 35,000 feet some 200 miles west of Tucson, Ariz., lent an odd greenish appearance to the sun which went through surprising (apparent) gyrations as an inversion layer was disturbed (A. P., no. date); Philadelphia, Pa., set a new daily maximum record of 99° F. on July 18, and 1 week later a new daily low (60.6° F.) on July 25; less meteorological but more refreshing was the all-time (since 1912) record surface water temperature of 81° F. recorded at Atlantic City, N. J., on July 22.

Not to be considered whimsical, however, were the floods—the worst in modern Japanese history—which occurred some 200 miles southwest of Tokyo about the 19th of July. Sudden cloudbursts and continuing heavy rains left more than 6,000 persons dead or missing and engulfed entire villages. Kyushu, recovering from the catastrophic floods of 3 weeks earlier which had left more than a million homeless, was also affected and reported waters rising again in debris-filled cities.

REFERENCES

1. Jay S. Winston, "The Weather and Circulation of June 1953—The Second Successive June With Record-Breaking Drought and Heat," *Monthly Weather Review*, vol. 81, No. 6, June 1953, pp. 162–168.
2. Thomas R. Reed, "The North American High-Level Anticyclone," *Monthly Weather Review*, vol. 61, No. 11, Nov. 1933, pp. 321–325.
3. Obie Y. Causey, "The Distribution of Summer Showers Over Small Areas," *Monthly Weather Review*, vol. 81, No. 4, Apr. 1953, pp. 111–114.
4. J. Namias and P. F. Clapp, "Confluence Theory of the High Tropospheric Jet Stream," *Journal of Meteorology*, vol. 6, No. 5, Oct. 1949, pp. 330–336.

RAINFALL IN MARITIME TROPICAL AIR OVER THE MIDWEST, JULY 16–18, 1953

H. E. BROWN AND C. F. THOMAS

WBAN Analysis Center, U. S. Weather Bureau, Washington, D. C.

INTRODUCTION

The rainfall over the Midwest from July 16–18, 1953 aroused the curiosity of all interested in the relationship between weather and the weather map. The fronts that are often invoked to explain the weather were absent. When rain occurs without the aid of fronts, as in this case, the meteorologist must seek other explanations of the phenomenon. This article presents an investigation of the possible causes in this instance of such precipitation and an attempt to find a model suitable for portrayal on the weather map. It is concluded that a theoretical model proposed by Bjerknes and Holmboe seems suitable.

THE WEATHER AND THE ANALYSIS

The rain fell from a patch of thunderstorms that moved from Kansas into Ohio. Scattered thunderstorms over Kansas on July 15 had moved and formed into a general rain area over Missouri by the 16th. The rainfall continued during the morning of the 17th when the patch was over Illinois and Indiana, and in the next 24 hours it moved over Michigan and Ohio (see figs. 1–4).

The rain patch was roughly 180 miles wide and 480 miles long along the north-northwest south-southeast axis (fig. 3) by July 17, and maintained approximately this size and shape for the next 24 hours while the axis moved with a uniform speed. The rain area took about 24 hours to move over a given station with a total precipitation averaging about ½ inch and a maximum total of 1¾ inches. The cloud bases in the rain area were from 8,000 to 12,000 feet, except that where the precipitation was heaviest, they lowered to about 800 feet.

Concurrent with the beginning of the rain on July 15 a warm front along the Gulf Coast was dissipating as shown by the frontal analysis of the weather map (fig. 2), and maritime tropical air had penetrated northward to the Canadian border. A moist tongue over Oklahoma and Kansas (fig. 1) at this time moved eastward with the rain (fig. 3). Aloft, an old cut-off cold vortex evolved into an open trough which moved eastward behind the rain patch (fig. 5). The trough aloft had extended downward to the surface by 0330 GMT July 18 (fig. 4) but earlier the surface analysis had had no feature associated with the rain.

The radiosonde observation for Green Bay, Wis., at 1500 GMT July 16 (fig. 6) is representative of the air mass except where precipitation was occurring. Note that the pseudo-wet-bulb curve decreases more rapidly in the vertical, between 910 and 430 mb., than the moist adiabatic curve, indicating convective instability. Saturation of a convectively unstable air mass will produce convective cells [1] which result in the formation of convective type clouds, assuming that sufficient condensation nuclei are present. The convective clouds in this air mass became thunderstorms when their tops reached above the freezing level which was about 2,000 feet above the base of the clouds.

Saturation of a convectively unstable air mass is most easily effected by adiabatic lifting. The lift may be classified as (1) orographic lifting, (2) frontal lifting, or (3) vertical motion resulting from convergence in the wind field; the latter process of course would operate also in the first two. The effect of each will be examined as applied to this rain. (Hereafter, horizontal divergence will be referred to simply as divergence.)

A lift of 2,000 feet would have been necessary for saturation of that layer of air having the highest moisture content, which was the layer nearest the surface. Considering the trajectory of the air mass from the Gulf Coast to the Great Lakes region, the maximum orographic lifting could have been only about 800 feet, which would not have been sufficient, alone, to fulfill the above condition.

Frontal lifting was considered as a possible factor in the explanation of precipitation because of the presence of a warm front along the Gulf Coast at the beginning of the period and the possibility that this front had not in reality dissipated or that a new front had formed in the same general area (fig. 2). A convenient method for determining the existence of fronts is the examination of thickness charts for temperature discontinuities. Twelve hours prior to the dissipation of the front on the 0330 GMT surface chart, the maximum temperature gradient expressed in terms of 1,000–850 mb. thickness (fig. 8) showed a gradient of 50 feet per 180 miles measured northward and normal to the surface position; however, a gradient of similar magnitude existed south of the front thus revealing no temperature discontinuity. The thickness chart for 1500 GMT, July 17 (fig. 9), 36 hours later,

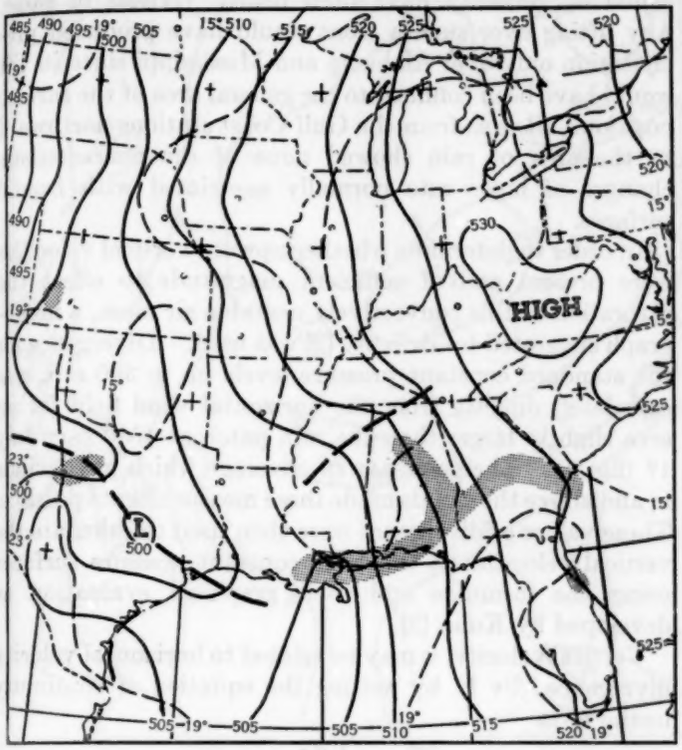

FIGURE 1.—850-mb. chart for 1500 GMT, July 15, 1953. Height contours (solid lines) are labeled in tens of feet and drawn for 50-foot intervals. Dew-point isopleths (light dashed lines) drawn for intervals of 4° C. Shaded areas indicate precipitation at the surface at 1530 GMT. Positions of predominant troughs indicated as heavy dashed lines.

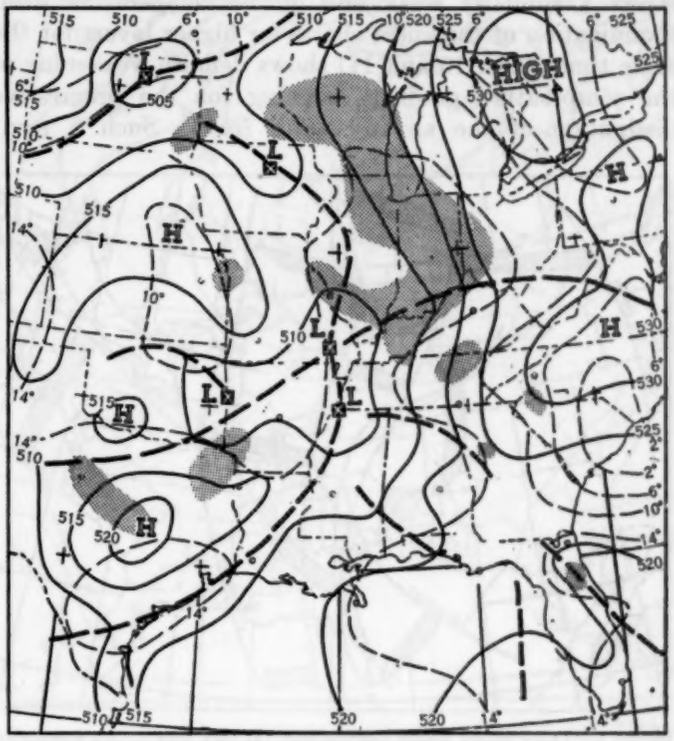

FIGURE 3.—850-mb. chart for 1500 GMT, July 17, 1953

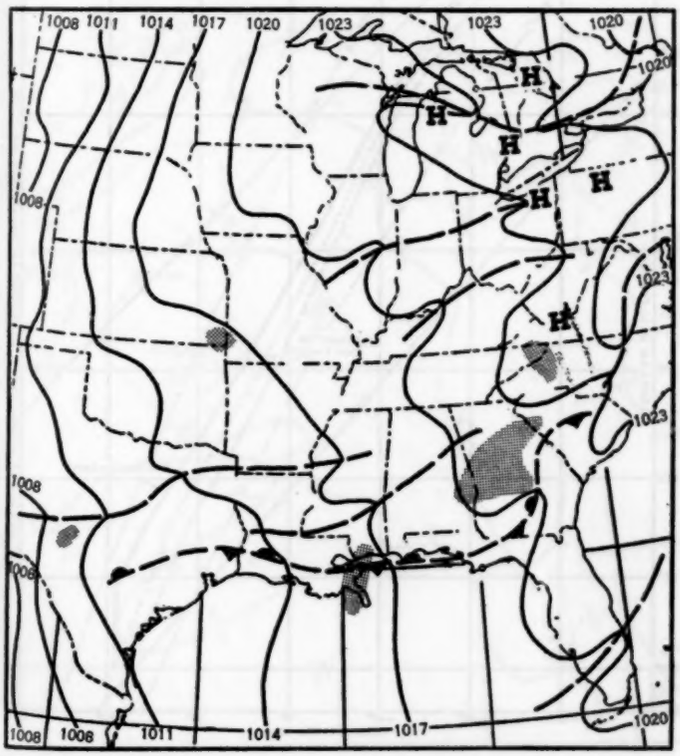

FIGURE 2.—Surface chart for 0330 GMT, July 16, 1953. Isobars (solid lines) drawn for 3-mb. intervals. Note the dissipating quasi-stationary front along the Gulf Coast area.

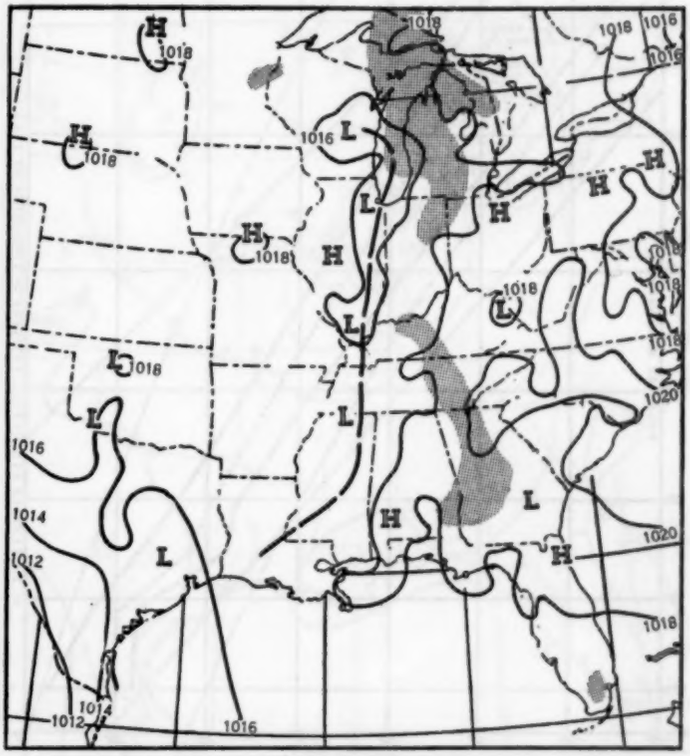

FIGURE 4.—Surface chart for 0330 GMT, July 18, 1953. Because of the extremely weak pressure gradient, isobars (here shown for 2-mb. intervals) were based on a detailed analysis using 1-mb. intervals with no attempt at smoothing.

266962—53——3

shows a similarly weak and diffuse temperature field. Examination of thickness charts for higher layers for the same times (figs. 10 and 11) shows definite weakening of the temperature gradient, arguing for the progressive dissipation of the already weak front. Such a front would of necessity have been nearly vertical in slope. Any lifting over such a front would have produced precipitation only over Alabama and Mississippi since its lift would have been confined to the general area of the surface position. RAOBS from the Gulf Coast stations northward to the area of rain showed none of the characteristic changes of lapse rate normally associated with frontal surfaces.

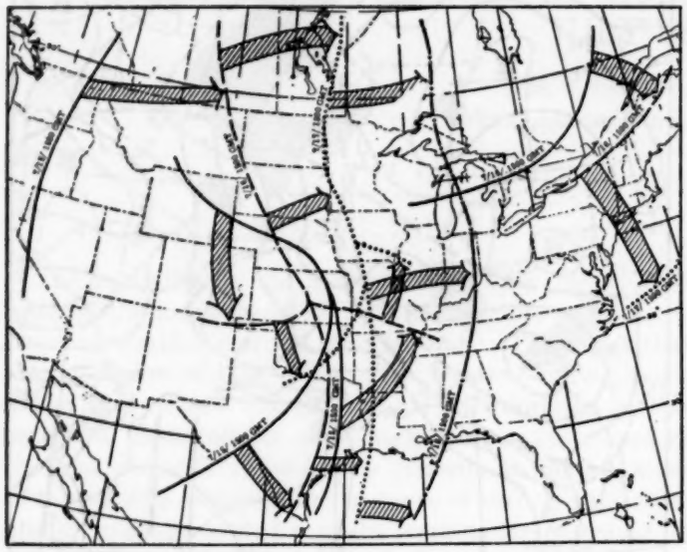

FIGURE 5.—24-hour 500-mb. trough positions from 1500 GMT, July 15, 1953, through 1500 GMT, July 18, 1953. The position at 1500 GMT, July 17, 1953 (the north-south dotted line) is that especially pertinent in its relation to the Bjerknes-Holmboe model referred to in the text.

In order to determine whether upward vertical velocities were present and of sufficient magnitude to effect the saturation of this convectively unstable air mass, a nomograph suggested by Bellamy [2] was used. Divergence for the standard constant pressure levels up to 300 mb. was calculated directly from the horizontal wind field for an area slightly larger than the rain patch at 1530 GMT July 17 (fig. 3). The good RAWIN coverage which gave winds in and above the clouds made these measurements possible. These values of divergence were then used to calculate the vertical velocities at the same constant pressure surfaces using the formulae and their graphical evaluation as developed by Kuhn [3].

Vertical velocity, w may be related to horizontal velocity divergence, div $\boldsymbol{V}$, by writing the equation of continuity in the form

$$\frac{\partial w}{\partial z}=-\frac{1}{\rho}\frac{d\rho}{dt}-\text{div}\,\boldsymbol{V}$$

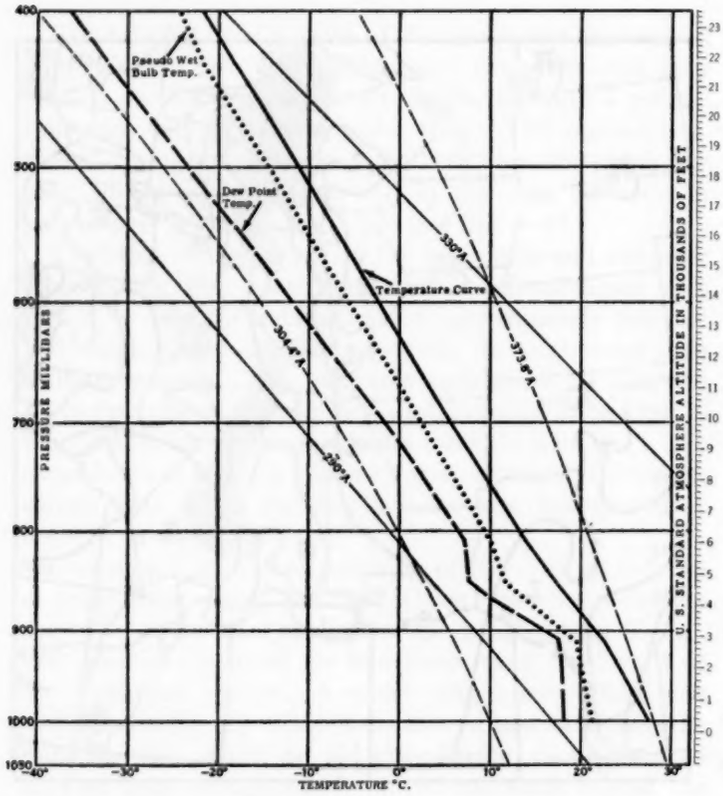

FIGURE 6.—Radiosonde observation from Green Bay, Wis. for 1500 GMT, July 16, 1953. Note that the lapse rate of the pseudo-wet bulb temperature curve is greater than or the same as the moist adiabatic lapse rate in the layer between 910 and 430 mb.

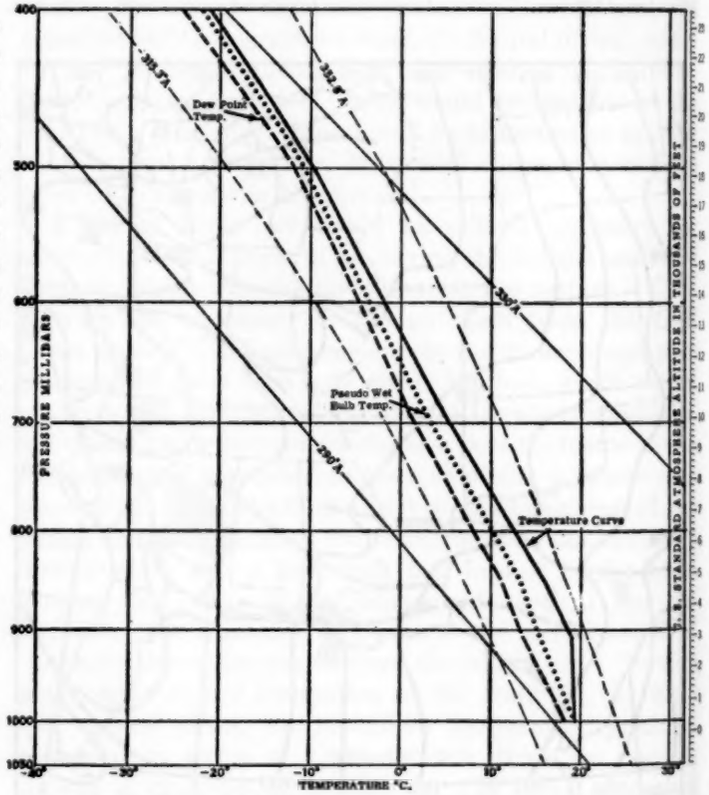

FIGURE 7.—Radiosonde observation from Green Bay, Wis. for 1500 GMT, July 17, 1953. Above 650-mb. the lapse rate of the temperature curve has decreased in 24 hours to slightly less than the moist adiabatic lapse rate.

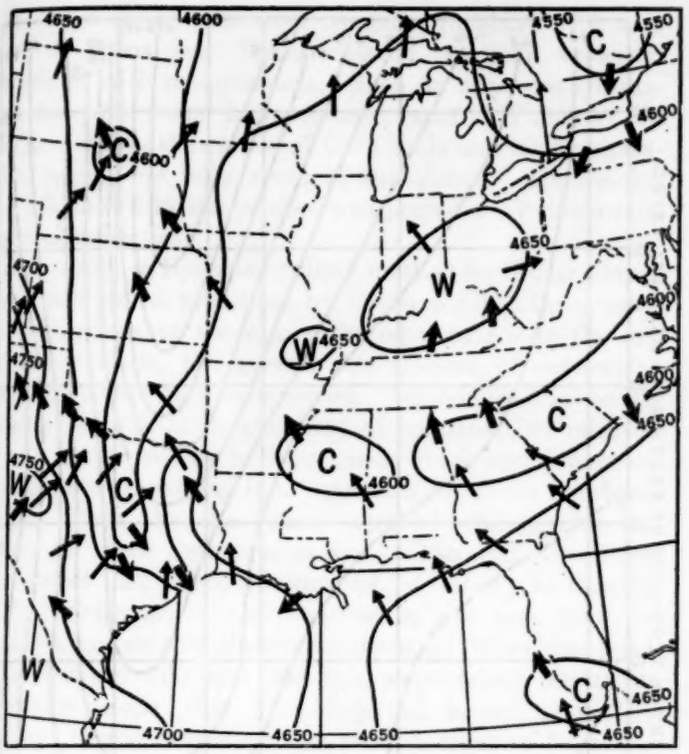

FIGURE 8.—1000-850-mb. layer thickness (or height difference) chart for 1500 GMT, July 15, 1953. Thickness isopleths are in feet for 50-foot intervals. Thin arrows indicate advection of warmer air and thick arrows advection of colder air. Note the generally weak gradients northward from the Gulf Coast.

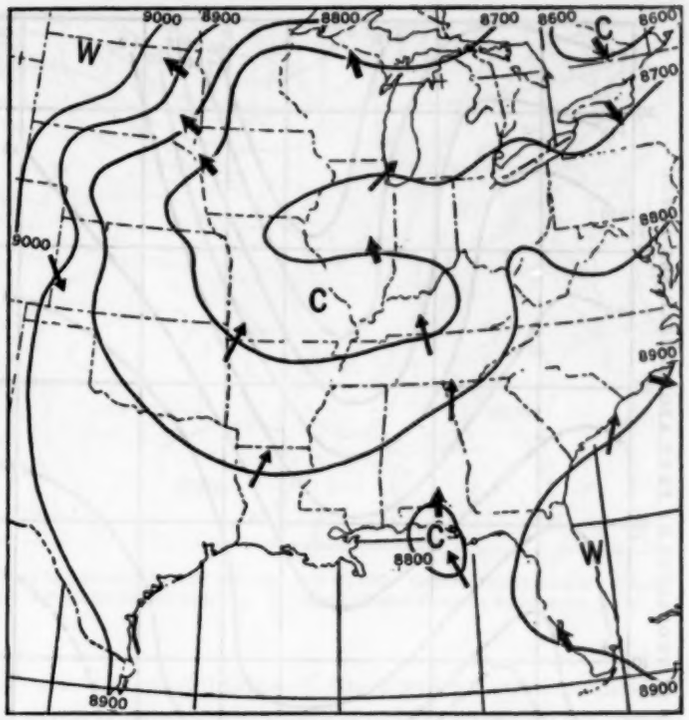

FIGURE 10.—700-500-mb. layer thickness chart for 1500 GMT, July 15, 1953. Thickness isopleths are in feet for 100-foot intervals.

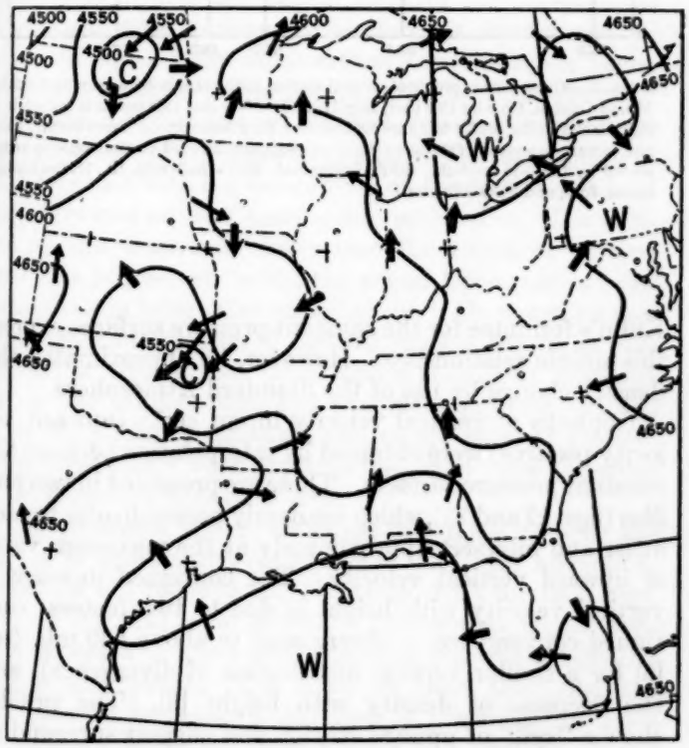

FIGURE 9.—1000-850-mb. layer thickness chart for 1500 GMT, July 17, 1953. Observe that over Illinois and Indiana, the general area of precipitation at this time (see fig. 3), the gradients are quite weak and some slight cold, rather than warm, advection is indicated.

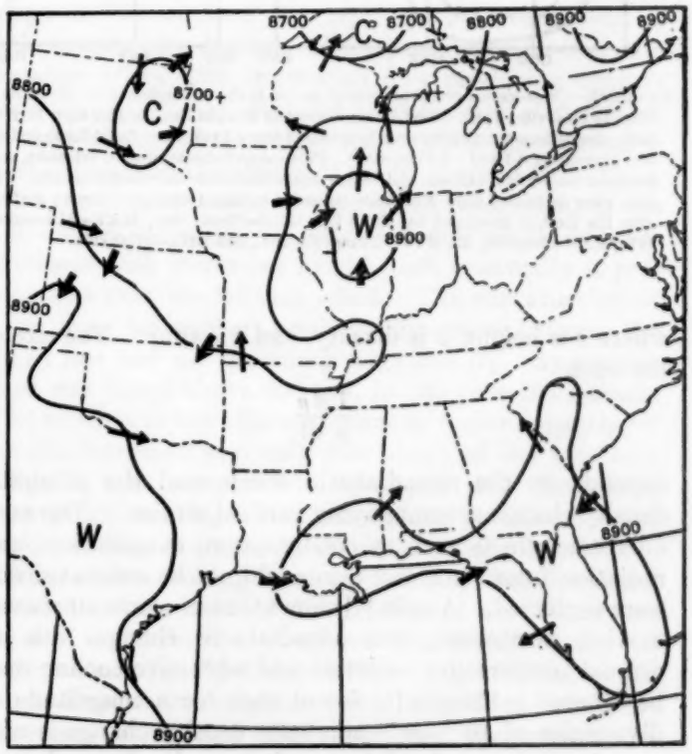

FIGURE 11.—700-500-mb. layer thickness chart for 1500 GMT, July 17, 1953.

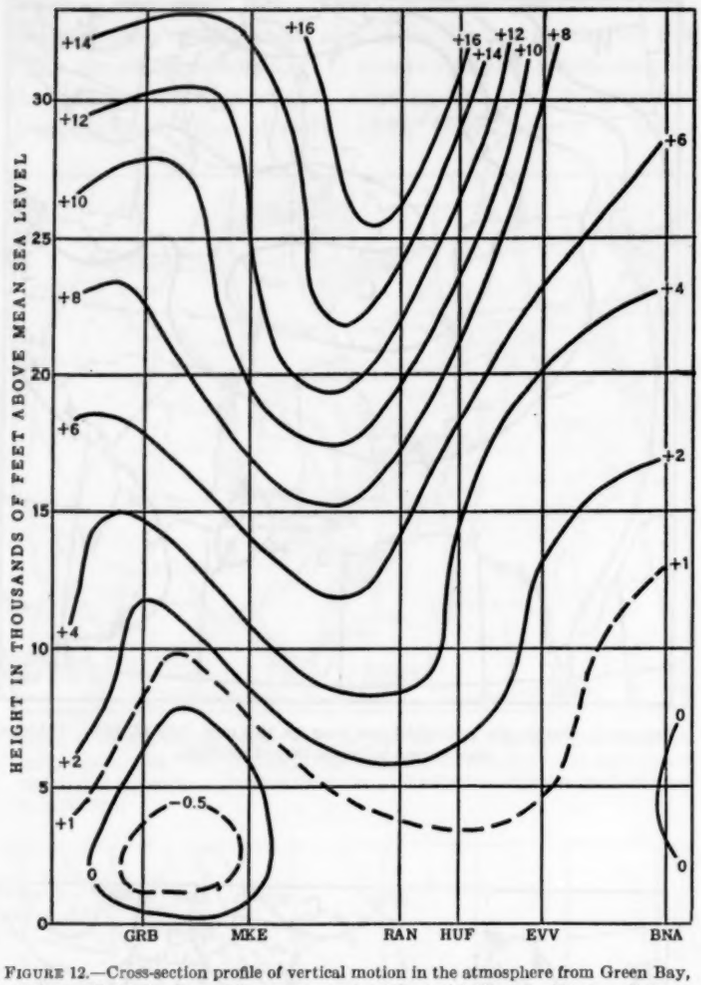

FIGURE 12.—Cross-section profile of vertical motion in the atmosphere from Green Bay, Wis., to Nashville, Tenn. (along an approximately straight line) for 1500 GMT, July 17, 1953. Isopleths are drawn for even intervals of every 2 cm. sec.$^{-1}$ (solid lines) and for odd intervals of +1 and −0.5 cm. sec.$^{-1}$. Plus values indicate upward velocities, zero indicates no vertical motion, and minus values represent downward motion. The data were calculated from divergence values at standard constant pressure surfaces after the method developed by Kuhn [3]. GRB=Green Bay, MKE=Milwaukee, Wis., RAN=Rantoul, Ill., EVV=Evansville, Ind., and BNA=Nashville.

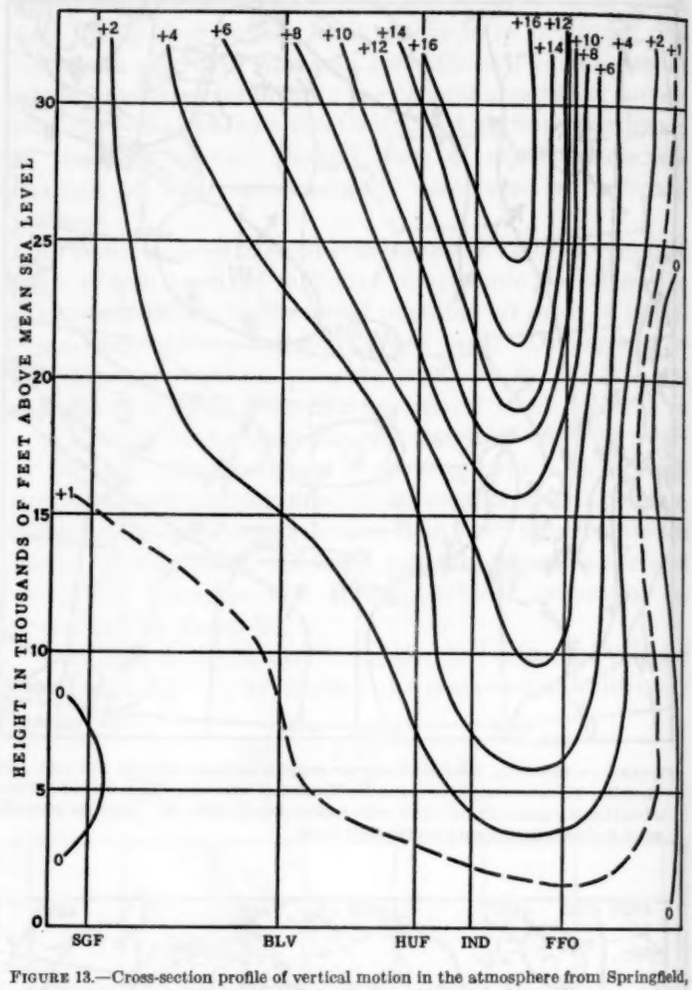

FIGURE 13.—Cross-section profile of vertical motion in the atmosphere from Springfield, Mo. to Dayton, Ohio for 1500 GMT, July 17, 1953. Note that this profile is not quite at right angles to the profile in figure 12; however, they intersect (at Terre Haute, Ind.) and picture two views of the same "cell" of maximum upward vertical velocity represented by the +16 isopleth. SGF=Springfield, BLV=Belleville, Ill., IND=Indianapolis, Ind., and FFO=Dayton.

where z is height, ρ is density, and t is time. The size of the term

$$\frac{1}{\rho}\frac{d\rho}{dt}$$

depends on the nonadiabatic effects and the adiabatic density change accompanying vertical motion. The nonadiabatic effects such as condensation, evaporation, and radiation from the cloud tops could not be estimated and were neglected. Austin [4] shows that in warm air masses moving northward, the nonadiabatic changes due to diurnal temperature variation and advective cooling may be ignored. Fleagle [5] found that for a magnitude of divergence of 10^{-5} sec^{-1} adiabatic density change is of a magnitude one order lower and may also be neglected. The neglect of these effects gives

$$\frac{\partial w}{\partial z} = -\text{div}\, \boldsymbol{V};$$

Kuhn's formulae for the constant pressure surfaces express this simple relationship. However, he approximated the density change by use of the Standard Atmosphere.

Isopleths of vertical velocity in cm sec^{-1} (upward velocity positive) were obtained by interpolation between the constant pressure surfaces. These are presented in two profiles (figs. 12 and 13), which are nearly perpendicular to each other and intersect approximately at the maximum value of upward vertical velocity. The continued increase of vertical velocity with height is due to two factors: continued convergence (−divergence) to above 500 mb. (see [6] for a similar vertical distribution of divergence), and the decrease of density with height [6]. The profiles show a "cell" of upward motion and suggest surrounding cells of downward motion. The north-south profile corresponds to the north-south axis of the instantaneous rain pattern for 1530 GMT July 17 (fig. 3). A comparison of the east-west profile with this rainfall pattern shows that

the edges of the rain area coincide, roughly, with zero vertical velocities. Thus, upward vertical velocities coincided with precipitation. Such an apparent correlation has been found in many more cases by Panofsky [7]. He also shows that areas of few clouds and no precipitation correspond with areas of subsidence. Apparently, the lift shown in the profiles was preceded by downward vertical velocities.

According to Bjerknes' "slice" method for lifting a layer to saturation as presented by Petterssen [8], the greater the lapse rate, or the nearer the lapse rate is to the dry adiabatic slope, the greater the amount of convective cloudiness that may be expected. Subsidence prior to the time of precipitation and heat of condensation released above 10,000 feet are both processes which would decrease the lapse rate causing it to approach the moist adiabatic slope. Thus, by the "slice" method, the greater the effect of these two processes, the less the convective cloudiness that would be expected. Contrary to Petterssen's conclusion, it was observed in this case that the greatest convective cloudiness occurred when the lapse rate between 700 and 500 mb. approached the moist adiabatic slope (fig. 7). Empirical investigations by Austin [1] and others confirm this observation for many cases. Austin says, "For the development of the vertical accelerations to force the cloud upward it seems desirable that there be a steep lapse rate of temperature. However, . . . a condition which gives rise to a high liquid water content does not appear to favor the development of vertical accelerations. Therefore, it should not be expected that a steep lapse rate of temperature is necessarily the most favorable condition for cumulus growth."

Cressman [9] has treated the "slice" method in a manner similar to that of Bjerknes but replaces the assumption of no divergence with the assumption of divergence such that the inflow and outflow compensate each other. His analysis of this treatment shows that the effect of vertical velocities is greatest "when the actual lapse rate exceeds the moist adiabatic value only slightly." Cressman further states that in a region of upward motion the lapse rate reaches an equilibrium value, with a stabilizing tendency due to the condensation and precipitation being opposed by a destabilizing tendency due to the upward motion. Thus Cressman's work explains the lapse rates observed in the situation presented here.

The processes which stabilized the lapse rate in the rain area apparently counteracted the cold advection, shown on the 700–500 mb. thickness chart for 1500 GMT, July 15 (fig. 10), over southern Illinois that might have been expected to move northeastward with the movement of the cold trough. The chart 48 hours later (fig. 11) indicates an increase of 200 feet in thickness (or midtroposphere warming) over Illinois and Indiana at the time of the rain. Definitely the cold trough did not release the rain by midtroposphere cooling, but rather by the dynamic effect of divergence.

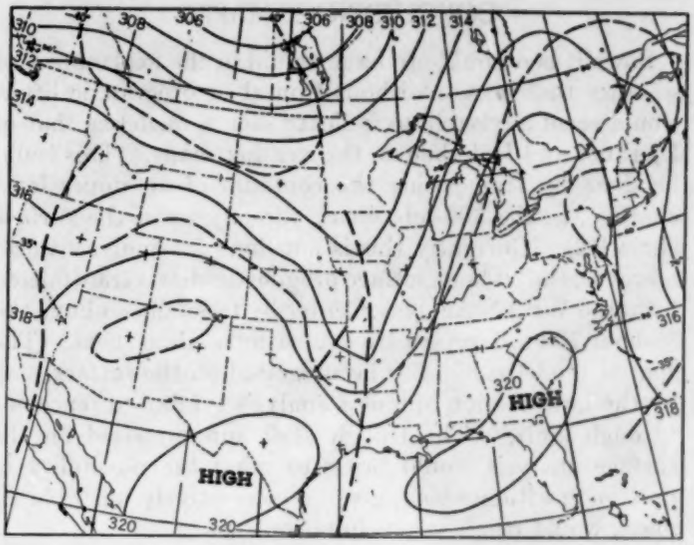

FIGURE 14.—300-mb. chart for 1500 GMT, July 17, 1953. Contours (solid lines) are in hundreds of feet for 200-foot intervals. Isotherms (dashed lines) are for intervals of 5° C.

From the assumptions of the gradient wind equation the divergence of the gradient wind is controlled by three factors: the solenoid term, the latitude effect, and the curvature effect [8]. At low levels, in a homogeneous air mass such as the one discussed here, the solenoid term is negligible. It may be neglected at higher levels when the isotherms are in phase with the contours as in this cold trough at 300 millibars (fig. 14). At low levels ahead of weak troughs the latitude effect predominates over the curvature effect with northward flow producing convergence [4] (see fig. 4). But the latitude effect depends on the first power of the wind speed while the curvative effect depends on the square of the wind speed [7]. Thus, with even slight increase of wind speed with height in the troposphere, the curvature effect becomes relatively more significant with increasing height until eventually it predominates over the latitude effect. The curvature effect in the upper troposphere produces divergence between the trough line and the preceding ridge line [7]. As convergence was found above 500 mb. in this case the latitude effect appears to have been effective in rather a deep layer (see the increased southerly flow south of the rain area in figs. 3, 4 as compared to figs. 1, 2) [10]. Low level convergence and high level divergence produce upward vertical motion as shown by the equation of continuity.

From such reasoning Bjerknes and Holmboe developed a model for the vertical distribution of the divergence ahead of and behind a trough such as the one described in this article (see fig. 1 in reference [11]). Ahead of the trough there is convergence below a level of nondivergence and divergence above. Behind the trough the convergence is above the level of nondivergence and the divergence is below. Empirical studies [7] have found this theoretical distribution of divergence to be a good approximation to the observed.

CONCLUDING REMARKS

Since it is desirable to have an aid in the explanation of weather that occurs without frontal or orographic lift it would seem advisable to indicate such a model as that of Bjerknes and Holmboe on the weather maps. This could be done by transposing the contours of an upper level chart, e. g. the 700-mb. chart, directly upon the surface chart [12]. Currently this is not done for analysis work, however, the 30-hour surface prognostic charts transmitted from the WBAN Analysis Center by facsimile do have the 36-hour 700-mb. prognostics superimposed on them. The spatial model could also be suggested on the surface map by the introduction of a new analysis symbol to represent "trough aloft." The trough aloft superimposed on the surface analysis would bring to mind the possibility of pretrough lifting which, given a convectively unstable air mass, would result in precipitation.

REFERENCES

1. J. M. Austin, "Cumulus Convection and Entrainment," *Compendium of Meteorology*, American Meteorological Society, Boston, 1951, pp. 694–701.
2. J. C. Bellamy, "Objective Calculations of Divergence, Vertical Velocity, and Vorticity", *Bulletin of the American Meteorological Society*, vol. 30, No. 2, Feb. 1949, pp. 45–49.
3. P. M. Kuhn, "A Generalized Study of Precipitation Forecasting. Part 2: A Graphical Computation of Precipitation" (to be published, *Monthly Weather Review*, vol. 81, No. 8, Aug. 1953).
4. J. M. Austin, "Cloudiness and Precipitation in Relation to Frontal Lifting and Horizontal Convergence", *Papers in Physical Oceanography and Meteorology*, Vol. IX, No. 3, Massachusetts Institute of Technology and Woods Hole Oceanographic Institution, Cambridge and Woods Hole, Massachusetts, August 1943.
5. R. G. Fleagle, "A Study of the Effects of Divergence and Advection on Lapse Rate", *Journal of Meteorology*, vol. 3, No. 1, Mar. 1946, pp. 9–13.
6. J. C. Thompson and G. O. Collins, "A Generalized Study of Precipitation Forecasting. Part 1: Computation of Precipitation from the Fields of Moisture and Wind", *Monthly Weather Review*, vol. 81, No. 4, Apr. 1953, pp. 91–100. (See fig. 3, p. 97, and equation (9), p. 95.)
7. H. A. Panofsky, "Large-Scale Vertical Velocity and Divergence", *Compendium of Meteorology*, American Meteorological Society, Boston, 1951, pp. 639–646.
8. S. Petterssen, *Weather Analysis and Forecasting*, McGraw-Hill Book Company, Inc., New York and London, 1940, see pp. 64–77 and 228.
9. G. P. Cressman, "The Influence of the Field of Horizontal Divergence on Convective Cloudiness", *Journal of Meteorology*, vol. 3, No. 3, Sept. 1946, pp. 85–88.
10. A. K. Showalter, "An Approach to Quantitative Forecast of Precipitation (III)", *Bulletin of the American Meteorological Society*, vol. 31, No. 1, Jan. 1950, pp. 23–25.
11. J. Bjerknes, "Extratropical Cyclones", *Compendium of Meteorology*, American Meteorological Society, Boston, 1951, pp. 577–598.
12. V. J. Oliver and M. B. Oliver, "Meteorological Analysis in the Middle Latitudes", *Compendium of Meteorology*, American Meteorological Society, Boston, 1951. (See p. 721, fig. 2.)

CORRECTION

MONTHLY WEATHER REVIEW, vol. 81, No. 6, June 1953, page 170: Maps in figures 3 and 4 should be interchanged. Map labeled figure 4 is for 1500 GMT, June 8, 1953.

U. S. GOVERNMENT PRINTING OFFICE: 1953

Chart I. A. Average Temperature (°F.) at Surface, July 1953.

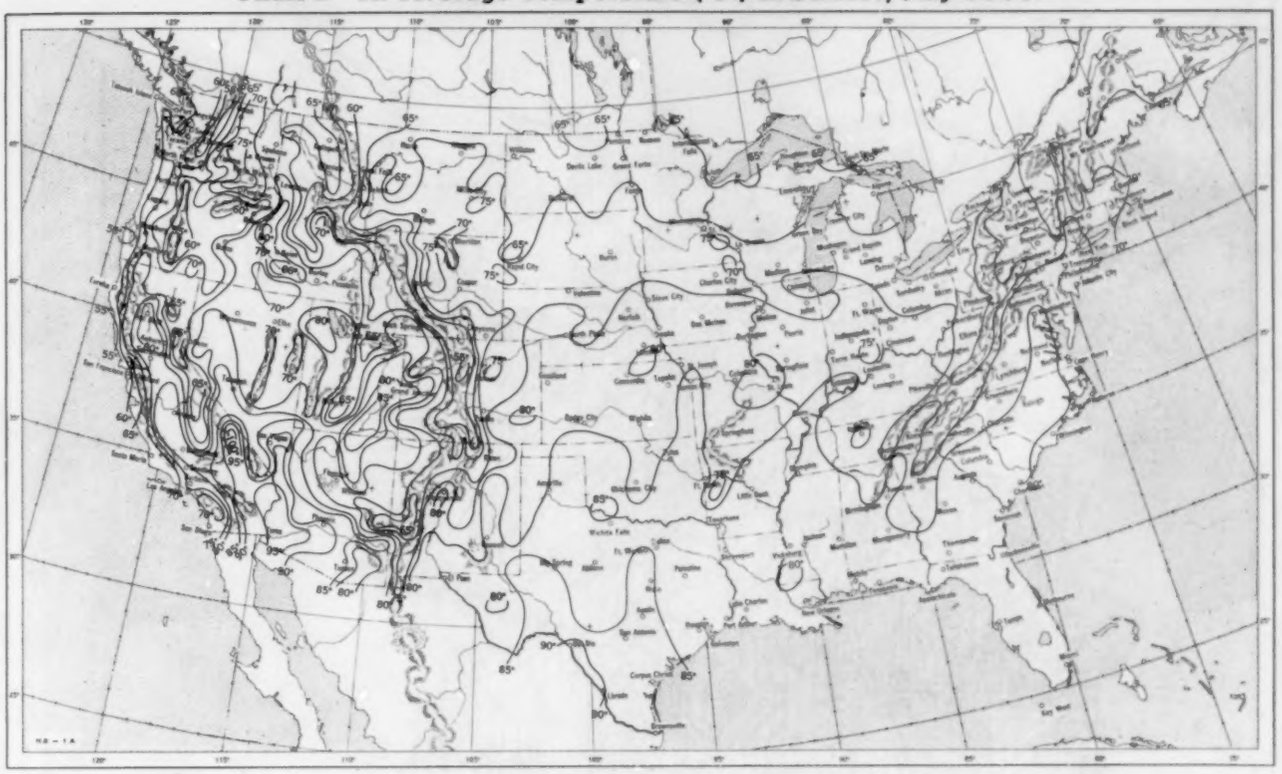

B. Departure of Average Temperature from Normal (°F.), July 1953.

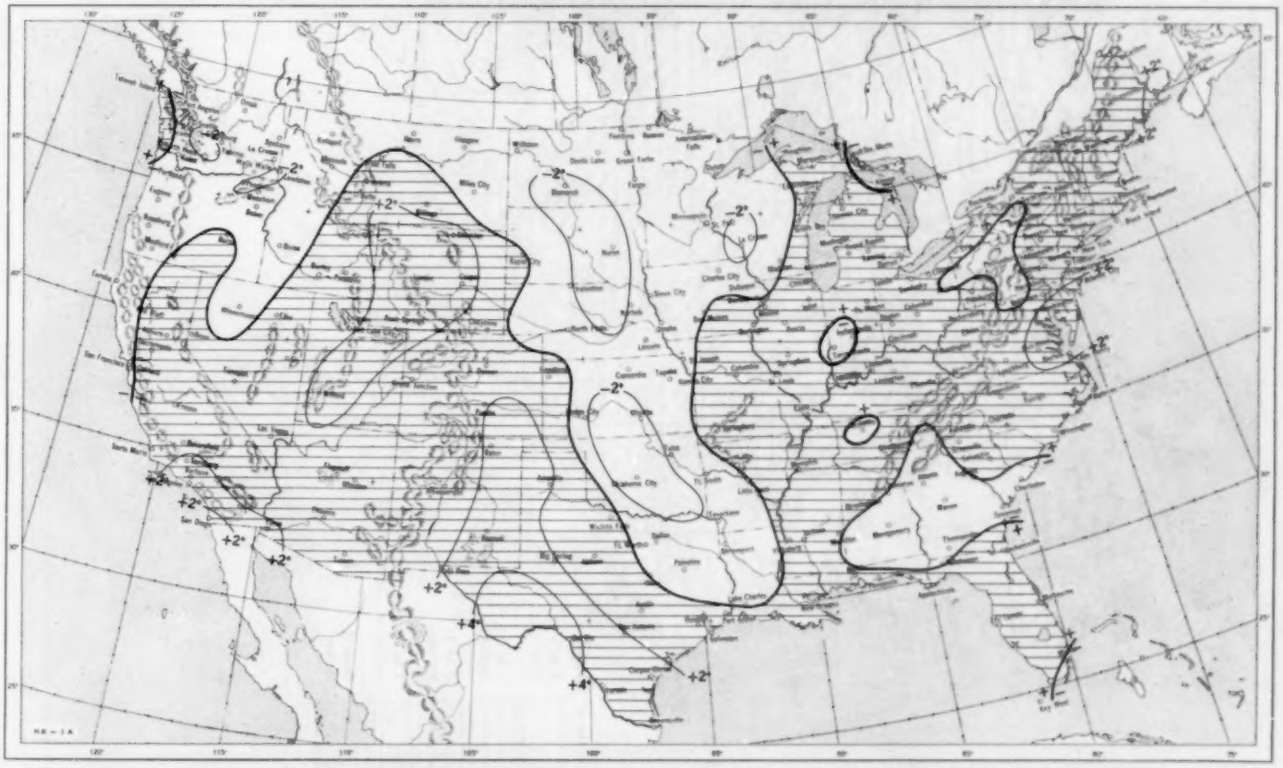

A. Based on reports from 800 Weather Bureau and cooperative stations. The monthly average is half the sum of the monthly average maximum and monthly average minimum, which are the average of the daily maxima and daily minima, respectively.

B. Normal average monthly temperatures are computed for Weather Bureau stations having at least 10 years of record.

Chart II. Total Precipitation (Inches), July 1953.

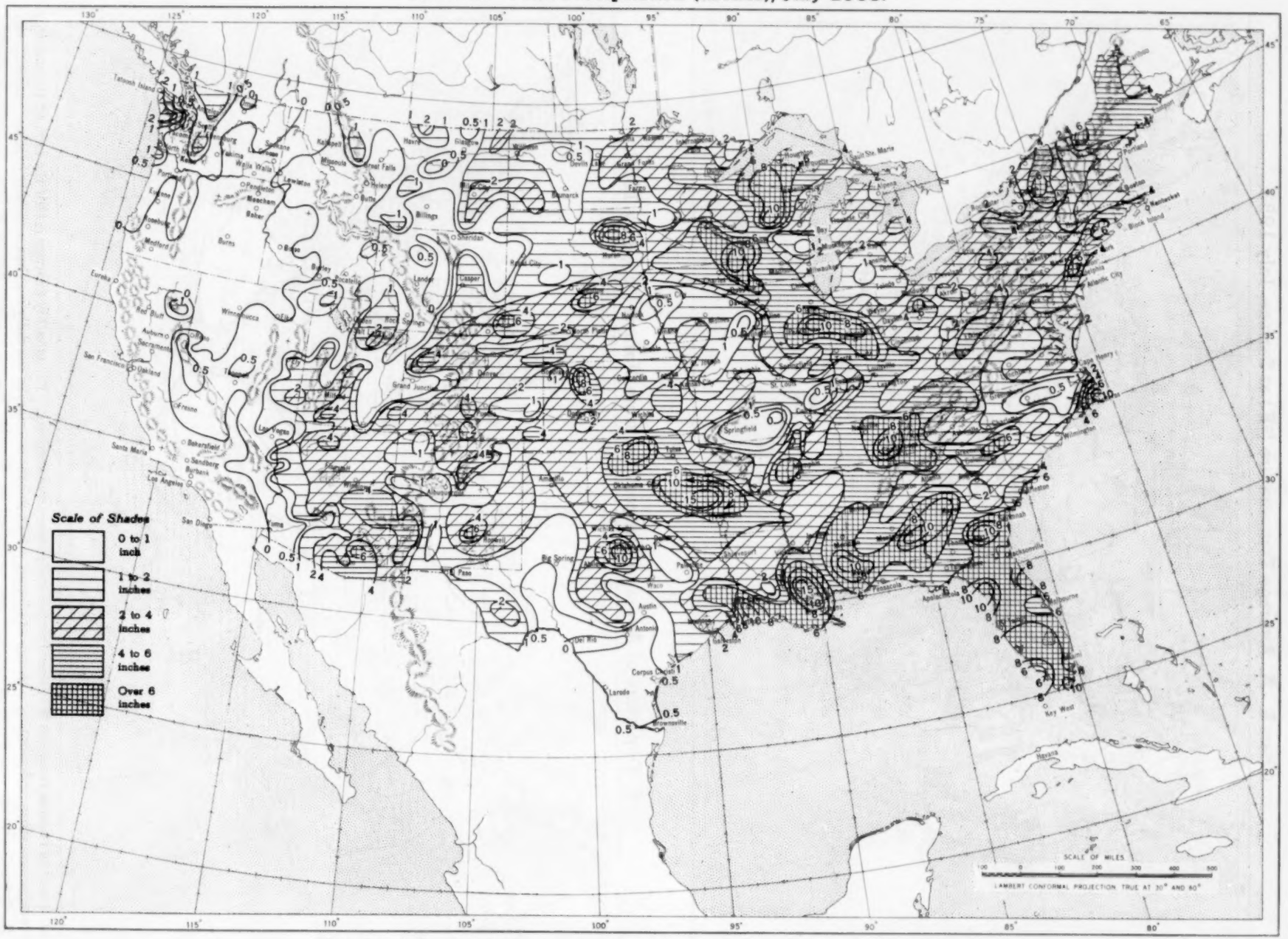

Based on daily precipitation records at 800 Weather Bureau and cooperative stations.

Chart III. A. Departure of Precipitation from Normal (Inches), July 1953.

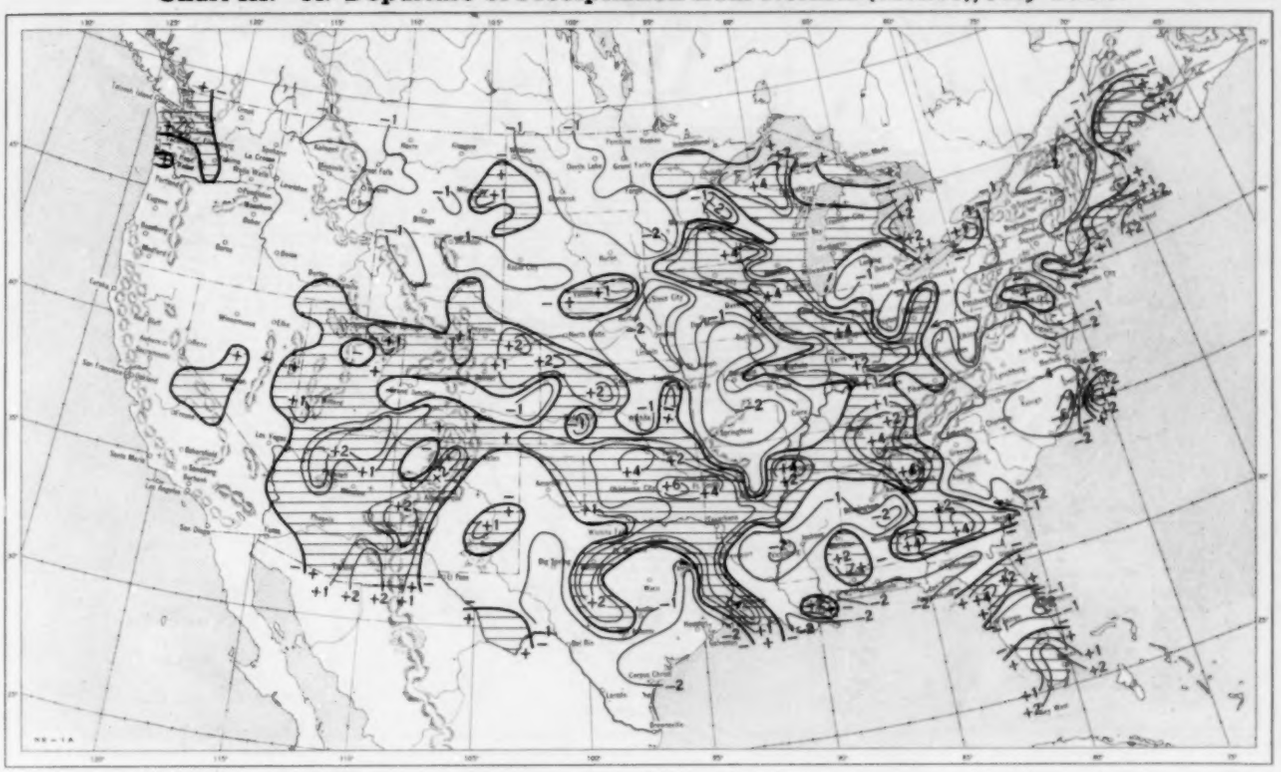

B. Percentage of Normal Precipitation, July 1953.

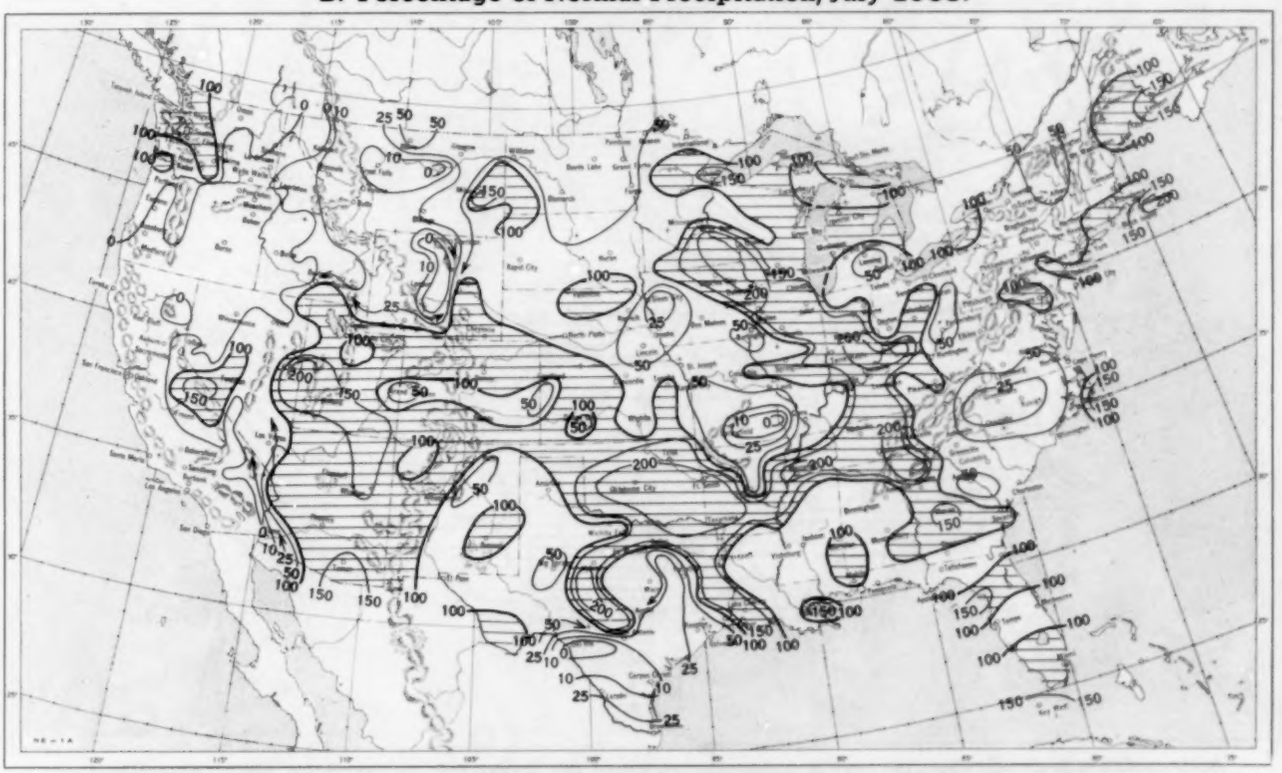

Normal monthly precipitation amounts are computed for stations having at least 10 years of record.

Chart VI. A. Percentage of Sky Cover Between Sunrise and Sunset, July 1953.

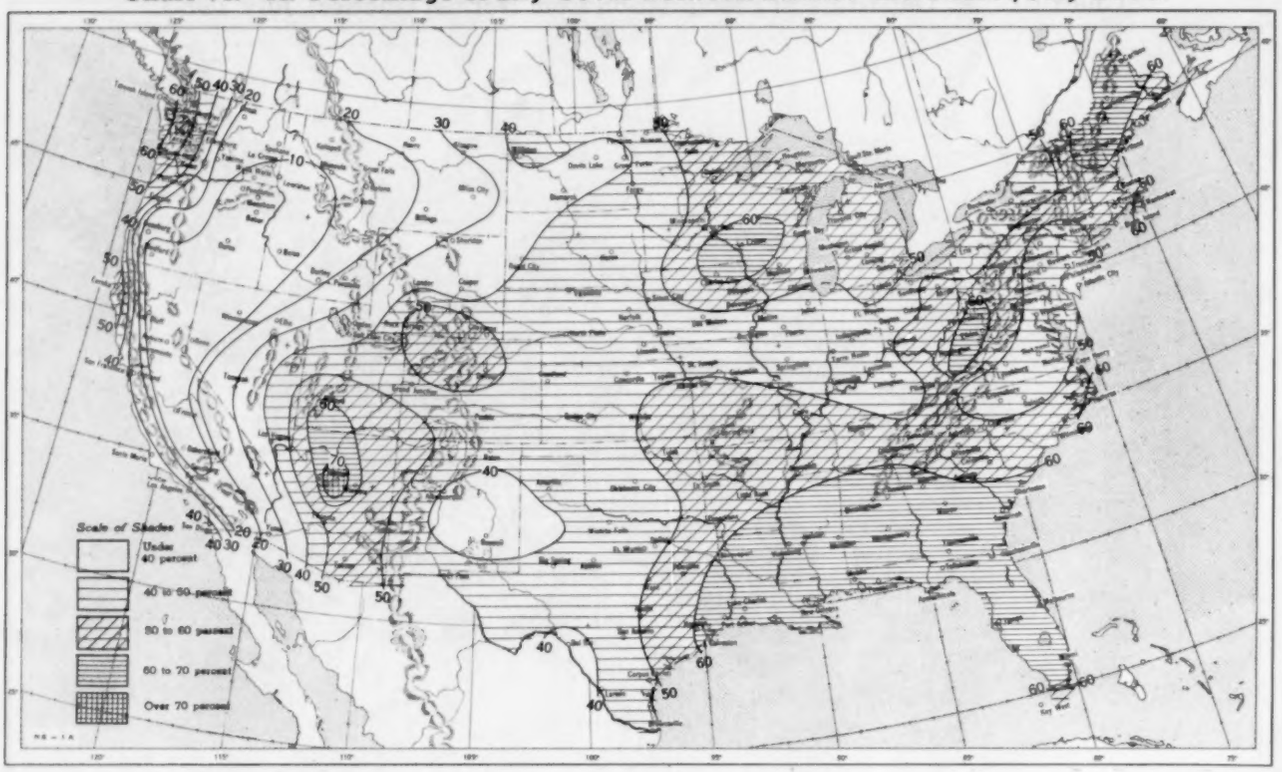

B. Percentage of Normal Sky Cover Between Sunrise and Sunset, July 1953.

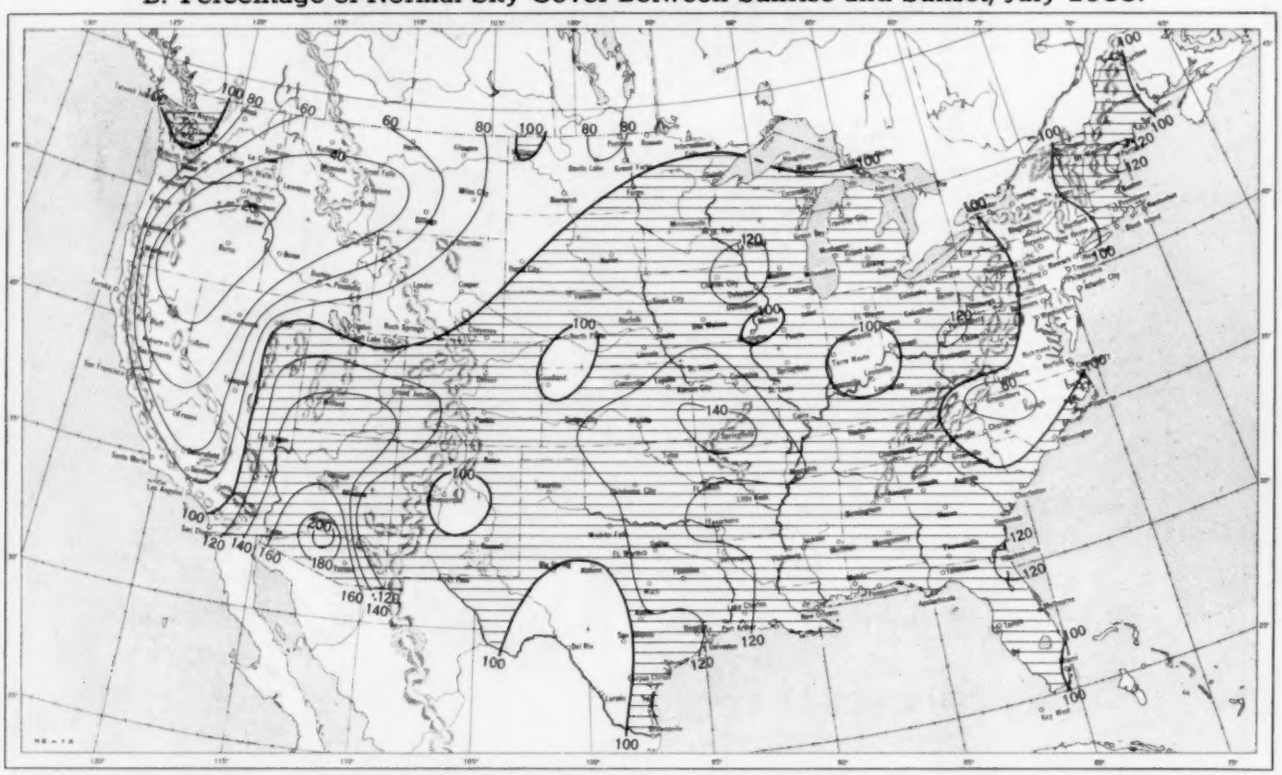

A. In addition to cloudiness, sky cover includes obscuration of the sky by fog, smoke, snow, etc. Chart based on visual observations made hourly at Weather Bureau stations and averaged over the month. B. Computations of normal amount of sky cover are made for stations having at least 10 years of record.

Chart VII. A. Percentage of Possible Sunshine, July 1953.

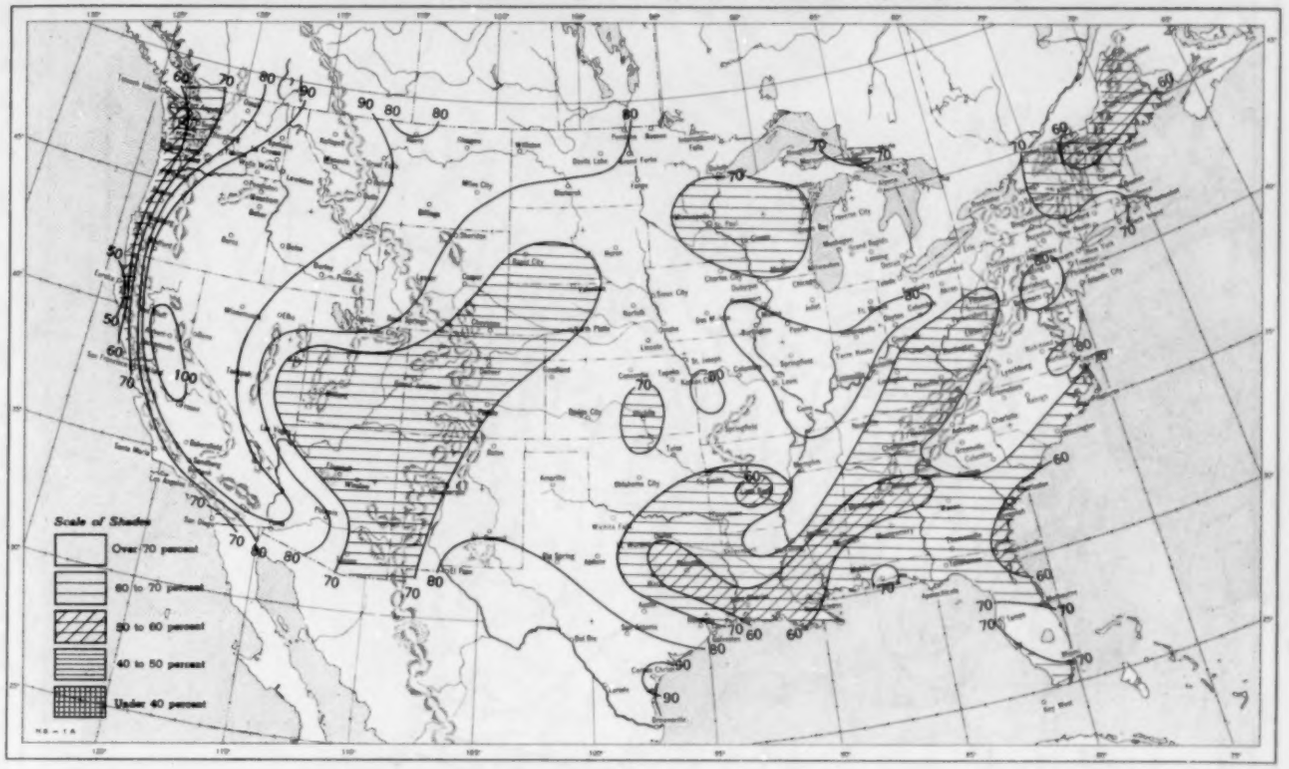

B. Percentage of Normal Sunshine, July 1953.

A. Computed from total number of hours of observed sunshine in relation to total number of possible hours of sunshine during month. B. Normals are computed for stations having at least 10 years of record.

Chart VIII. Average Daily Values of Solar Radiation, Direct + Diffuse, July 1953. Inset: Percentage of Normal Average Daily Solar Radiation, July 1953.

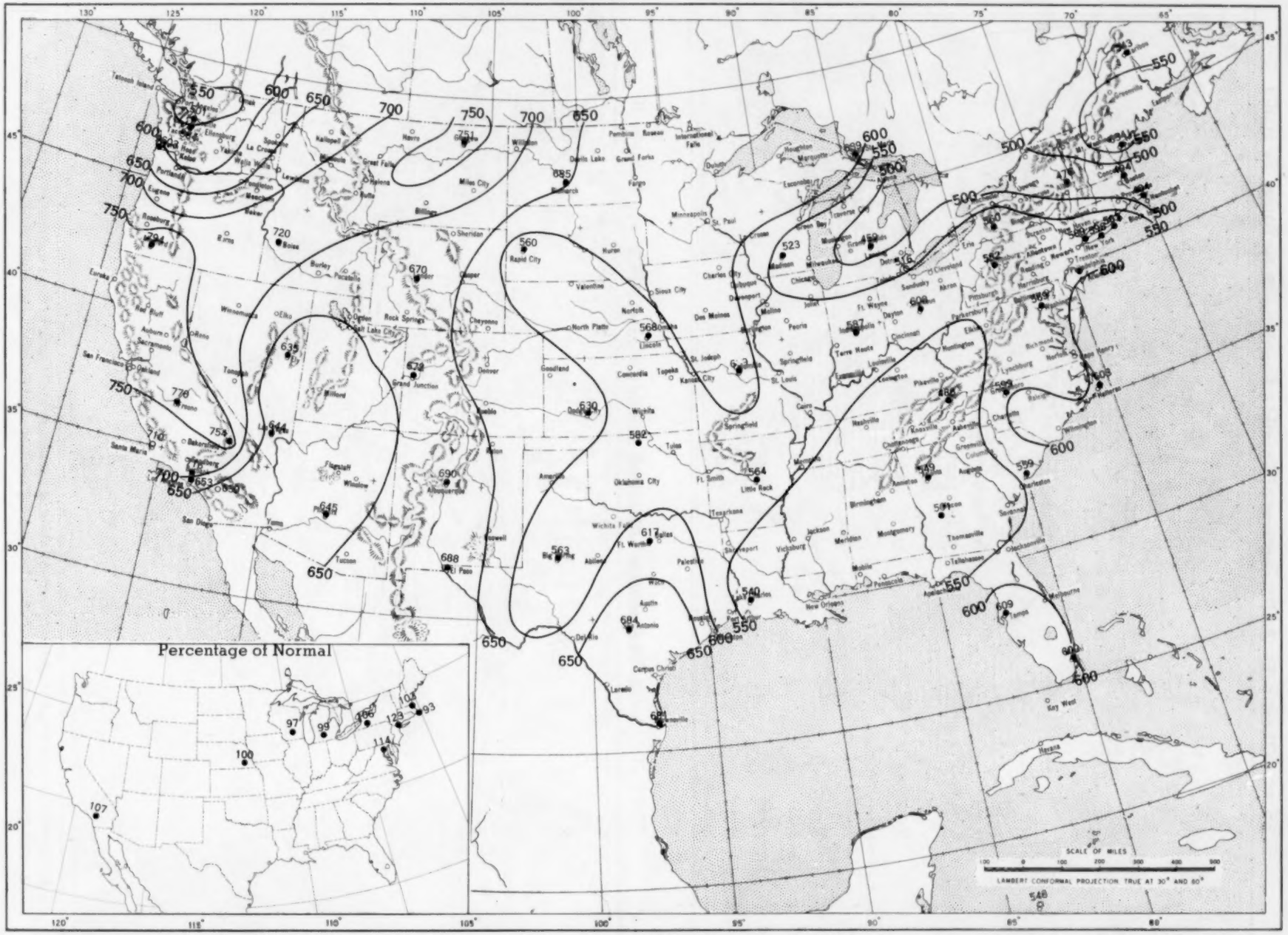

Chart shows mean daily solar radiation, direct + diffuse, received on a horizontal surface in langleys (1 langley = 1 gm. cal. cm. $^{-2}$). Basic data for isolines are shown on chart. Further estimates are obtained from supplementary data for which limits of accuracy are wider than for those data shown. Normals are computed for stations having at least 9 years of record.

Chart IX. Tracks of Centers of Anticyclones at Sea Level, July 1953.

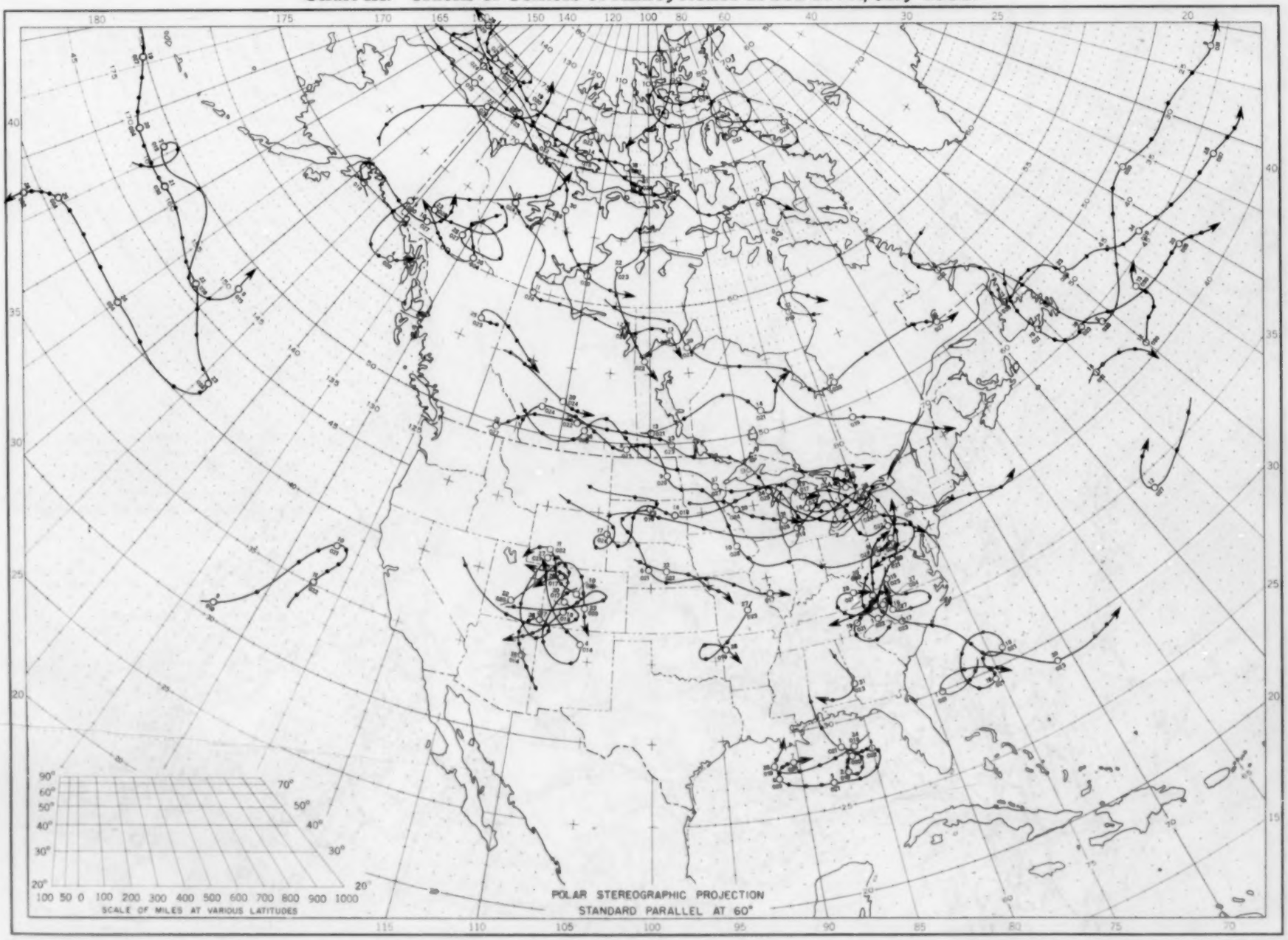

Circle indicates position of center at 7:30 a. m. E. S. T. Figure above circle indicates date, figure below, pressure to nearest millibar. Dots indicate intervening 6-hourly positions. Squares indicate position of stationary center for period shown. Dashed line in track indicates reformation at new position. Only those centers which could be identified for 24 hours or more are included.

Chart X. Tracks of Centers of Cyclones at Sea Level, July 1953.

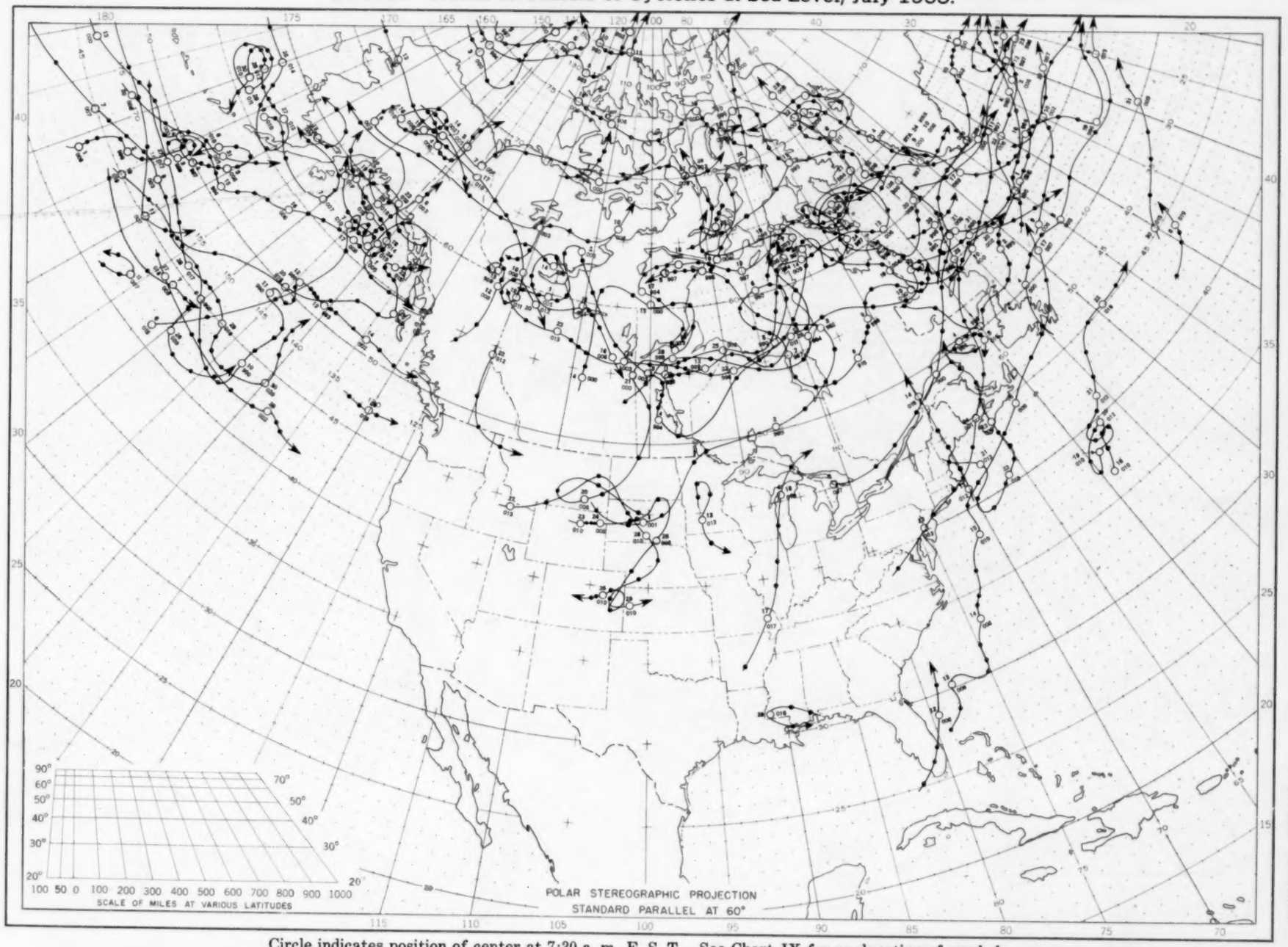

Circle indicates position of center at 7:30 a. m. E. S. T. See Chart IX for explanation of symbols.

Chart XI. Average Sea Level Pressure (mb.) and Surface Windroses, July 1953. Inset: Departure of Average Pressure (mb.) from Normal, July 1953.

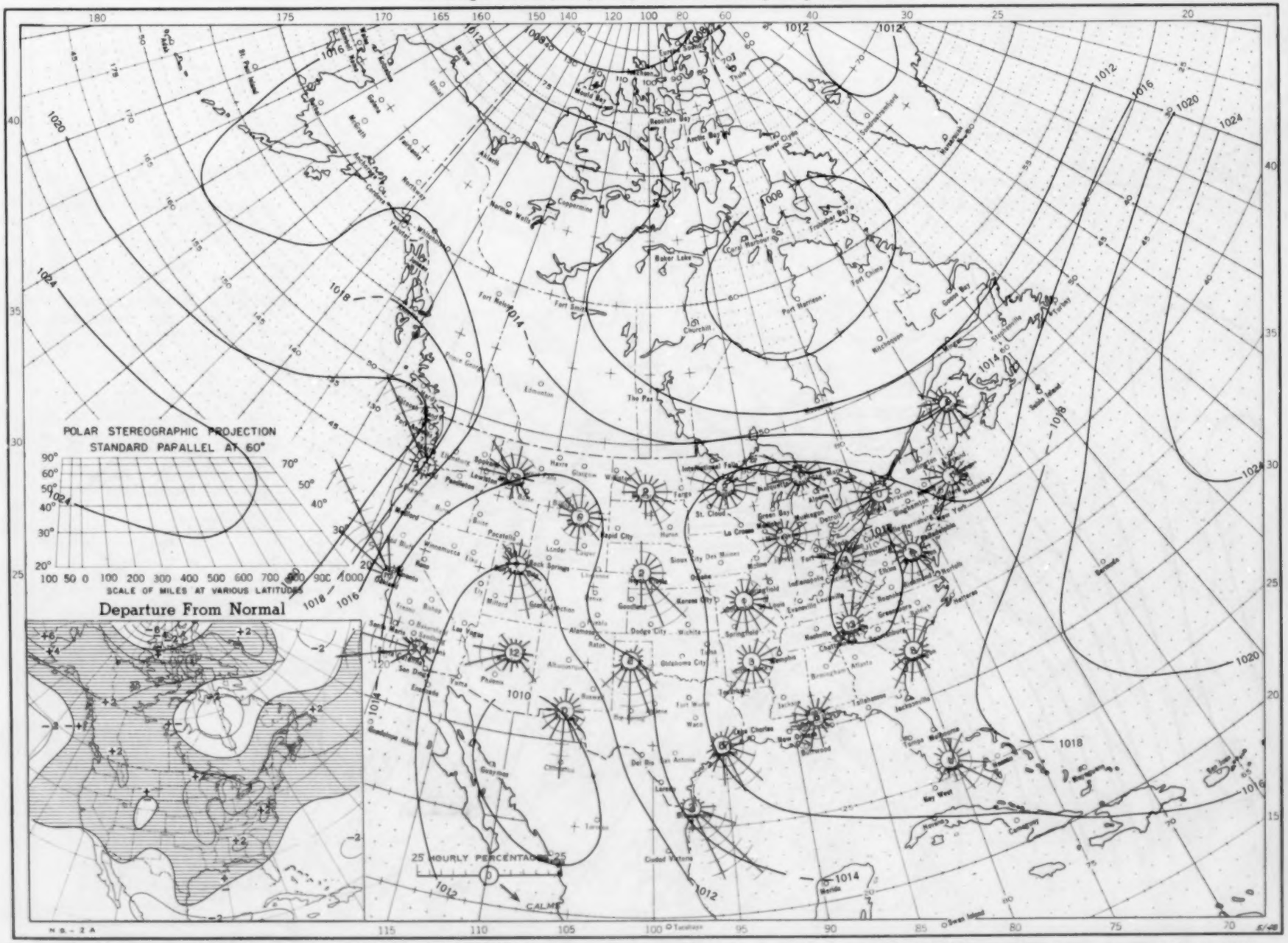

Average sea level pressures are obtained from the averages of the 7:30 a. m. and 7:30 p. m. E. S. T. readings. Windroses show percentage of time wind blew from 16 compass points or was calm during the month. Pressure normals are computed for stations having at least 10 years of record and for 10° intersections in a diamond grid based on readings from the Historical Weather Maps (1899-1939) for the 20 years of most complete data coverage prior to 1940.

Chart XII. Average Dynamic Height in Geopotential Meters (1 g.p.m. = 0.98 dynamic meters) of the 850-mb. Pressure Surface, Average Temperature in °C. at 850 mb., and Resultant Winds at 1500 Meters (m.s.l.), July 1953.

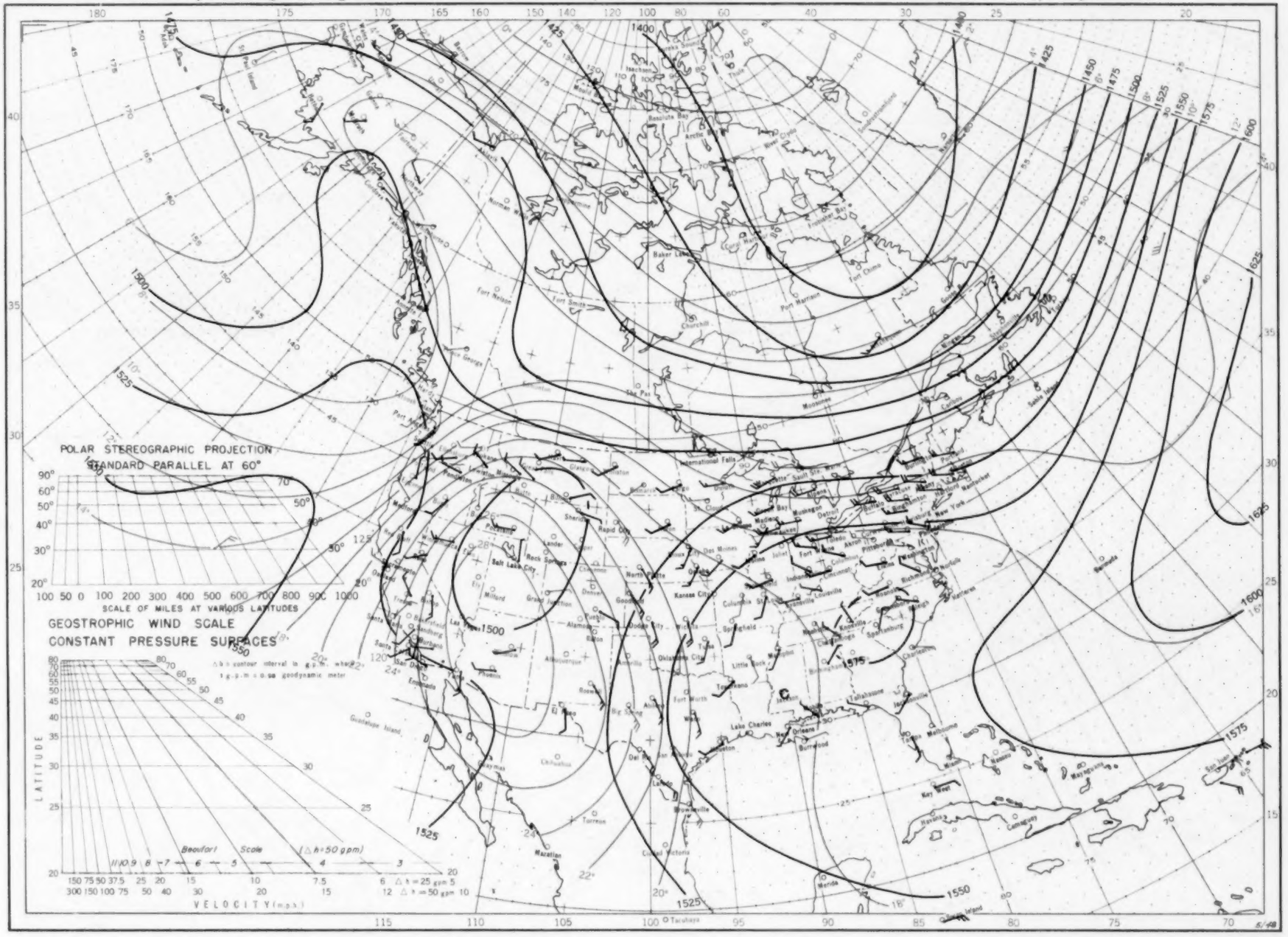

Contour lines and isotherms based on radiosonde observations at 0300 G. M. T. Winds shown in black are based on pilot balloon observations at 2100 G. M. T.; those shown in red are based on rawins taken at 0300 G. M. T.

Chart XIII. Average Dynamic Height in Geopotential Meters (1 g.p.m.. = 0.98 dynamic meters) of the 700-mb. Pressure Surface, Average Temperature in °C. at 700 mb., and Resultant Winds at 3000 Meters (m.s.l.), July 1953.

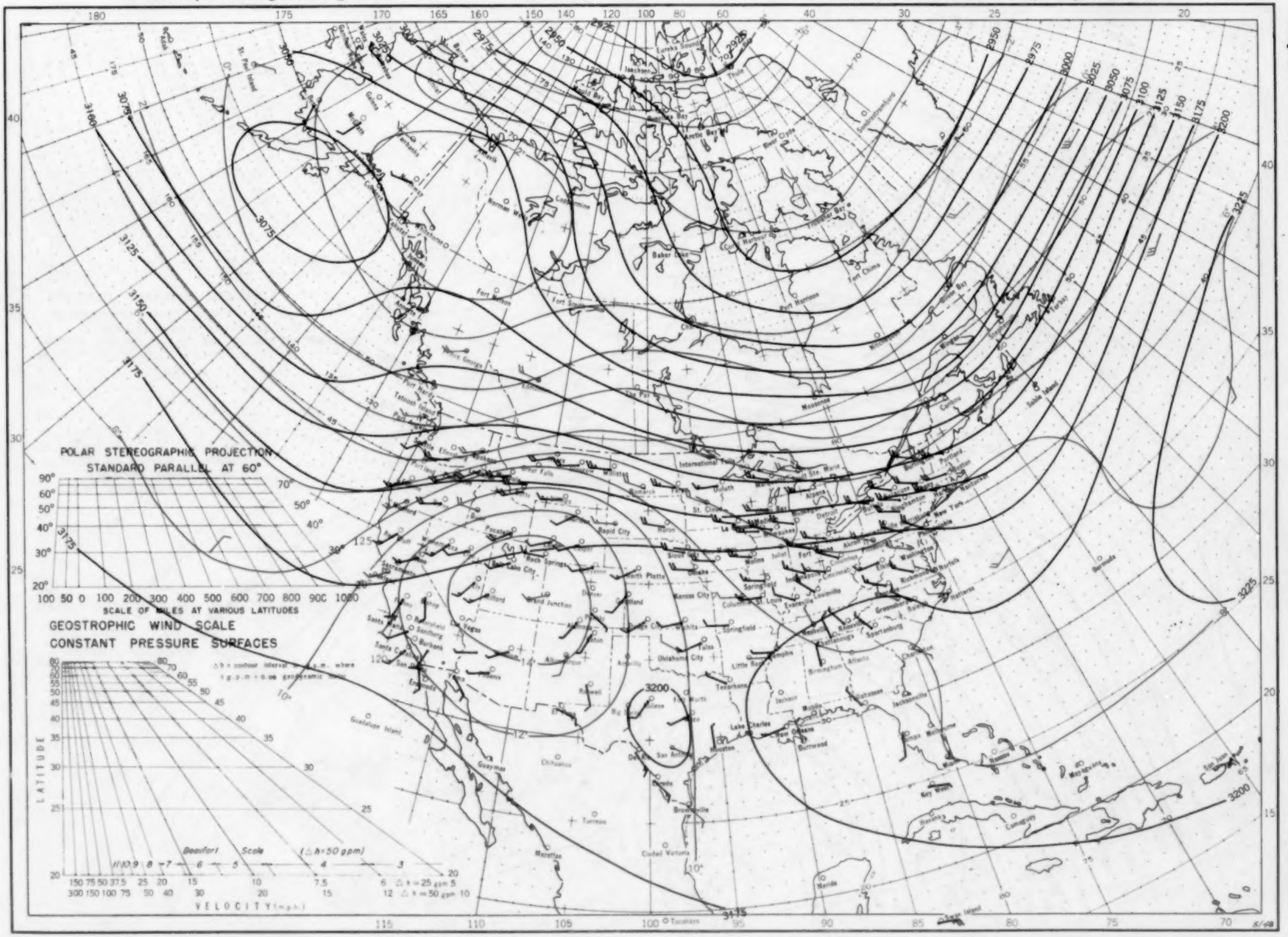

Contour lines and isotherms based on radiosonde observations at 0300 G. M. T. Winds shown in black are based on pilot balloon observations at 2100 G. M. T.; those shown in red are based on rawins taken at 0300 G. M. T.

Chart XIV. Average Dynamic Height in Geopotential Meters (1 g.p.m. = 0.98 dynamic meters) of the 500-mb. Pressure Surface, Average Temperature in °C. at 500 mb., and Resultant Winds at 5000 Meters (m.s.l.), July 1953.

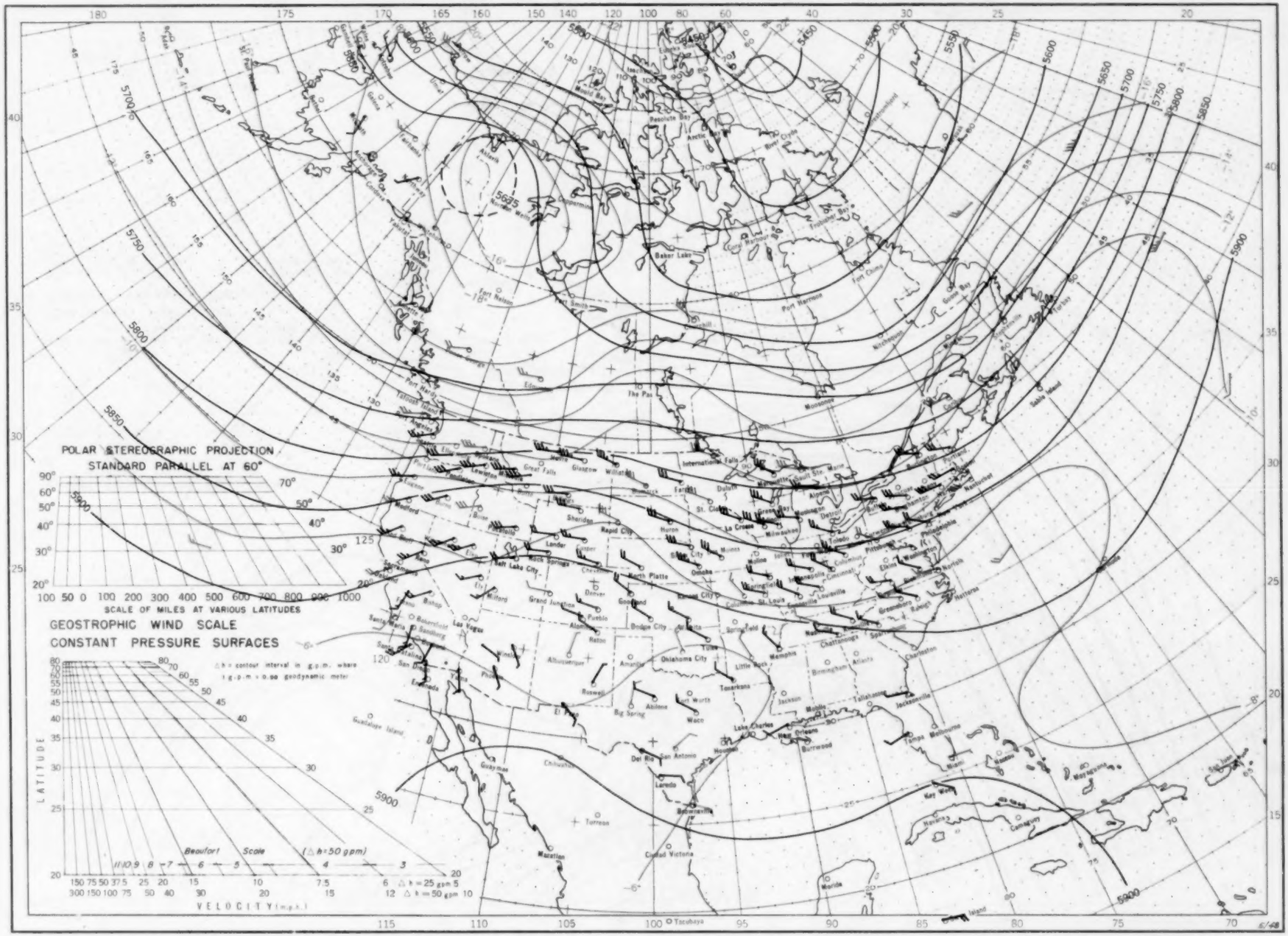

Contour lines and isotherms based on radiosonde observations at 0300 G. M. T. Winds shown in black are based on pilot balloon observations at 2100 G. M. T.; those shown in red are based on rawins at 0300 G. M. T.

Chart XV. Average Dynamic Height in Geopotential Meters (1 g.p.m. = 0.98 dynamic meters) of the 300-mb. Pressure Surface, Average Temperature in °C. at 300 mb., and Resultant Winds at 10,000 Meters (m.s.l.), July 1953.

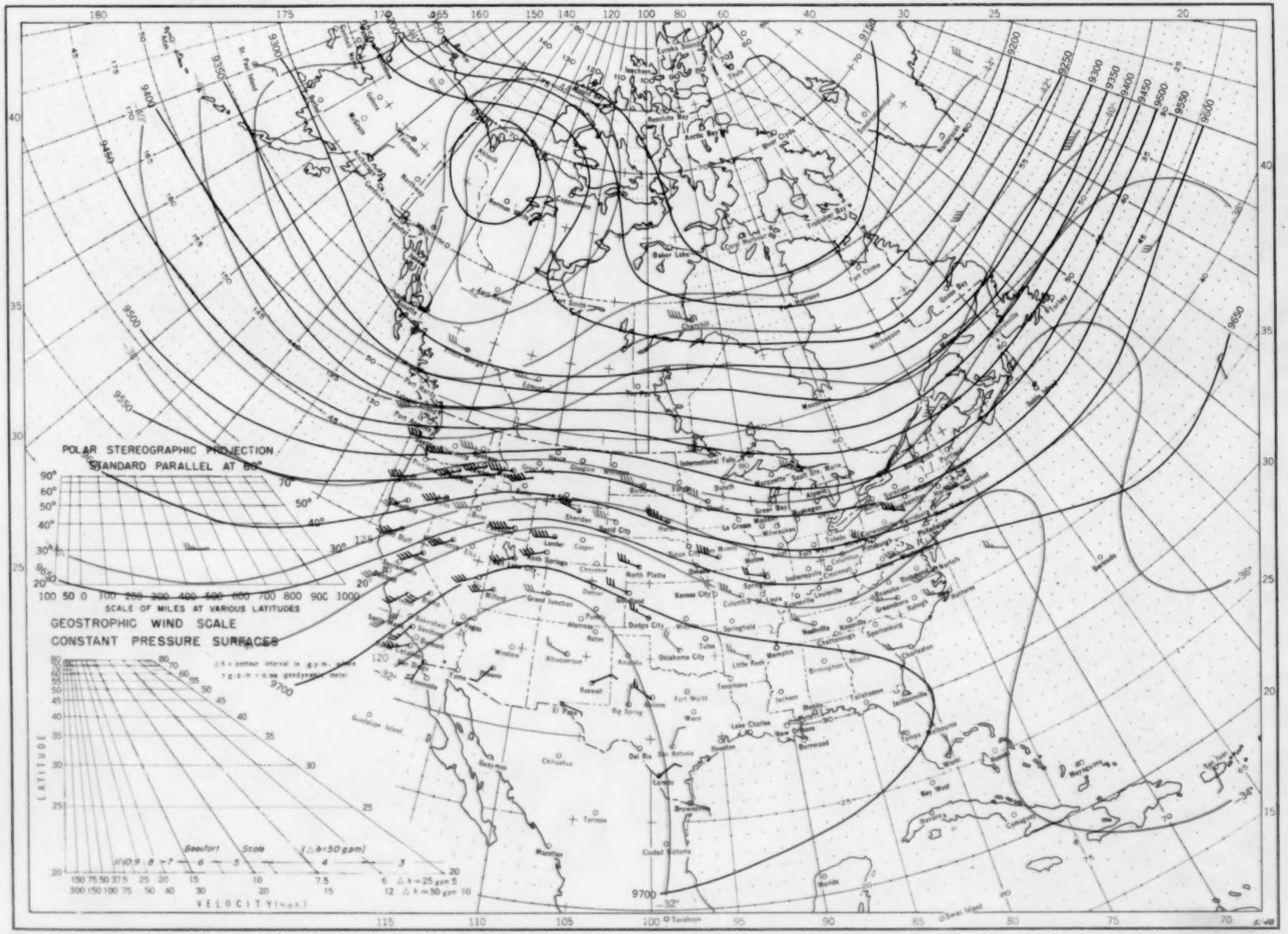

Contour lines and isotherms based on radiosonde observations at 0300 G. M. T. Winds shown in black are based on pilot balloon observations at 2100 G. M. T.; those shown in red are based on rawins at 0300 G. M. T.